



UNIVERSITÀ DEGLI STUDI DI PALERMO



PhD in Cell Biology and Technological Sciences of Drugs  
Department of Biological Chemical and Pharmaceutical Technologies  
SSD: BIO/06

**BIOLOGICAL EFFECTS OF JAHA, A NEW HISTONE  
DEACETYLASE INHIBITOR, ON CANCER CELLS FROM  
HUMAN BREAST EPITHELIUM**

PhD STUDENT:  
**Mariangela Librizzi**

SCIENTIFIC COORDINATOR:  
**Prof. Patrizia Diana**

TUTOR:  
**Prof. Claudio Luparello**

COORDINATOR OF CELL BIOLOGY:  
**Prof. Gabriella Sconzo**

XXV CYCLE (2012-2014)  
YEAR OF AWARD 2015

DOTTORATO



*"The science does not exclude errors;  
indeed, sometimes these lead to the truth."*

*(Jules Verne)*

## Table of contents

<b>Abstract</b> .....	<b>pag.1</b>
<b>Preface</b> .....	<b>pag.3</b>
<b>Acknowledgements</b> .....	<b>pag.5</b>
<b>List of Abbreviations</b> .....	<b>pag.6</b>
<b>1. Introduction</b> .....	<b>pag.13</b>
1.1 Breast cancer .....	pag.13
1.2 Triple-negative breast cancer .....	pag.14
1.3 Epigenetic control of gene expression .....	pag.14
1.4 DNA Methylation .....	pag.17
1.5 Histone acetylation .....	pag.17
1.6 Histone deacetylases .....	pag.18
1.6.1. Classification and localization .....	pag.18
1.6.2 Mechanism of action .....	pag.20
1.6.3 Structure of the HDACs .....	pag.21
1.7 Histone deacetylase inhibitors .....	pag.23
1.8 Short-chain fatty acids .....	pag.25
1.9 Hydroxamic acids .....	pag.26
1.10 Epoxides .....	pag.26
1.11 Cyclic Peptides .....	pag.26
1.12 Benzamides .....	pag.27
1.13 Hybrid Compounds .....	pag.27
1.14 HDACi mechanism of action .....	pag.27
1.15 HDACi and cell cycle inhibition .....	pag.31
1.16 HDACi and apoptosis .....	pag.32
1.17 HDACi and autophagy .....	pag.32
1.18 Effects of HDAC on cell motility and angiogenesis .....	pag.34
1.19 Therapeutic uses of HDACis .....	pag.35
<b>2. Aim of the research</b> .....	<b>pag.37</b>
<b>3. Materials and Methods</b> .....	<b>pag.40</b>

<b>3.1 Materials</b> .....	<b>pag.40</b>
3.1.1 Chemicals .....	pag.40
3.1.2 Consumables .....	pag.42
3.1.3 Equipment .....	pag.44
3.1.4 Buffers and Solutions .....	pag.45
3.2 Methods .....	pag.46
3.2.1 HDACis .....	pag.46
3.2.2 Cell cultures and viability assay .....	pag.46
3.2.3 Apoptosis Assay .....	pag.47
3.2.4 Cell Cycle Analysis .....	pag.47
3.2.5 Evaluation of ROS Production .....	pag.47
3.2.6 Mitochondrial Membrane Potential (MMP) Assay .....	pag.48
3.2.7 Autophagy Assays .....	pag.48
3.2.8 Migration Assay .....	pag.49
3.2.9 Total RNA Isolation .....	pag.49
3.2.10 Genomic DNA isolation .....	pag.51
3.2.11 Reverse Transcription Reaction .....	pag.52
3.2.12 Conventional PCR reaction .....	pag.53
3.2.13 Primer Sequences used for PCR amplification .....	pag.54
3.2.14 Differential Display-PCR .....	pag.55
3.2.15 Real Time Polymerase Chain Reaction .....	pag.58
3.2.16 Methylation Sensitive Restriction Endonucleases Multiplex PCR .....	pag.59
3.2.17 SDS-PAGE and Western blotting analysis .....	pag.61
3.2.18 Liquid chromatography-tandem mass spectrometry analysis .....	pag.62
3.2.19 Bioinformatic Analysis .....	pag.64
3.2.20 Statistical Analysis .....	pag.69
<b>4. Results</b> .....	<b>pag.70</b>
4.1 Effect of JAHA and homo-JAHA treatment on cell viability/proliferation .....	pag.70
4.2 JAHA-induced non-apoptotic death on MDA-MB231 cells .....	pag.71
4.3 Alterations of MDA-MB231 cell cycle cells after JAHA treatment .....	pag.72
4.4 JAHA-induced decrease of MMP in MDA-MB231 cells .....	pag.73
4.5 JAHA-induced increase in reactive oxygen species production in MDA-MB231 cells.....	pag.74
4.6 Autophagy inhibition in MDA-MB231 breast cancer cells treated with JAHA .....	pag.75
4.7 Inability of JAHA to affect MDA-MB231 cell motile behaviour .....	pag.79

4.8 Effect of JAHA on ERK and AKT signaling pathways.....	pag.82
4.9 JAHA influence on DNMT1 protein expression in MDA-MB231 cells .....	pag.84
4.10 Epigenetic effects of JAHA on genomic methylation status in MDA-MB231 cells.....	pag.85
4.11 Differentially-Expressed Genes in MDA-MB231 cell treated with JAHA .....	pag.87
4.12 Differentially-Expressed Proteins in MDA-MB231 cell treated with HDACis .....	pag.93
<b>5. Discussion .....</b>	<b>pag.97</b>
<b>6. Conclusion.....</b>	<b>pag.107</b>
<b>7. Future work .....</b>	<b>pag.108</b>
<b>References .....</b>	<b>pag.109</b>
<b>Sitography .....</b>	<b>pag.125</b>

## ***Abstract***

*The histone deacetylase inhibitors (HDACis) are a class of chemically heterogeneous anticancer agents of which suberoylanilide hydroxamic acid (SAHA) is a prototypical member. SAHA derivatives may be obtained by the three-dimensional manipulation of the SAHA aryl cap, such as the incorporation of a ferrocene unit like that present in Jay Amin hydroxamic acid (JAHA) and homo-JAHA (Spencer et al., 2011). These metal-based SAHA analogues have been tested for their cytotoxic activity toward triple-negative MDA-MB231 breast cancer cells. The results obtained indicate that of the two compounds tested, only JAHA was prominently active on breast cancer cells with an  $IC_{50}$  of 8.45  $\mu$ M at 72 h of treatment. For this reason JAHA only was used for the subsequent experiment at 8.45  $\mu$ M concentration. Biological assays showed that exposure of MDA-MB231 cells to the HDACi resulted in cell cycle perturbation with an alteration of S phase entry and a delay at  $G_2/M$  transition and in an early production of reactive oxygen species followed by mitochondrial membrane potential (MMP) dissipation and autophagy inhibition. No annexin binding was observed after short-(5 h) and longer (24 and 48 h) term incubation with JAHA, thereby excluding the promotion of apoptosis by the HDACi (Librizzi et al., 2012). An in vitro “scratch assay” has also been performed to measure migration of cells treated with JAHA for 24 h, but preliminary indications suggested that JAHA had no effect on the motile behaviour of MDA-MB231 cells. Subsequently, in order to identify protein signatures associated to its cytotoxic activity, we utilized a proteomic approach to reveal protein expression changes after 18, 24 and 48 h of exposure. Protein identification was performed by mass spectrometry, and a total of eleven differentially-expressed proteins were visualized. In parallel, Differential Display (DD) gene expression analysis was used to identify gene signatures in the MDA-MB231 human breast cancer cell line after exposure to JAHA. The result obtained by DD-PCR were confirmed by Real Time PCR analysis. Further study were required to compare the reported signature pattern with that obtained after exposure of MDA-MB231 cells with the parental molecule SAHA, and to understand the biological implications of the expression changes found. A further set of assays was designed to check the effect of JAHA on the intracellular signaling pathways of MDA-MB231 breast cancer cells. Concerning the MEK pathway JAHA repressed MAP kinase (ERK) activation after 18 h and up to 30 h of treatment, and also down-regulated DNA (cytosine-5-)-methyltransferase 1 (DNMT1), a downstream ERK target, already at 18 h with an increase up to 48 h of exposure.*

*To check the occurrence of changes in the extent of global DNA methylation, genomic DNA was submitted to MeSAP (Methylation Sensitive Restriction Arbitrarily-Primed) PCR (Naselli et al., 2014) using AfaI and then HpaII enzymes followed by PCR amplification with an arbitrary primer binding preferentially to guanine and cytosine (GC)-rich regions of DNA, including CpG islands. Preliminary indications suggest the ability of JAHA to induce hypomethylation patterns in tumoral breast cancer cells after 30 h of the treatment. Collectively, these data demonstrate that the HDACi JAHA, by inhibiting ERK activity, regulates DNMT1 expression and ultimately DNA methylation. Although caution must be exercised in extrapolation of the vitro results to the in vivo situation for which research on animals and human trials are needed, nevertheless JAHA treatment possesses the potential for its development as an agent for prevention and/or therapy of “aggressive” breast carcinoma, thus prompting us to get more insight into the molecular basis of its anti-breast cancer activity.*

## Preface

This research was supported by: a grant from the University of Palermo/Italy (R.S. ex 60% and FFR) to C.L. and a grant from research and training acknowledged from the National Operational Programme for Research and Competitiveness 2007-2013 (PON R & C) PON 01\_01059.

One publication “in extenso” and a number of communications to congresses (see list of publications) were produced from the present research.

## List of Publications

### Peer-reviewed journal publication

Librizzi M., Longo A., Chiarelli R., Amin J., Spencer J., Luparello C. Cytotoxic effects of Jay Amin hydroxamic acid (JAHA), a ferrocene-based class I histone deacetylase inhibitor, on triple-negative MDA-MB231 breast cancer cells. *Chem. Res. Toxicol.*, 2012 November 19; 25 (11): 2608-16.

### Communications to congresses

1) Librizzi M., Debski J., Dadlez M., Spencer J., Luparello C. Gene and Protein Signatures Associated to Treatment of MDA-MB231 Breast cancer cells with JAHA, a novel Histone Deacetylase Inhibitor. Congresso Ricerca di base, interdisciplinare e traslazionale in ambito Biologico e Biotecnologico, 26-27 June 2014 Palermo, Italy.

2) Librizzi M., Chiarelli R., Segreto C., Caradonna F., Spencer J., Bosco L., Roccheri M.C., Luparello C. The effect of the HDACi JAHA on DNA Methylation of breast cancer cells by downregulating DNMT1 through ERK signaling. Congresso Ricerca di base, interdisciplinare e traslazionale in ambito Biologico e Biotecnologico, 26-27 June 2014 Palermo, Italy.

3) Librizzi M., Longo A., Chiarelli R., Amin J., Spencer J., Tobiasch E., Luparello C. Cytotoxic effect of a novel histone deacetylase inhibitor, JAHA, on triple-negative breast cancer cells. BIT Congress-Europe BIT's Major Diseases Clinical Summit, 5-7 November 2013 Warsaw, Poland.



4) Librizzi M., Longo A., Chiarelli R., Amin J., Spencer J., Tobiasch E., Luparello C. JAHA, a novel histone deacetylase inhibitor: cytotoxic effect on triple-negative breast cancer cells. 86° Congresso SIBS Società di Biologia Sperimentale, 24-25 October 2013 Palermo, Italy.

5) Librizzi M., Longo A., Chiarelli R., Amin J., Spencer J., Tobiasch E., Luparello, C. Effetto citotossico di un nuovo inibitore delle deacetilasi istoniche, JAHA, su cellule di tumore mammario umano triplo negativo. Meeting Biotecnologie ricerca di base interdisciplinare translazionale in ambito biomedico, 27-28 June 2013 Palermo, Italy.

6) Librizzi M., Longo A., Chiarelli R., Amin J., Spencer J., Luparello C. JA47, a new histone deacetylase inhibitor that induces cytotoxic effects on triple-negative MDA-MB231 breast cancer cells in vitro. Convegno Annuale dell'Associazione Italiana di Colture Cellulari (Onlus AICC), 21-23 November 2012 Palermo, Italy.

7) Librizzi M., Longo A., Agnello M., Amin J., Spencer J., Luparello C. Cytotoxic effects induced by JA47, a novel histone deacetylase inhibitor (HDACi), on MDA-MB231 breast cancer cells. SIBBM Società Italiana di Biofisica e Biologia Molecolare Frontiers in Molecular Biology, Epigenetics in Development and Disease, 24-26 May 2012 Palermo, Italy.

## **Acknowledgements**

Most importantly, I would like to thank my supervisor Professor Claudio Luparello for his support, kindness and the help given to me throughout my project.

I would like to thank Dr. John Spencer (University of Sussex, UK) who provided me with the chemical tools that made the realization of this project possible.

I would like to thank Prof. Edda Tobiasch of the University of Applied Sciences of Bonn-Rhein-Sieg (D) and Prof. Michał Dadlez of the University of Warsaw (PL) for hosting me in their lab during my thesis internship.

I would to thanks Prof. Fabio Caradonna, Prof. Maria Carmela Roccheri, Dr. Roberto Chiarelli and Dr. Liana Bosco of the University of Palermo for their generous contributions to this research.

There are many colleagues that I have had the pleasure to work during the course of this doctoral study which I'd also like to thank.

In conclusion I would like to thank my family, because of their devoted support given to me that made my study feasible. They unquestioningly gave me the time and space that I needed, showed great patience and understanding of my necessities, particularly when my mind was elsewhere, and through their actions helped me to remain motivated and to complete this work in a timely fashion.

## **List of Abbreviations**

$\lambda$  - wavelength

°C - degrees centigrade

$\mu\text{g}$  - microgram

$\mu\text{l}$  - microliter

$\mu\text{M}$  - micromolar

x g - relative centrifugal force (RCF)

**ADP** - adenosine diphosphate

**AgNO<sub>3</sub>** - silver nitrate

**AHNAK** - neuroblast differentiation-associated protein

**AKT** - protein kinase

**AMP** - adenosine monophosphate

**APL** - acute promyelocytic leukemia

**APS** - ammonium peroxydisulfate

**Arg** - arginine

**Asp** - aspartic acid

**ATP** - adenosine triphosphate

**AVO** - acidic vesicular organelle

**BCA** - bicinchoninic acid method

**BCIP/NBT** - 5-bromo-4-chloro-3'-indolylphos. p-toluidine salt/nitro-blue tetrazolium chloride

**BDNF** - brain-derived neurotrophic factor

**BHT** - butylated hydroxytoluene

**bp** - base pair

**BSA** - bovine serum albumin

**CDK** - cyclin-dependent kinase

**CDR** - complementarity determining region

**CH<sub>3</sub>COOH** - acetic acid

**cm** - centimeter

**cm<sup>2</sup>** - square centimeter

**CO<sub>2</sub>** - carbon dioxide

**DAG** - diacylglycerol

**DD** - death domain

**DD-PCR** - differential display-PCR

**DDD** - double digested DNA

**DED** - death effector domain

**DISC** - death inducing signalling complex

**DMSO** - dimethyl sulfoxide

**DNA** - desoxyribonucleic acid

**DNMT1** - DNA methyltransferase 1

**dNTPs** - desoxyribonucleotides

**DRAM** - damage-regulated autophagy modulator

**DTT** - dithiothreitol

**EDTA** - ethylene diamine tetracetic acid

**EGTA** - ethylene glycol tetracetic acid

**ER** - endoplasmic reticulum

**ERBB 2** - epidermal growth factor receptor

**ERGIC 2** - ER-Golgi intermediated compartment

**ERK** - extracellular signal regulated kinase

**ExoSAP-IT** - exonuclease I and shrimp alkaline phosphatase

**FACS** - fluorescence-activated cell sorter

**FADD** - FAS associated death domain protein

**FBS** - fetal bovine serum

**FDR** - false discovery rate

**FITC** - fluorescein isothiocyanate

**g** - gram

**GAPDH** - glyceraldehyde-3-phosphate dehydrogenase

**h** - hour

**H** - hydrogen

**H2A** - histone 2A

**H2B** - histone 2 B

**H3** - histone 3

**H4** - histone 4

**HAT** - histone acetylase

**HDAC** - histone deacetylase

**HDACi** - histone deacetylase inhibitor

**HDC** - high-dose chemotherapy

**HDLP** - histone deacetylase-like protein

**HER2** - human epidermal growth factor receptor 2

**HIF** - hypoxia inducible factor

**His** - histidines

**H<sub>2</sub>O** - water

**HPLC** - high performance liquid chromatography

**HRP** - horseradish peroxidase

**l** - liter

**LiCl** - lithium chloride

**IAPs** - inhibitors of apoptosis

**IDI 1** - isopentenyl-diphosphate delta isomerise

**IC<sub>50</sub>** - half maximal inhibitory concentration

**IPG** - immobilized pH gradient

**iTRAQ** - isobaric tags for relative and absolute quantitation

**JAHA** - Jay Amin hydroxamic acid

**JC1** - dye for mitochondrial membrane potential

**K** - lysine

**LC3** - microtubule-associated protein 1A/1B-light chain 3

**LC - MS** - liquid chromatography-mass spectrometry

**LC-MS - MS/MS** - liquid chromatography coupled to tandem mass spectrometry

**LRCH 1** - leucina-rich-repeat and calponin homology domain containing protein 1

**M** - molar

**MAPK** - mitogen activated protein kinases

**MBD 1** - methyl-CpG-binding protein 1

**MED 25** - mediator of RNA Polymerase II trascription subunit25

**MeSAP-PCR** - methylation-sensitive arbitrarily-primed polymerase chain reaction

**mg** - milligramme

**MgCl<sub>2</sub>** - magnesium chloride

**min** - minute

**ml** - milliliter

**M-MLV RT** - moloney murine leukemia virus reverse transcriptase

**mM** - millimolar

**MMP** - mitochondrial membrane potential

**mRNA** - messenger RNA

**MS** - mass spectrometry

**MS/MS** - tandem mass spectrometry

**MTT** - 3-(4,5-dimethylthiazol-2-yl)-2,5-diphenyltetrazolium bromide

**Na<sub>2</sub>CO<sub>3</sub>** - sodium carbonate

**NAD** - nicotin-amide-dinucleotide

**NAALAD2** - inactive\_N-acetylated-alpha-linked acidic peptidasi-like protein 2

**NCBI** - National Center for Biotechnology Information

**NFK-B** - nuclear factor kappa light chain enhancer of activated B cells

**NGF** - nerve growth factor

**NHE** - normal hydrogen electrode

**nM** - nano molar

**NOS** - nitric oxide synthase

**NSCLC** - non-small cell lung cancer cells

**NTRK 2** - neurotrophic tyrosine receptor kinase 2

**ODDD** - oxygen-dependent degradation domain

**PBS** - phosphate-buffered saline

**PCR** - polymerase chain reaction

**PK1** - pyruvate dehydrogenase kinase

**pH** - pondus hydrogenii

**Phe** - phenylalanine

**PI** - propidium iodide

**PI3** - fosfoinositide 3-chinasi

**PKε** - protein kinase C epsilon

**PKι** - protein kinase C iota

**p62/SQSTM1** - p62/sequestosome 1

**PMF** - peptide mass fingerprinting

**PMSF** - phenylmethanesulfonyl fluoride

**PR** - partial remission

**PSMs** - peptide spectrum match

**pVHL** - von hippel–lindau tumor suppressor

**R** - arginine

**RAD 50** - DNA protein repair

**RNA** - ribonucleic acid

**ROS** - reactive oxygen species

**rpm** - revolution per minute

**RPMI** - Roswell Park Memorial Institute

**rRNA** - ribosomal RNA

**RS** - random sequence

**RT** - room temperature

**RT** - reverse transcriptase

**RT-PCR** - real time-PCR

**S** - serine

**SAHA** - suberoylanilide hydroxamic acid

**SDD** - single digested DNA

**SDS** - sodium dodecyl sulphate

**SDS-PAGE** - sodium dodecylsulfate-polyacrylamide gel electrophoresis

**sec** - second

**SGD** - saccharomyces genome database

**SIRT** - sirtuin

**SMAC** - second mitochondria-derived activator of caspases

**T** - threonine

**TBE** - tris-borate/EDTA

**TBP 2** - thioredoxin-binding protein 2

**TBS** - tris buffered saline



**TBS-T** - tris-buffered saline and tween 20

**TCA** - trichloroacetic acid

**TE** - tris-EDTA

**TEMED** - N, N, N', N'-tetramethylethylene-diamine

**TFA** - trifluoroacetyl acid

**TNBC** - triple-negative breast cancer

**TNF** - tumor necrosis factor

**TNFR** - tumor necrosis factor receptor

**TPA** - tissue polypeptide antigen

**TPX** - trapoxin

**tRNA** - transfer RNA

**TRAIL** - TNF related apoptosis-inducing ligand

**TRX** - thioredoxin

**TSA** - trichostatin A

**Tyr** - tyrosine

**VDUP1** - vitamin D3 up-regulated protein 1

**VEGF** - vascular endothelial growth factor

**YWHAB** - tyrosine 3-monooxygenase tryptophan 5-monooxygenase activation protein, beta polypeptide

# 1. Introduction

## 1.1 Breast cancer

Breast cancer is the most common cancer diagnosed in women globally. More than 1 million women are affected by the disease each year and it is estimated that 400,000 women will die due to breast cancer (Laurentiis et al., 2010). Cancer is generally characterized by uncontrolled cell division, cell transformation, and escape of apoptosis, invasion, angiogenesis and metastasis. One of the challenges of treating breast cancer is the heterogeneity between various tumors (Polyak, 2011). Breast cancer can be classified in multiple ways. Traditionally, classification was histological, separating breast cancers into ductal, lobular, nipple, or not otherwise specified. However, molecular classification using immunohistochemistry to reflect the hormone-responsiveness of the tumors and other cell markers has become increasingly useful for dictating treatment and prognosis. The molecular subtypes of breast cancer, which are based on the presence or absence of estrogen receptors (*ER*), progesterone receptors (*PR*), and human epidermal growth factor receptor-2 (*HER2*), include: luminal A (*ER+* and/or *PR+*; *HER2-*), luminal B (*ER+* and/or *PR+*; *HER2+*), basal-like (*ER-*, *PR-*, and *HER2-*), and *HER2*-enriched (*ER-*, *PR-*, and *HER2+*) (Hsiao et al., 2010; Viale, 2012), (figure 1.1).

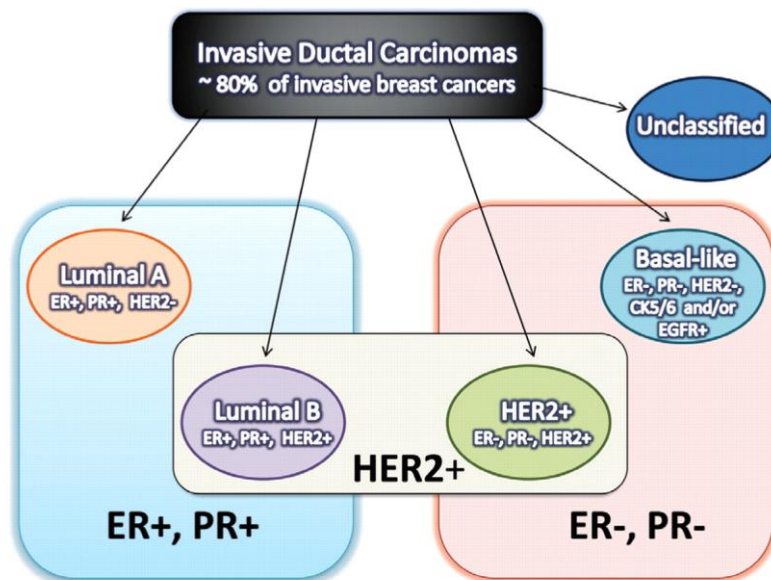


**Figure 1.1.** Molecular subtypes of breast cancer – hormone receptor and growth factor status. ER – Estrogen Receptor, PR – Progesterone Receptor, ERBB2/HER2 – Human Epidermal growth factor Receptor 2 (<http://www.labmed.ascpjournals.org>).

It is important to note that not all tumors in a specific histological subtype belong to the same molecular classification. Additionally, the hormone responsiveness does not determine the molecular subtype. For example, not all tumors with HER2+ receptors are of the HER2-enriched mRNA subtype, and not all tumors in the HER2-enriched mRNA subtype are clinically HER2 receptor-positive. In addition a variety of genetic and epigenetic changes has been implicated in the development of breast cancer, in particular somatic gene mutations, copy number aberrations, exon sequencing changes, alterations in miRNA and protein expression levels, and changes in methylation and acetylation levels.

## **1.2 Triple-negative breast cancer**

Of the estimated 1 million cases of breast cancer diagnosed annually worldwide, approximately 170,000 will harbour the triple-negative phenotype (Anders et al., 2009). Triple-negative breast cancer (TNBC) does not express the ER, PR or the HER2 receptor hence the triple-negative status. Although most basal like cancers do not express ER, PR and HER2 receptors some do, therefore the small overlap between basal like and TNBC is generally insensitive to the standard targeted drugs for breast cancer as many current therapies tend to target the receptors, for example, Herceptin and anti-oestrogen therapies (Zordoky et al., 2014). Since TNBC does not have any of the receptors, it is much more difficult to treat and there is often a poor prognosis. Therefore, the testing of new or pre-existing novel drugs in the treatment of triple-negative breast cancer is paramount.

## **1.3 Epigenetic control of gene expression**

In eukaryotes DNA is packaged into chromatin fibers to achieve compaction, enabling the entire genome to fit into the nucleus, and allowing DNA transcription, replication, and repair, when necessary (figure 1.2).

The nucleosome is the basic repeating unit of chromatin polymer and consists of 146 bp of DNA wrapped around a histone octamer (Marks et al., 2001). Histones are small basic proteins conserved throughout evolution and consist of a globular domain flanked by a carboxy-terminal and a lysine rich amino-terminal tail composed of positively charged residues. The core histone octamer is formed by two copies of each of histones H2A, H2B, H3 and H4 organized in an H3-H4 tetramer and two H2A-H2B dimers.

The binding of Histone H1 to linker DNA sequences between nucleosomes leads to a further chromatin compaction, by mechanisms that remain poorly defined (figure 1.3).

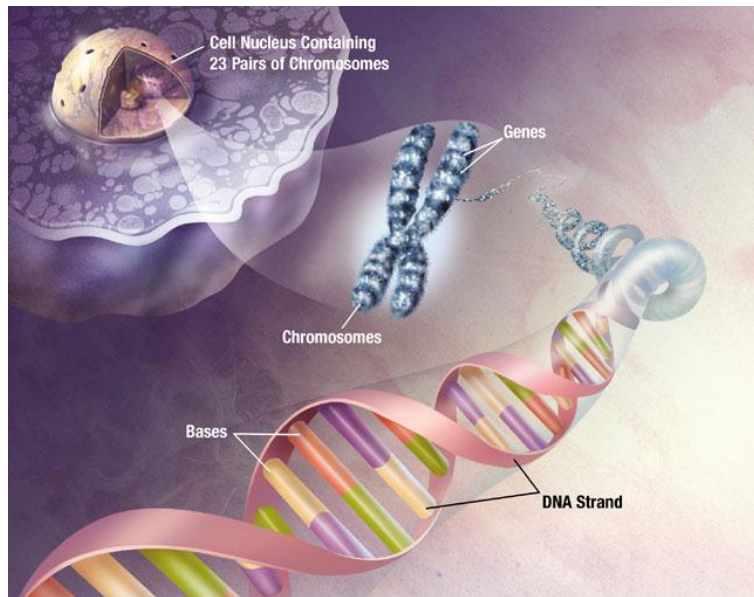


**Figure 1.2.** Organization of DNA into chromatin, nucleosome fibers are packaged into higher order structures giving rise to chromosomes (<http://www.bouzoki.files.wordpress.com>).

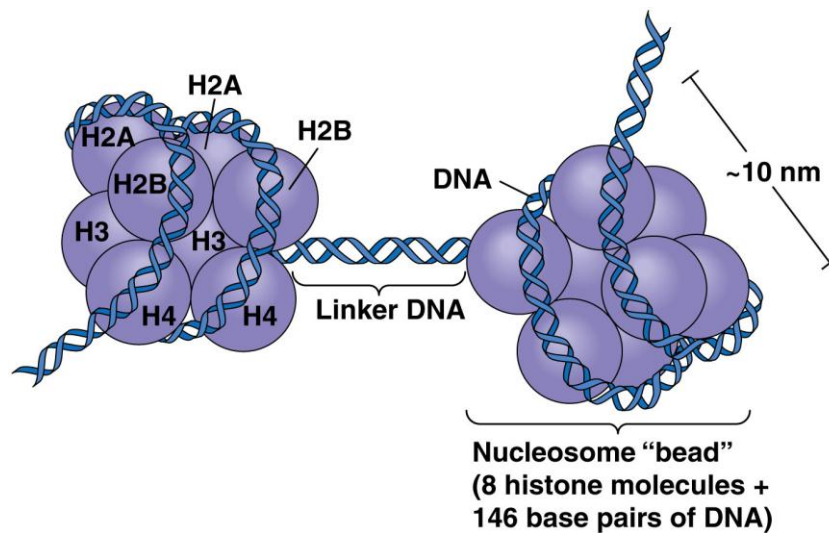


**Figure 1.3.** Schematic representation of a nucleosome. DNA is wrapped around core histone octamer which contains two H3-H4 tetramers centrally located and two flanking H2A-H2B dimers. Histone H1 links nucleosomes into higher order structures (<http://www.mun.ca>).

Histone lysine tails protruding from the nucleosome are sites of post-translational modifications including acetylation, methylation and ubiquitination of lysine (K) residues, phosphorylation of serine (S) and threonine (T) residues, methylation of arginine (R) and ADP ribosylation of glutamic acid residues (Zhang et al., 2001), (figure 1.4).

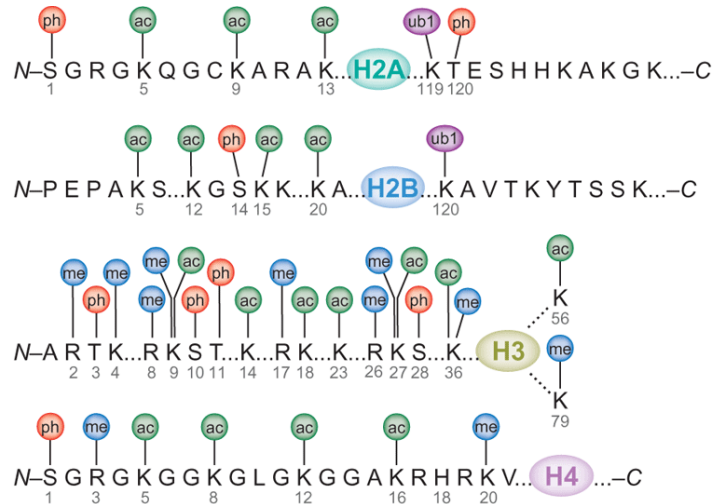


**Figure 1.4.** Histone modifications include acetylation (ac), methylation (me), phosphorylation (ph) and ubiquitination (ub1). Most of the known histone modifications occur on the N-terminal tails of histones, with some exceptions including ubiquitination of the C-terminal tails of H2A and H2B and acetylation and methylation of the globular domain of H3 at K56 and K79, respectively. Globular domains of each core histone are represented as coloured ovals (<http://www.nature.com>).

Strahl (2000) proposed that distinct histone modifications, on one or more tails, act sequentially or in combination to form a 'histone code' that is read by other proteins leading to distinct downstream events. This theory states that posttranslational modifications can act through two mechanisms that are not mutually exclusive: (i) by structurally changing the chromatin fiber through internucleosomal contacts thus regulating the access of transcription factors to the DNA; and (ii) by generating docking sites for effector molecules that, in turn, initiate distinct biological processes. The histone code is part of the epigenetic information found into the cells. The term “epigenetics” refers to mitotically and meiotically heritable changes in gene expression that are not coded in the DNA sequence itself (Egger et al., 2004). Indeed, DNA methylation is another well studied epigenetic mechanism. Methylation at the C-5 position of cytosine residues present in CpG dinucleotides by DNA methyltransferases (DNMTs) is generally considered to facilitate static long-term gene silencing (Lund et al., 2004).

## **1.4 DNA Methylation**

DNA methylation and histone modifications are two principal factors in epigenetic phenomena. These two mechanisms perform a crucial function in carcinogenesis and tumor progression. DNA methylation is controlled by DNA methyltransferase (DNMT), an enzyme that catalyzes the transfer of a methyl moiety from S-adenosyl-1-methionine to the 5-position of cytosines in the CpG dinucleotide (Robertson, 2001). DNMT overexpression has been detected in a variety of malignancies, including lung, prostate, and colorectal tumors (Eads et al., 1999; Lin et al., 2007; Manoharan et al., 2007). Because DNA methylation is a reversible biochemical process, DNMT may be a viable target for the treatment of cancer. Since two cytidine analogues, 5-azacytidine and 5-aza-2'deoxyctidine, have been reported in the 1980s, several DNMT inhibitors are currently under investigation for their possible utility in treating a variety of tumors (Schneider et al., 2007; Mai et al., 2009). It has become widely accepted that histone modification and DNA methylation are intricately interrelated in terms of affecting chromatin structure and gene expression (Hashimshony et al., 2003). Because these two parameters have long been implicated in the regulation of cellular response, histone deacetylase (HDAC) inhibitors and DNMT inhibitors might be considered potential targets for the cancer.

## **1.5 Histone acetylation**

To date, acetylation is the most extensively studied histone posttranslational modification and involves the transferring of an acetyl group from the metabolic intermediary acetyl coenzyme to the  $\epsilon$ -amino group of a lysine residue. The primary effect produced by acetylation is the partial neutralization of the positive charge of the histones, thus decreasing their affinity for the DNA, altering nucleosome-nucleosome interactions and enabling chromatin decondensation to allow transcriptional activation (Jenuwein et al., 2001; Vaquero et al., 2003). Although it is known that the four core histones (H2A, H2B, H3, and H4) can be acetylated in their N-terminal tails, the H3 and H4 modifications are mainly responsible for the effect on transcription. The balance between acetylated and deacetylated states of chromatin is regulated by histone acetyltransferase (HAT) and histone deacetylase (HDAC) enzymes (Marks et al., 2001; Minucci et al., 2006). HATs transfer acetyl groups to amino-terminal lysine residues in histones, which results in local expansion of chromatin and increased accessibility of transcription factors to DNA, whereas HDACs catalyse the removal

of acetyl groups, leading to chromatin condensation and transcriptional repression (figure 1.5).

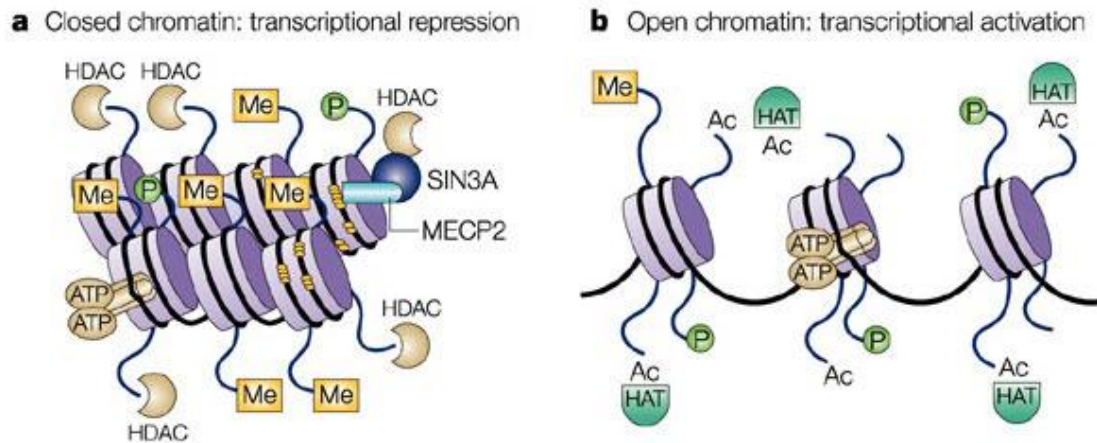


**Figure 1.5.** Schematic representation of the equilibrium between HDAC and HAT activities (Johnstone, 2002).

## 1.6 Histone deacetylases

### 1.6.1. Classification and localization














The HDACs can be divided into two families (table 1.1), (Tauton et al., 1996) the  $Zn^{+2}$  dependent HDAC family composed of class I (HDACs 1, 2, 3 and 8), class II a/b (HDACs 4, 5, 6, 7, 9 and 10), and class IV (HDAC 11) and (Glaser et al., 2002)  $Zn^{+2}$ -independent NAD-dependent class III SIRT enzymes.

Zn -Dependant HDAC		NAD- Dependant HDAC
Inhibited by TSA		Inhibited by Nicotinamide
Class I	Class II	Class III
HDAC 1	HDAC 4-7	SIRT 1-7
HDAC 2	HDAC 9	
HDAC 3	HDAC 10	
HDAC 8		
HDAC 11		

**Table 1.1.** Classification of HDAC family.



Based on their homologies to yeast HDACs, mammalian HDACs can be divided into four classes (table 1.2) (Glaser, 2007). Class I comprises HDAC1, 2, 3 and 8, which are related to the yeast HDAC rpd3, and these HDACs are located in the nuclei of the cells. Class IIa/b HDACs, homologous to yeast hda1, have both histones and non-histone proteins as substrates, are primarily localized to the cytoplasm but they can shuttle to nucleus through association with 14-3-3 proteins. Specifically, HDAC 4, 5, 7 and 9 fall into Class IIa, whereas Class IIb contains the HDAC6 and 10, which have two catalytic sites (Dokmanovic et al., 2005). It was reported that HDAC11 has a conserved domain in the catalytic region of both Class I and Class II enzymes (Fischle et al., 2002) and it has been grouped to Class IV HDAC. Zn<sup>+2</sup>-independent and NAD-dependent Class III HDACs are homologues to yeast sir2, and they are virtually unaffected by the HDAC inhibitors that are now in clinical trials. At present, the applications of HDAC inhibitors in therapy of cancer or other diseases are mainly pointed to Zn<sup>+2</sup>-independent Class I and II HDACs.

	Structure and Length	Cellular localization
<b>Class I</b>		
HDAC1	 482 aas	Nucleus
HDAC2	 488 aas	Nucleus
HDAC3	 428 aas	Nucleus/Cytoplasm
HDAC8	 377 aas	Nucleus
<b>Class IIa</b>		
HDAC4	 1084 aas	Nucleus/Cytoplasm
HDAC5	 1122 aas	Nucleus/Cytoplasm
HDAC7	 855 aas	Nucleus/Cytoplasm
HDAC9a	 1011 aas	Nucleus/Cytoplasm
HDAC9b	 879 aas	Nucleus/Cytoplasm
<b>Class IIb</b>		
HDAC6	 1215 aas	Nucleus/Cytoplasm
HDAC10	 669 aas	Nucleus/Cytoplasm
<b>Class IV</b>		
HDAC11	 347 aas	Nucleus
		

**Table 1.2.** The classification of HDACs in mammals (Lucio-Eterovic et al., 2008).

The class II enzymes are characterized by either a large N-terminal domain or a second catalytic domain (HDAC 6 which contains both a histone and a tubulin deacetylase catalytic domain). The class III SIRT<sup>s</sup> are NAD<sup>+</sup> dependent deacetylases with non-histone proteins as substrates (in mammalian cells) and have been linked to regulation of calorific utilization of



cells (only in yeast the SIR proteins are known to be histone deacetylases) (Bolden et al., 2006). HDACs do not function independently but rather in concert with multi-protein complexes (e.g., NCoR, SMRT, MEF, MeCP2, Sin3A, etc.), (Ng et al., 2000) that are recruited to specific regions of the genome that in turn generate the unique spectrum of expressed and silenced genes that are characteristic of the expression profiles responsible for the malignant phenotype of cancer cells.

### 1.6.2 Mechanism of action

The mechanism of action of the HDAC enzymes involves removing the acetyl group from the histones comprising the nucleosome. Hypoacetylation results in a decrease in space between the nucleosome and the DNA which is wrapped around it. Tighter wrapping of the DNA diminishes accessibility for transcription factors, leading to transcriptional repression (figure 1.6), (Strahl et al., 2000; Wade, 2001).

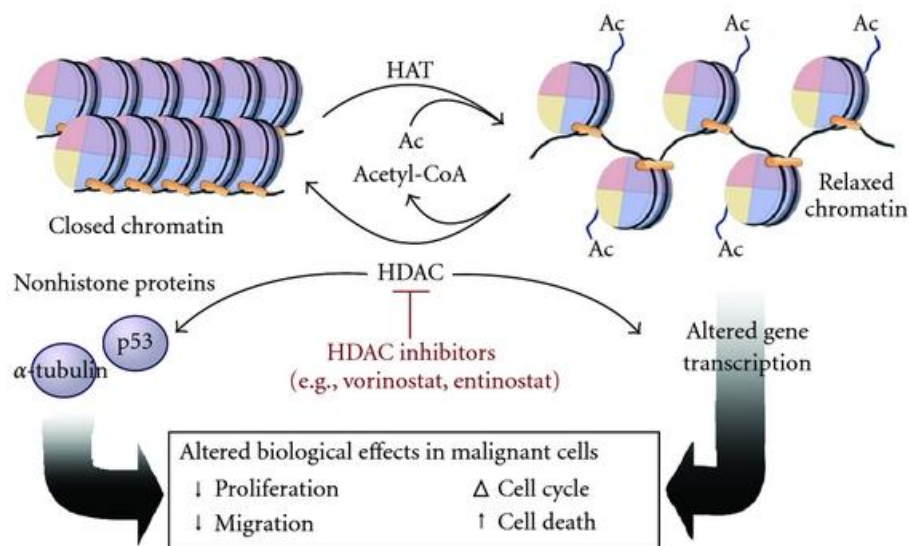


**Figure 1.6.** HAT and HDAC mechanism of actions (<http://www.hindawi.com>).

The catalytic domain of HDAC is formed by a stretch of ~390 amino acids consisting of a set of conserved amino acids. The active site consists of a gently curved tubular pocket with a wider bottom (Finnin et al., 1999). Removal of an acetyl group occurs via a charge-relay system consisting of two adjacent histidine residues, two aspartic residues (located approx. 30 amino acids from the histidines and separated by approx. 6 amino acids), and one tyrosine residue (located approx. 123 amino acids downstream from the aspartic residues) (Buggy et

al., 2000). An essential component of the charge-relay system is the presence of a  $Zn^{+2}$  ion. This atom is bound to the zinc binding site on the bottom of the pocket. However, other cofactors are required for HDAC activity since most recombinantly expressed enzymes are found to be inactive. HDACi function by displacing the zinc ion and thereby rendering the charge-relay system dysfunctional. TSA, with its hydroxamic acid group and its five-carbon atom linker to the phenyl group, has the optimal conformation to fit into the active site (Finnin et al., 1999). There have been indications that histone hypoacetylation frequently occurs in tumor cells, and the disorder of histone acetylation level is associated with carcinogenesis (Mahlknecht et al., 2000). Abnormal transcriptional silencing of certain cancer-related genes mediated by overexpression of HDACs that are recruited by transcription factors may be a cause of carcinogenesis.

### 1.6.3 Structure of the HDACs

The structure of the histone deacetylase catalytic core, as revealed by the crystal structure of a homologue from the hyperthermophilic bacterium *Aquifex aeolicus*, that shares 35.2% identity with human HDAC1 over 375 residues, deacetylates histones *in vitro*. It consists of a central eight-stranded parallel  $\beta$ -sheet and sixteen  $\alpha$ -helices as shown in figure 1.7.

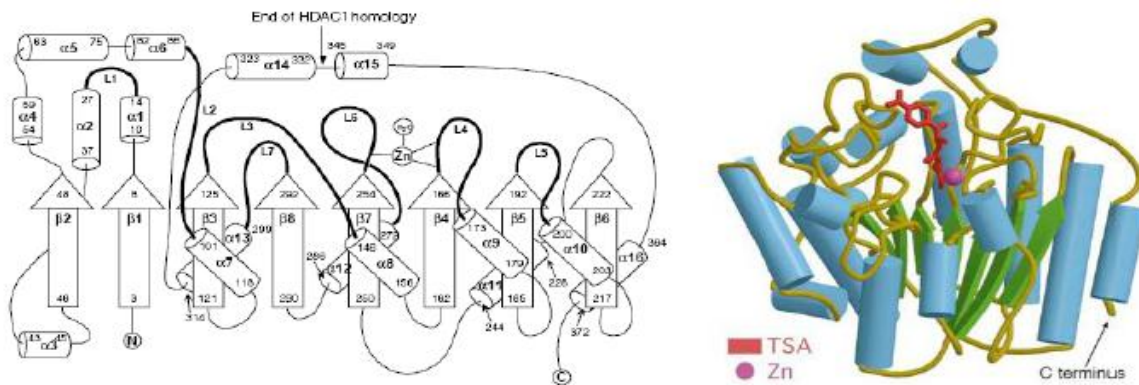


**Figure 1.7.** HDLP structure (Finnin et al., 1999).

Four helices pack on either face of the  $\beta$ -sheet, forming the core  $\alpha/\beta$  structure characteristic of this class of folds. Most of the remaining eight helices are clustered near one side of the  $\beta$ -sheet. Large, well-defined loops originate from the carboxy-terminal ends of the  $\beta$ -strands (loops L1-L7; figure 1.7). The extra helices and the large L1-L7 loops are associated with a significant extension of the structure beyond the core  $\alpha/\beta$  motif. This gives rise to two

prominent architectural features: a deep, narrow pocket and an internal cavity adjacent to the pocket (figure 1.8).

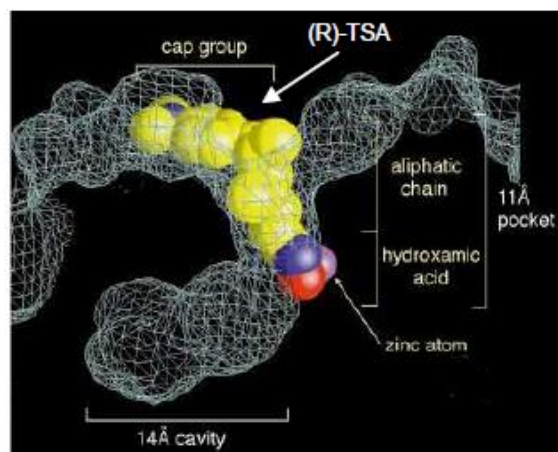


**Figure 1.8.** Space-filling representation of TSA in the active-site pocket (Finnin et al., 1999).

The pocket has a tube-like shape with a depth of  $\sim 11 \text{ \AA}$ . The pocket opening constricts halfway down to  $\sim 4.5$  by  $5.5 \text{ \AA}$ , but becomes wider at the bottom. The pocket and its immediate surroundings are made up of seven loops. These originate from strands near the centre of the sheet (L3-L7) and from the additional helices that pack near the ends of the strands. The walls of the pocket are covered with hydrophobic and aromatic residues that are identical in HDAC1 (Pro22, Gly140, Phe141, Phe198, Leu256 e Tyr296). Of particular significance are Phe 141 and Phe 198, whose phenyl groups face each other in parallel at a distance of  $7.5 \text{ \AA}$ , marking the most slender portion of the pocket. In the crystal structure of the zinc-reconstituted enzyme, the zinc ion is positioned near the bottom of the pocket, just beyond its narrowest point. It is coordinated by Asp 168, His 170, Asp 258 and a water molecule. The protein ligands are arranged in a tetrahedral geometry, but the position of the water molecule, which also hydrogen-bonds to His 131, deviates from this geometry by  $\sim 25^\circ$ . In addition to the zinc ligands, the bottom of the pocket contains two histidines (His 131 and His 132), two aspartic acids (Asp 166 and Asp 173) and a tyrosine (Tyr 297), all of which are identical in HDAC1. The Asp 166-His 131 charge-relay pair is positioned deeper inside the pocket, and is more buried than the Asp 173-His 132 charge relay, which is partially solvent exposed. The internal cavity is made up of portions of the L3 and L7 loops as they emerge from the  $\beta$ -strands and the  $\alpha 1$ -L1- $\alpha 2$  segment. The L1 loop, which demarcates the cavity from the solvent, has higher temperature factors than the rest of the structure, indicating some inherent flexibility that may allow the transient exchange of the cavity contents with the bulk solvent. The cavity is lined primarily with hydrophobic residues and is particularly rich in

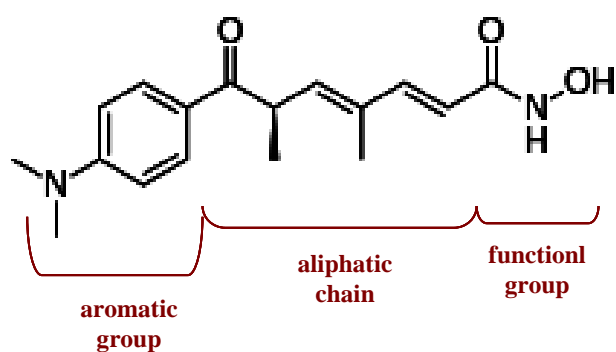
glycine residues. There are only two charged residues in the cavity and these are contributed by the L1 loop (Arg 27 and His 21). The function of the cavity is not clear. It is possible that it provides space for the diffusion of the acetate product away from the catalytic centre, which may otherwise be crowded and shielded from the solvent when the substrate is bound. The HDLP-HDAC1 homology maps mainly to the hydrophobic core and to the L1-L7 loops, with the portions of the loops that make up the pocket and adjacent cavity having the highest level of conservation. Specifically, all of the polar residues in the active site and the hydrophobic residues that make up the walls of the pocket are identical. Among the residues that make up the internal cavity, the ones closest to the active site are either identical or conservatively substituted. The HDLP active-site residues that are identical in HDAC1 are also conserved in the class II histone deacetylases. One exception is Asp 173 of the exposed charge-relay system, which is an asparagine in some class II HDACs. The 375-amino-acid HDLP protein corresponds to the histone deacetylase catalytic core that is conserved across the HDAC family. The one region likely to have a less similar structure is the 40-residue C terminus of HDLP (335-375), which has significantly lower homology to HDAC1 (Finnin et al., 1999).

## **1.7 Histone deacetylase inhibitors**

Natural and synthetic inhibitors of HDAC have not only contributed to the discovery of HDAC enzyme molecules and the elucidation of their functions but have also developed as attractive therapeutic agents for diseases including cancer. After the disclosure of the crystal structure of the HDAC-like protein bound to the inhibitor, the momentum of research on HDAC inhibitors increased, and several inhibitors are currently under clinical trials. One of the most important developments in this field of research was the isolation of specific HDAC inhibitors from natural sources. In the early 1990s, trichostatin A (TSA) and other fungal antibiotics such as trapoxin (TPX) were shown to inhibit HDAC at nanomolar concentrations and to allow the induction of histone hyperacetylation in living cells (Yoshida et al., 1995; Kijima et al., 1993). In addition, it is becoming increasingly clear that reversible acetylation of proteins other than histones is one of the key post-translational modifications controlling the activity of proteins. The HDACi have been widely used as powerful tools for identification and functional analysis of the acetylated non-histone proteins. The clinical importance of the HDAC inhibitors has been emphasized, in particular for cancer treatment. These agents act selectively in altering the transcription of relatively few of the expressed genes (generally 2% to 10% of expressed genes are increased or decreased in their rate of

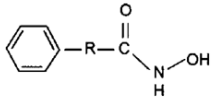
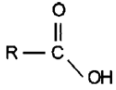
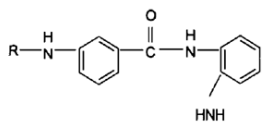
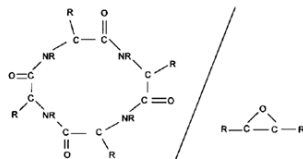
transcription), (Van Lint et al., 1996; Butler et al., 2002). The first compound described as an inhibitor of HDAC activity was sodium butyrate (Candido et al., 1978).

The effect of butyrate as a noncompetitive inhibitor was shown with a partially purified enzyme (Cousens et al., 1979). However, its effective concentration exceeds millimolar levels, which raised the possibility that it affects other enzymes, the cytoskeleton and membranes. Therefore, butyrate should be used with caution. TPX, which had been discovered to induce morphological reversion of transformed phenotype to normal in several oncogene transformed cells, was also shown to inhibit HDAC (Kijima et al., 1993). In contrast to TSA, TPX was an irreversible inhibitor of HDAC. Cocrystallization of the bacterial histone deacetylase-like protein (HDLP) with TSA demonstrated that TSA mimics the substrate and that TSA binds by inserting its long aliphatic chain into the tube-like HDLP pocket and inhibits the enzyme activity by interacting with the zinc and active-site residues through its hydroxamic acid at one end of the aliphatic chain (Finnin et al., 1999). Hydroxamic acid, a functional group of the inhibitor, coordinates the zinc through its carbonyl and hydroxyl groups, resulting in the formation of a penta-coordinated zinc. The classes of compounds that have been identified as strong HDAC inhibitors have basic structures mimicking that of TSA, which possesses an aromatic group as a cap, an aliphatic chain for a spacer, and a hydroxamic acid as a functional group interacting with the active-site zinc. The functional groups include carboxylates, hydroxamic acids, electrophilic ketones containing epoxyketones, anilides, and thiols (figure 1.9).



**Figure 1.9.** Basic structure of the HDACi (TSA) ([http://www.en.wikipedia.org/wiki/Trichostatin\\_A](http://www.en.wikipedia.org/wiki/Trichostatin_A)).

Several structurally distinct classes of HDC inhibitors have been developed, including hydroxamic acid, cyclic peptides, electrophilic ketones, short-chain fatty acids, and benzamides (Drummond et al., 2005; Beckers et al., 2007), (table 1.3).

Class / Structure	Drugs	Clinical trial (phase)
<b>Hydroxamic acid</b> 	SAHA LAQ-824 LBH589A	I – III I I
<b>Carboxylic acid</b> 	Phenylbutyric acid Valproic acid Pivanex	II II II
<b>Benzamide</b> 	MS-275 CI-994	II II/III
<b>Cyclic tetrapeptide/Epoxide</b> 	Depsipeptide (FK228)	II

**Table 1.3.** HDAC inhibitors in clinical trials as anticancer agents (Lee et al., 2007).

## 1.8 Short-chain fatty acids

This class of compounds is characterized by a short plasma half-life, non-specificity and low power due to the short aliphatic chain which limits the contact with the catalytic pocket of HDACs. Some require high concentrations of the order of millimolar, to exert their inhibitory action; are therefore not suitable for clinical use. Sodium butyrate causes cell cycle arrest in G<sub>2</sub>/M and cell death by apoptosis; it promotes the acetylation of histones and maturation of granulocytes in acute myeloid leukemia and, in humans, selectively inhibits the growth of tumor cells in the prostate and carcinoma of the cervix. Sodium valproate inhibits HDAC at millimolar concentrations; has been shown to reduce the growth of endometrial cells in humans and, in acute myeloid leukemia, reduces cell proliferation and induces apoptosis (Miller et al., 2003; Yoshida et al., 2003; Marks et al., 2007).

## **1.9 Hydroxamic acids**

This class of inhibitors is very similar for both HDAC class I and class II; they contain the function hydroxamic acid that binds with high affinity to the catalytic residue by HDAC and prevents the substrate access to the zinc ion. The general structure of these molecules consists of a hydrophobic linker that allows the hydroxamic group of chelating the cation on the bottom of the pocket while the rest of the molecule blocks access to the pocket itself. Most of the molecules belonging to this group show a high power, acting on micro and nanomolar doses *in vitro*, but are reversible inhibitors of Class I and II HDAC. Trichostatin (TSA) was one of the first HDAC inhibitors identified and is often used as a reference (Yoshida et al., 2003). It was developed as an antifungal but is relatively unstable; its toxicity and its lack of specificity, however, have led to the search for other molecules. As mentioned previously, the design of many inhibitors, however, was inspired by its structure. The TSA blocks the proliferation and triggers apoptosis in hepatocellular carcinoma cells, blocks the cell cycle in HeLa cells and ovaries cancer cells. Simple hydroxamic acids such as SAHA have shown activity in submicromolar doses. SAHA is a second generation polar-planar compound that induces cell growth arrest, differentiation and/or apoptosis and it is under clinical trial for the treatment of haematological and non-haematological tumors.

## **1.10 Epoxides**

These molecules may act by chemically modification in the nucleophile active site with the epoxy group and forming hydrogen bonds with the ketone; they are likely to block the HDAC through the reaction of the epoxy molecule with zinc or with an amino acid of the active site, forming a covalent bond. The high reactivity of the epoxy group drastically reduces the bioavailability of these molecules and makes them of little interest from the pharmacological point of view. The only inhibitors belonging to this class are a series of natural compounds with an *in vitro* significant activity as the trapoxina (TPX) A and B (Miller et al., 2003; Marks et al., 2007).

## **1.11 Cyclic Peptides**

Cyclic peptides such apidicin, have a molecule of ethylketone, and the depsipeptide inhibit HDAC at nanomolar doses (Miller et al., 2003).

It seems that the apidicin interacts with the catalytic site and inhibits cell proliferation in several cancers. The depsipeptide is a natural product derived from *Chromobacterium violaceum* and shows potent antitumor activity with a mechanism still not well known.

## 1.12 Benzamides

The mechanism of action of this group of inhibitors is unknown but it seems that they inhibit histone deacetylation and cellular proliferation at the level of the transition between G<sub>1</sub> and S phases of the cell cycle. MS275 and some of its derivatives inhibit HDACs in vitro at micromolar doses; it is assumed that the diaminophenyl group is very important for the purposes of its inhibitory activity; probably both amino functions chelate the metal ion in the catalytic site. MS275 induces cell cycle arrest in G<sub>1</sub> increasing the expression of the cyclin-dependent kinase inhibitor (CDKI) p21Waf-1/Cip1. MS275 has demonstrated antiproliferative activity in several human tumor cell lines (lung, breast, colon, leukemia, ovary and pancreas) (Beckers et al., 2007).

## 1.13 Hybrid Compounds

The compounds are composed of semi-synthetic hybrid (Müller et al., 2012) born from the union of cyclic tetrapeptides and hydroxamic acid groups of TSA or SAHA; they can reversibly inhibit HDAC at nanomolar concentrations and showed selectivity of action for HDAC1 and HDAC4.

## 1.14 HDACi mechanism of action

Activation of differentiation programmes, inhibition of the cell cycle and induction of apoptosis are the key antitumor activities of HDACis. These biological effects are due to HDACi-dependent alteration in the acetylation level of histones, transcription factors and other proteins. In fact, the inhibition of HDACs causes the release of these enzymes from transcription factor complexes and the recruitment of HATs which acetylate histones favoring decondensation of chromatin structure and activation of transcription of tumor-suppressor genes or other genes crucial for the normal functioning of cells (Marks et al., 2001). Although histone deacetylation has a fundamental role in regulating gene expression, HDAC inhibitors seem to directly affect transcription of only a relatively small number of genes (2-10%).



Different HDAC inhibitors activate a common set of genes indicating that certain loci are more susceptible to these compounds than others, in particular those that control cell growth and survival (Johnstone, 2002). Moreover, HDAC substrates include also non-histone proteins such as transcription factors (e.g. p53, E2F), signal transduction mediators (e.g. STAT3), DNA repair enzymes (e.g. Ku70), chaperone proteins (e.g. Hsp90), structural proteins ( $\alpha$ -Tubulin), steroid receptors (ER $\alpha$ ). HDACis induce an increase in acetylation level of these proteins affecting their function, stability or protein-protein interaction (Xu et al., 2005; Spange et al., 2009).

In fact, p53 acetylation increases its stability and binding to DNA leading to transcriptional activation of different p53 target genes including pro-apoptotic genes (e.g. *Bax*) (Minucci et al., 2006). Moreover, acetylation in the DNA-binding domains of Ku70 reduces its ability to repair drug-induced DNA damage, thereby sensitizing cancer cells to agents producing DNA double-strand break as radiations. This effect may account for the increase of tumor cell sensitivity to chemotherapy and radiotherapy following HDACi treatment (Minucci et al., 2006). One of the main effects of HDACis is inhibition of the cell cycle which is a necessary event in cellular differentiation. Almost all HDACis activate transcription of the cyclin-dependent kinase (CDK) inhibitor p21/WAF1 encoded by the *CDKN1A* gene inducing acetylation of histones at the level of this locus. However, the induction of p15/INK4b (*CDKN2B*), p16/INK4a (*CDKN2A*) and p27/Kip1 (*CDKN1B*) CDK inhibitors at transcriptional level has also been reported (Marks et al., 2001). The increase in the level of p21/WAF1 or other CDK inhibitors causes hypophosphorylation of retinoblastoma tumor-suppressor protein RB and arrest of cell cycle in G<sub>1</sub> phase (Johnstone, 2002). Analysis of the cell-cycle profiles of tumor cells treated with HDAC inhibitors indicates that the cells often arrest in G<sub>1</sub>, but sometimes accumulate in the G<sub>2</sub> phase of cell cycle. In fact, it has been demonstrated that SAHA at low concentration predominantly induces G<sub>1</sub> arrest, while high concentration induces both G<sub>1</sub> and G<sub>2</sub>/M arrests in bladder carcinoma cell lines (Richon et al., 2000). Furthermore, SAHA has been also reported to inhibit the growth of pancreatic cancer cells and non-small cell lung cancer cells (NSCLC) in a dose-dependent manner inducing G<sub>2</sub>/M cell cycle arrest, apoptosis and differentiation. Most tumor cells that do not arrest in G<sub>1</sub>, after HDACi treatment, replicate their DNA and subsequently arrest in G<sub>2</sub> checkpoint (Johnstone, 2002), (figure 1.10).

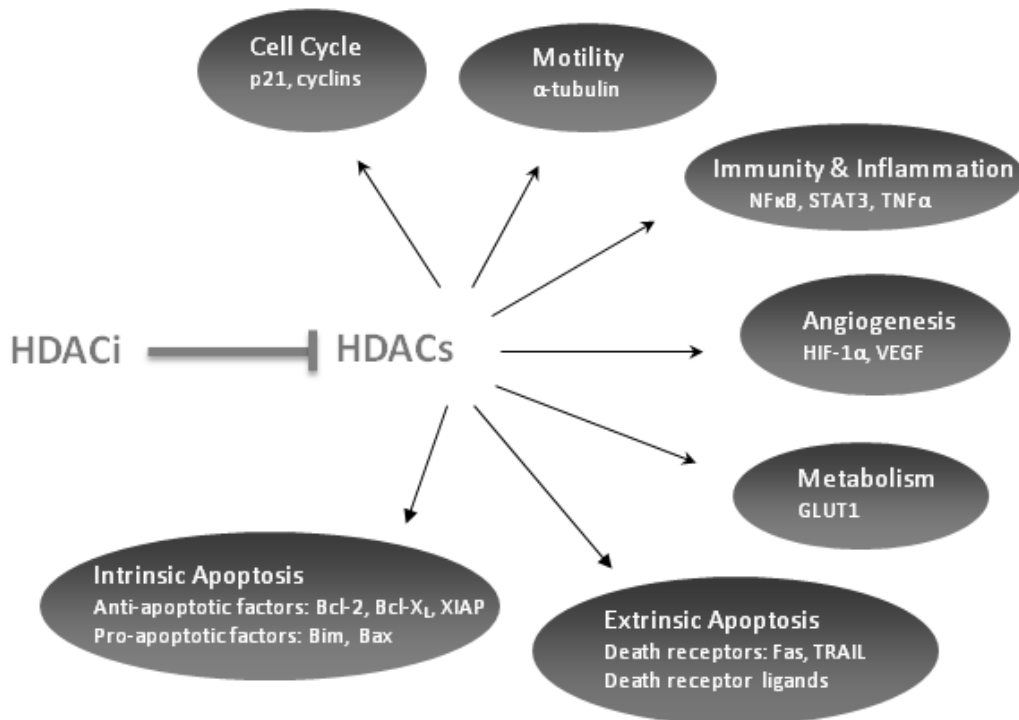


**Figure 1.10.** Multiple HDACi-activated antitumor pathways. HDACi can induce transformed cell growth arrest, terminal differentiation, cell death and/or inhibition of angiogenesis. The cell death pathways identified in mediating HDACi-induced transformed cell death include apoptosis via the intrinsic and extrinsic pathways, mitotic catastrophe/cell death, autophagic cell death, senescence and reactive oxygen species (ROS)-facilitated cell death (<http://www.discoverymedicine.com>).

However, many tumor cell lines accumulating replicated DNA and hyperacetylated histones undergo apoptosis (Johnstone, 2002). In this context, HDACis can induce cell death of tumor cells activating both mitochondrial (intrinsic) and death-receptor (extrinsic) pathways of apoptosis. The pathway activated depends on the cell type and class of HDAC inhibitor used. The intrinsic apoptosis pathway is usually triggered in response to stress conditions such as cytotoxic drugs, UV irradiation, and requires disruption of the mitochondrial membrane by Bcl-2 family pro-apoptotic members Bax and Bak. Following a death stimulus, the cytosolic monomeric Bax translocates to the mitochondria where it becomes an integral membrane protein and oligomerizes giving rise to voltage dependent anion channels which lead to mitochondrial outer membrane permeabilization (Johnstone et al., 2007). This event induces the release from the mitochondria of cytochrome c and other pro-apoptotic factors, such as Smac/DIABLO (Second Mitochondria-derived Activator of Caspases). Cytochrome c binds and activates Apaf-1 which in turn activates caspase-9 starting caspase cascade (Johnstone, 2002).

Smac/DIABLO binds and antagonizes the caspase inhibitors IAPs (inhibitors of apoptosis). Caspases are cysteine aspartate proteases expressed as inactive zymogens (pro-caspase) and proteolytically processed to an active state after an apoptotic stimulus. Initiator caspases (e.g. caspase-2, -8, -9 and -10) cleave inactive pro-forms of effector caspases, thereby activating them. Effector caspases (e.g. caspase-3, -6 and -7), in turn, cleave other protein substrates within the cell, to trigger the apoptotic process. Bcl-2 family also includes pro-apoptotic Bad and Bim, and antiapoptotic Bcl2 and BclxL proteins. Bad and Bim stimulate activation of the intrinsic pathway preventing the antiapoptotic function of Bcl2 and BclxL. HDACis can alter the balance of expression of pro- and anti-apoptotic genes to induce a pro-apoptotic response. Indeed, SAHA causes upregulation of proapoptotic (*Bax and Bim*) and downregulation of antiapoptotic (*IAP, Bcl-2, Bcl-xL*) genes. Different HDACis induce also the cleavage of the pro-apoptotic protein Bid resulting in a C-terminal fragment (tBid) which translocates to mitochondria and induces the oligomerization of Bax and Bak opening the mitochondrial voltage-dependent anion channel (Johnstone et al., 2003). The extrinsic pathway of apoptosis is mediated by death receptors including Fas (Apo-1 or CD95), tumor necrosis factor (TNF) receptor-1 (TNFR-1), TNF-related apoptosis-inducing ligand (TRAIL or Apo2-L) receptors (DR-4 and DR-5). All death receptors are characterized by a cysteine-rich extracellular domain and an intracellular cytoplasmic sequence motif known as the death domain (DD). The binding of Fas-Ligand (Fas-L), TNF $\alpha$  and TRAIL ligands induce trimerization of their receptors and clustering of the receptor DD leading to the recruitment of the adaptor protein FADD (FASAssociated Death Domain-containing protein or MORT1) which interacts with the death domain of the receptors through its own death domain. FADD also contains a death effector domain (DED) near its amino terminus, which facilitates binding to the DED of procaspase-8 and its activation. This complex (receptor-FADD-procaspase-8) of interacting proteins is referred to as the death inducing signalling complex (DISC) (Johnstone et al., 2007). Procaspase-8 is activated by autoproteolytic processing and the resulting active caspase-8 cleaves and activates downstream effector caspases such as caspase-3, -6, and -7. Caspase-8 can also proteolytically activate Bid which can start the mitochondrial pathway amplifying the apoptotic signaling. HDACis can upregulate the expression of both death receptor and their ligands in transformed cells but not in normal cells (Xu et al., 2005). Indeed, it has been reported that Fas and FasL are induced in human neuroblastoma cells by hydroxamates, in nude mice xenograft of human osteosarcoma cells by FK228 and mouse model of acute promyelocytic leukaemia by valproic acid. TRAIL is induced at mRNA level in acute myeloid leukaemia cells by SAHA and MS-275 and both TRAIL and DR5 are

induced in the mouse model of APL by valproic acid. TNF $\alpha$  is upregulated by FK228 in human promyelocytic leukemia cells (Xu et al., 2005). Therefore, extrinsic apoptotic pathway can account for HDACi-induced cell death in many transformed cells.

## **1.15 HDACi and cell cycle inhibition**

As reported previously, the inhibition of HDAC results in the increase of the acetylation levels of histone proteins and other proteins causing a series of events that differ between them according to the spectrum of selectivity of the inhibitor towards the various HDAC based on the cellular context of the tumor. In most cases the antitumor activity is based on the ability to activate programs of differentiation, inhibit the progression of the cell cycle and induce apoptosis. It also seems to be very important the ability to activate the immune response and inhibition of angiogenesis. The acetylation of p53 is increased during cellular stress (Luo et al., 2000), stopping the repression by Mdm-2 (Tang et al., 2008; Palani et al., 2010), increasing the affinity for the DNA (Harms et al., 2007), reducing the ubiquitin-mediated degradation of the transcription factor and increasing the expression of p21 WAF1/Cip1 (Zhao et al., 2006). A number of studies have demonstrated the activation of p53 after the inhibition of HDAC (Zhao et al., 2006; Condorelli et al., 2008). However, some work reported that apoptosis and induction of p21 determined by the inhibition of HDACs can be induced in a p53 independent manner, a remark that this may be clinically relevant for the tumors treatment with p53 mutated (Gui et al., 1999, Saito et al., 1999; Sowa et al., 1999; Peart et al., 2003; Lindemann et al., 2004). The histones hyperacetylation leads the relaxation of chromatin structure and facilitates the expression of several regulatory genes. Treatment with HDAC inhibitors, in fact, causes an increase in the expression of the cyclin-dependent kinase inhibitor p21 WAF1, the repression of genes encoding for cyclins A and D, and the inhibition of thymidylate synthetase, which is involved in DNA synthesis. These events are likely to contribute to the arrest of the cell cycle phases G<sub>1</sub>/S, in particular they increase the levels of p21 WAF1 tumor suppressor, which binds and inhibits the activity of CDK, induce hypophosphorylation of pRb, p107 and p130 proteins, the suppression of cell proliferation and cell-cycle arrest in G<sub>1</sub> phase. In normal cells, the HDACi activate a cell cycle control at the G<sub>2</sub> phase that is missing in many cancer cells; the loss of this control causes aberrant mitoses in cancer cells that lead to death. This block in G<sub>2</sub> phase by treatment with HDACi could be the basis of selective action on tumor cells (Dokmanovic et al., 2005; Drummond et al., 2005).

## 1.16 HDACi and apoptosis

As already discussed, apoptosis, also known as programmed cell death, is a genetically regulated process of fundamental importance for tissue homeostasis and development. Apoptosis is morphologically characterized by the formation of protuberances ("blebs") in the cytoplasmic membrane, cell shrinkage, chromatin condensation, exposure of phosphatidylserine, DNA degradation and cell fractionation in smaller vesicles that are internalized by phagocytic cells (Meech et al., 2001; Cory et al., 2002). Apoptosis is achieved through the activation of cysteine proteases known as caspases (Thornberry et al., 1998), mediated by two "pathway" (extrinsic) mediated by receptor and the mitochondrial pathway (intrinsic) (Johnstone, 2002). The apoptosis pathways are finely regulated at different levels and the dysregulation may be the cause of human diseases including cancer (Rossi et al., 2003; Vermeulen et al., 2005). The correlation between the proper function of HDAC and cell survival has been widely demonstrated; it is known, in fact, as the inactivation of HDAC6 interfere with cell survival by triggering an apoptotic mechanism of cell death (Hideshima et al., 2005). HDAC inhibitors induce apoptosis probably through the activation of different mechanisms. The treatment with these molecules seems primarily able to alter the expression of genes involved in the proapoptotic response; it is in fact increased the transcription of genes such as *TRAIL*, *Fas* and *Bak* and decreased the transcription of genes such as *XIAP* and *bcl-2*. In addition the HDAC inhibitors would also be able to induce apoptosis through the increased production of oxygen radicals. High levels of TBP2 (thioredoxin-binding protein 2), generally low in cancer cells can be the cause of apoptosis. SAHA, HDAC inhibitor, selectively increases the expression of TBP2, which binds and inactivates reduced thioredoxin. This protein is important for the redox reactions of the cell, the action of SAHA increases the sensitivity of the cell to oxidative stress and can cause apoptosis.

## 1.17 HDACi and autophagy

Autophagy, is a process preserved through evolution in which the proteins and cellular organelles are sequestered in autophagosomes and finally degraded after fusion with lysosomes.

Three forms of autophagy have been described: macroautophagy, microautophagy and chaperone-mediated autophagy (figure 1.11) which differ in their physiological functions and transport mode (Reggiori et al., 2002; Wang et al., 2003).

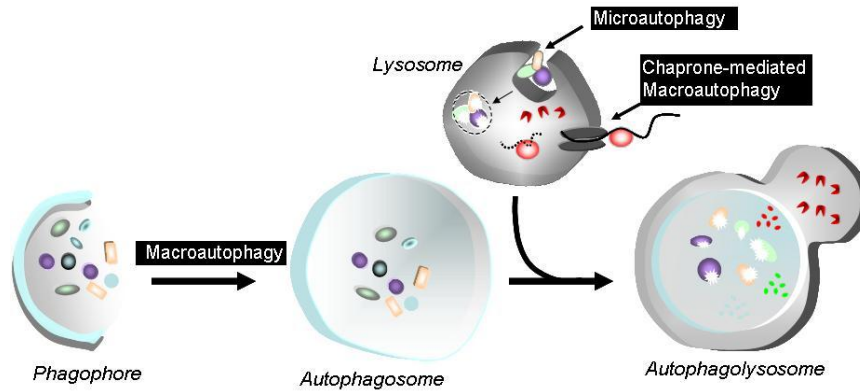


**Figure 1.11.** Three forms of autophagy: macroautophagy, microautophagy and chaperone-mediated autophagy (<http://www.autophagy.lu>).

The double cell membrane invaginates, melts, forming a vesicle, called autophagosome, which fuses with the lysosome, an acid organelle, forming the autolysosome (figure 1.12). The lysosomal acid hydrolases degrade the components in their elementary forms (free nucleotides, fatty acids, amino acids) that can be used to recover ATP and other molecules critical for the biosynthetic pathway in hypoxia or nutrient depletion conditions. (Noda et al., 1998; Levine et al., 2004; Carew et al., 2010).

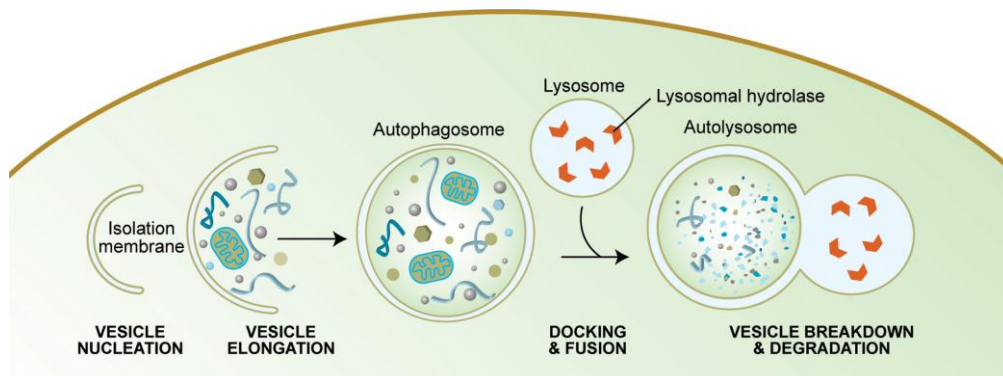


**Figure 1.12.** Schematic diagram of the cellular events during autophagy (<http://www.wormbook.org>).

Autophagy involves a complex "pathway" of cellular events characterized by different proteins. One of the key proteins in the autophagy regulation is TOR kinase that inhibits the autophagic process in the presence of growth factors and abundant nutrients (Noda et al., 1998). Although p53 can positively regulate autophagy through a stress induced protein known as DRAM (Damage-Regulated Autophagy Modulator); a p53 target gene (Crighton et al., 2006).

TOR regulates more than 30 genes called "autophagy-related" which encode for proteins essential for the autophagy (Klionsky et al., 2003), including beclin 1 and LC3, which is used in the laboratory to monitor the autophagy process. This protein can be in two forms: LC3-I and LC3-II. The form LC3-I is predominant in normal cell and diffuse into the cell; when autophagy is induced, LC3-I is cleaved in the form LC3-II (Tanida et al., 2004 a and 2004 b) and inserted in the membrane of the autophagosome (Kabeya et al. 2000). It was shown as HDACs are required for autophagy, in particularly for the fusion of lysosomes with autophagosomes (Iwata et al., 2005). The role of autophagy in cancer and its potential interest as a therapeutic target are still controversial. There are experimental evidences that support the theory that autophagy acts as a tumor suppressor gene and therefore could be stimulated to reduce the occurrence of breast cancer (Liang et al., 1999, Qu et al., 2003; Karantza et al., 2007; Mathew et al., 2007). However, there are other experimental evidence showing as the survivor effects induced by autophagy may actually help the cancer cells to proliferate, especially in stressful conditions such as high proliferative rate, the hypoxic conditions in solid tumors and the lack of nutrients in the metastatic conditions (Paglin et al., 2001; Abedin et al., 2007; Apel et al., 2008; Qadir et al., 2008; Samaddar et al., 2008).

### **1.18 Effects of HDAC on cell motility and angiogenesis**

Cell motility plays a crucial role in tumor metastasis. The studies on this matter reveal that overexpression of HDAC6 increases the motility. (Hubbert et al., 2002). Another aspect related to tumor development is the angiogenesis. In tumors the formation of new blood vessels can be realized from a preexisting vascular thanks to the recruitment of circulating cells such as endothelial progenitor cells derived from bone marrow, macrophages and fibroblasts (Adams et al., 2007; Kerbel, 2008). These cells together with the malignant cytotypes are capable to secrete proangiogenic factors including vascular endothelial growth factor (VEGF) produced by induction of the transcription factor hypoxia inducible factor 1 alpha (HIF-1alpha), which induces the formation of new blood vessels (Kim et al., 2001). It was shown that the hypoxic conditions regulate the function of HDACs both directly and indirectly (Kim et al., 2001; Mahon et al., 2001). Specifically it has been shown that hypoxic conditions in different cell lines in vitro, increase the expression of mRNA for HDAC1, HDAC2 and HDAC3 and other proteins (Kim et al., 2001). In addition, overexpression of HDAC1 average the reduced expression of p53 and pVHL that induces the overexpression of HIF-1  $\alpha$  and its target transcriptional VEGF, that situation is reversed when using the histone

deacetylase inhibitor trichostatin A (TSA) both in vitro and in vivo (Kim et al., 2001). The condition by which the reduction in the expression of p53 and pVHL in turn helps to reduce the expression of the inhibitory factor HIF-1  $\alpha$ , thus allowing the induction of angiogenesis in endothelial cells has also been described (Mahon et al., 2001). These results clearly demonstrate that the HDACs indirectly regulate the activity of HIF-1  $\alpha$  in hypoxic conditions. But the HDACs also act directly on HIF-1  $\alpha$  to regulate its activity. It has been shown, for example, that HDAC1 and HDAC3 directly regulate the stability and transcriptional activity of HIF-1  $\alpha$  through the interaction with the oxygen-dependent degradation domain (ODDD) of HIF-1  $\alpha$  (Kim et al., 2007). These studies demonstrate that the HDACs play a critical role in angiogenesis induced by hypoxia and they represents a new strategy in cancer therapy through they ability to inhibit angiogenesis itself. At present there are numerous preclinical and clinical studies that confirm an anti-angiogenic role of HDACi in the treatment of multiple cancers.

## **1.19 Therapeutic uses of HDACis**

HDACis mediate a number of molecular changes within cancer cells. These changes in gene expression or protein activity and stability can lead to cells that arrest during the cell cycle, apoptose or differentiate. Recent research has also shown that the HDACis can decrease angiogenesis in some tumors by inhibiting hypoxia-inducible factor 1 alpha activity, suggesting additional pathways by which the HDACi can be effective at decreasing tumorigenesis (Kim et al., 2007; Qian et al., 2006). In cancers that poorly respond to chemotherapy, treatment with HDACis can increase the sensitivity of the cancer cells to other drugs and treatments such as radiotherapy (Munshi et al., 2005; Hahn et al., 2008). Combination of retinoic acid and HDACi therapy has shown promise in cell culture models of acute promyelocytic leukemia (APL). In APL, a chromosomal translocation produces the fusion protein PML-RARalpha which aberrantly retains deacetylases and the methyl-CpG-binding protein 1 (MBD1) at the promoters of retinoic acid-responsive genes, thus inhibiting normal differentiation of these cells (Fenrick et al., 1998; Villa et al., 2006). Inhibiting HDAC activity, or that of DNA methyltransferases, in combination with providing an excess of retinoic acid, relieves this repression and allows differentiation to proceed (Fenrick et al., 1998; Villa et al., 2006). Interestingly, the treatment of cells with HDAC inhibitors also indirectly causes proteasomal degradation of the PML-RARalpha fusion protein (Kramer et al., 2008). The HDACi currently used in clinical trials inhibit Class I and II zinc-dependent HDACs.



Little is known about how the HDACs mediate these effects preferentially over non-cancerous cells. In addition, it is unclear which HDACs are necessary to mediate these anticancer effects. The loss of HDAC2 protein was reported in some colon cancer and endometrial cell lines and interestingly, this renders the colon cancer cells resistant to TSA (Ropero et al., 2006). RNAi experiments that knock-down individual HDACs showed that HDACs 1, 3 and 8 were all independently important for cancer cell growth, as knock down of any one was sufficient to inhibit growth in specific cancer cell types (Glaser et al., 2003; Vannini et al., 2004). These findings suggest that HDAC-specific inhibitors could be effective in some cancers, though it is not clear if they would be as effective as the inhibitors that target multiple HDACs. The current HDACis which are showing promise in multiple tumor types are not without toxic side effects. It will be important to determine which HDACs need to be inhibited in specific cancer types in order to obtain the maximum effectiveness of the drugs while at the same time minimizing the unwanted toxicity and off-target side effects of these drugs.

## **2. Aim of the research**

The histone deacetylase inhibitors (HDACis) are an emerging class of chemically heterogeneous anticancer agents, which restore a relaxed, hyperacetylated, chromatin structure potentially leading to re-expression of silenced genes and/or silencing of downstream genes, ultimately inducing death, apoptosis, and cell cycle arrest in cancer cells also via nonhistone-targeted mechanisms such as perturbations of p53, cytokine signaling pathways, and angiogenesis (Dickinson et al., 2010; Kim et al., 2011). HDACis are grouped in different categories on the basis of their chemical nature, and the implication of this molecular diversity is that the precise mechanism through which these compounds work is still poorly understood. Suberoylanilide hydroxamic acid (SAHA), is a prototypical HDACi targeting class I and II HDAC approved in 2006 by the Food and Drug Administration for treatment of cutaneous T cell lymphoma, (Mann et al., 2007) which has been subjected to several manipulations of the core structure to probe the effect of such modifications on both HDAC inhibitory activity and cytotoxic effect on cancer cells. Some Authors (Spencer et al., 2011) have recently reported the synthesis of metal-based SAHA analogues incorporating a ferrocene unit, e.g. Jay Amin hydroxamic acid (JAHA) and homo-JAHA. JAHA if compared with parental SAHA, displayed similar broad inhibitory profiles toward class I HDACs, including HDAC8, although homo-JAHA was less potent toward HDAC6 and more effective toward HDAC8, whereas none of them was active on class IIa HDACs. The ability of these compounds to restrain the growth of the estrogen receptor-positive, low malignant, MCF-7 breast tumor cells prompted us to extend the investigation to other neoplastic cell lines, more representative of breast cancer histotypes with poor outcome, and also to get more insight into the molecular mechanism of the cytotoxic induction. Triple-negative breast cancers lack expression of estrogen and progesterone receptors and are human epidermal growth factor receptor 2 (HER2)/neu negative, thereby being poorly responsive to hormonal therapies and to HER2-targeting drugs and usually associated with worse prognosis than other breast tumor types (Kassam et al., 2009). For these reason the present work was aimed to evaluate the possibility of an innovative therapy for triple-negative breast cancer based on HDACis, investigating the effects and mechanisms of action of novel metal-based SAHA analogues on an in vitro model system of triple-negative human breast cancer, i.e. MDA-MB231 cells. The realization of this project was made possible thanks to the collaboration with Dr. John Spencer of the School of Science, University of Sussex, UK, who provided us with two newly-synthesized derivatives of SAHA, i.e. JAHA and homo-JAHA (figure 2.1). JAHA (N<sup>1</sup>-

(ferrocenyl)-N<sup>8</sup>-hydroxyoctanediamide) is an organometallic analogue of SAHA containing a ferrocene group consisting of two cyclopentadienyl rings bound on opposite sides of a central metal atom. The incorporation of protein ligands in organometallic parts provides the possibility of a better integration in space and ensures a better affinity that could not be obtained with rather simple planar aromatic groups or alicyclic rings (Meggers, 2009).

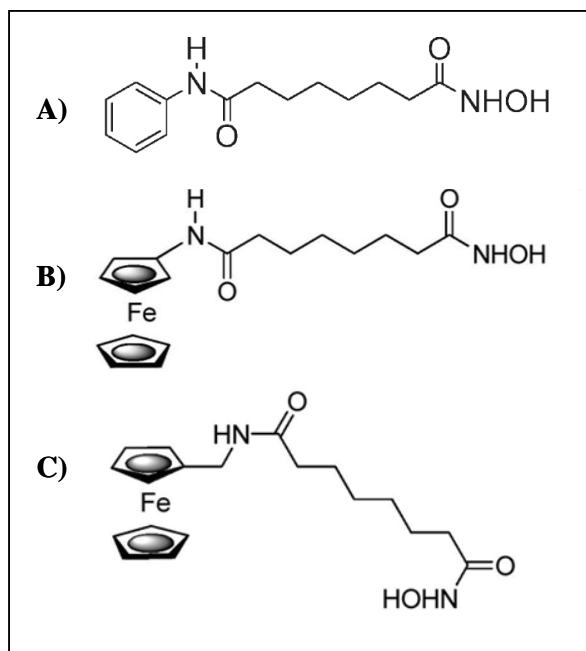


**Figure 2.1.** Chemical structures of the compounds which have been examined in this study. (A) Suberoylanilide hydroxamic acid (SAHA),  $C_{14}H_{20}N_2O_3$ , molecular weight 264.3202. (B) JAHA,  $C_{18}H_{24}FeN_2O_3$ , molecular weight 372.2398. (C) Homo-JAHA,  $C_{19}H_{26}FeN_2O_3$ , molecular weight 396.35. JAHA and Homo-JAHA were provided by courtesy of Dr. John Spencer, University of Sussex, UK (Spencer et al., 2011).

JAHA is able to bind the enzyme in a similar manner to SAHA, using the interactions between the hydroxyamate and the zinc of the catalytic site, with a hydrogen bond between the amide portion of the ligand and the Asp 10. The ferrocenyl group of JAHA easily fits into the pocket defined by the amino acids Tyr100, Phe152, and Tyr306 (figure 2.2); this region of the enzyme is considered malleable and able to adapt the structures of different ligands. The homologous homo-JAHA was synthesized to evaluate the effect of the introduction of a methylene group as a spacer in JAHA (Spencer et al., 2011).

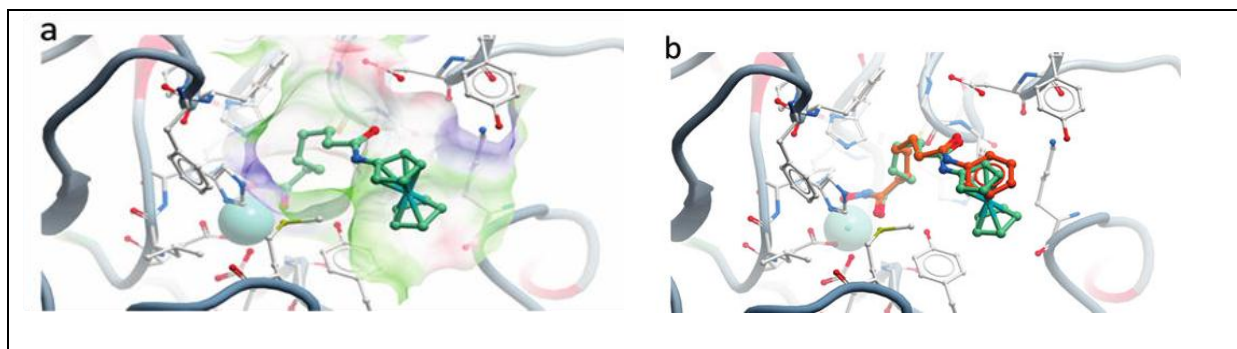


**Figure 2.2.** Model of JAHA binding to HDAC8 (a) and comparison between JAHA and SAHA (b) (Spencer et al., 2011). The zinc ion is colored in cyan. The residues in the binding pocket are represented according to the models "ball and stick". In blue the nitrogen, oxygen in red, carbon in grey; JAHA is represented in green and SAHA in orange.

Because so far little is known about the biological role of these compounds in experimental models "in vitro", the purpose of this research is therefore to estimate the effects related to the use of homo-JAHA and JAHA at different concentrations and at different times on MDA-MB231 cells, considering first the survival dose-dependent time, calculating the  $IC_{50}$  by MTT and performing biological and molecular assay to evaluate the cytotoxic effect of this compounds on MDA-MB231 breast cancer cells.

## 3. Materials and Methods

### 3.1 Materials

#### 3.1.1 Chemicals

Acetic Acid	Carlo Erba Reagenti, Rodano, Italy
Acrilamide solution	Sigma-Aldrich, Steinheim, Germany
Acrylamide-bisacrylamide (29:1 ratio)	FISHER Molec. Biology, Trevose, USA
Agarose	Sigma-Aldrich, Steinheim, Germany
AgNO <sub>3</sub>	Sigma-Aldrich, Steinheim, Germany
APS	Sigma-Aldrich, Steinheim, Germany
β-mercaptoethanol	Invitrogen, Paisley, UK
Boric acid	Carlo Erba Reagenti, Rodano, Italy
Bromophenol blue	Sigma-Aldrich, St. Louis, USA
Butylated hydroxytoluene	Sigma-Aldrich, St. Louis, USA
Chloroform	Sigma-Aldrich, St. Louis, USA
Coomassie Blue	Sigma-Aldrich, St. Louis, USA
DEPC treated water	Invitrogen, Paisley, UK
DMSO	Sigma-Aldrich, St. Louis, USA
DNA Loading Dye 6X	Invitrogen, Paisley, UK
DTT	Thermo Scientific, Waltham, MA, USA
EDTA	Santa Cruz, Heidelberg, Germany
EGTA	Santa Cruz, Heidelberg, Germany
Ethanol 96%	Carlo Erba Reagenti, Rodano, Italy
Ethanol absolute	Carlo Erba Reagenti, Rodano, Italy
Ethidium bromide	Sigma-Aldrich, St. Louis, USA

Formaldehyde 37%	Promega, Madison, USA
Formic acid	Thermo Scientific, Waltham, MA, USA
Glycerol	Sigma-Aldrich, St. Louis, USA
Glycine	Invitrogen, Paisley, UK
HCl	Carlo Erba Reagenti, Rodano, Italy
Hydroxyurea	Sigma-Aldrich, St. Louis, USA
Iodoacetamide	Appli Chem, St. Louis, Missouri, USA
IPG Buffer	GE Healthcare Life Sciences, Milan, Italy
Isopropanol	Sigma-Aldrich, St. Louis, USA
LiCl	Invitrogen, Paisley, UK
Methanol	Sigma-Aldrich, St. Louis, USA
NaCl	Sigma-Aldrich, St. Louis, USA
Na <sub>2</sub> CO <sub>3</sub>	Riede-de Haen GmbH, Seelze, Germany
N, N-methylene bis-acrilamide solution	Sigma-Aldrich, St. Louis, USA
Non-fat dry milk	Euroclone, Milan, Italy
PMSF	Sigma-Aldrich, St. Louis, USA
SDS	Sigma-Aldrich, St. Louis, USA
Silanization solution	Fluka Chemie AG, Buchs, Switzerland
Sodium thiosulfate	Sigma-Aldrich, St. Louis, USA
TEMED	Sigma-Aldrich, St. Louis, USA
Terminator™ 5'-Phosphate-Dep. Exonuclease	Epicentre, Madison, USA
Trichloroacetic acid	Sigma-Aldrich, St. Louis, USA
Trifluoroacetic acid	Sigma-Aldrich, St. Louis, USA
Triton X-100	Sigma-Aldrich, St. Louis, USA
Trizma base	Sigma-Aldrich, St. Louis, USA
Tween 20	Sigma-Aldrich, St. Louis, USA

Urea	Invitrogen, Paisley, UK
$\lambda$ -Methacryloxypropyltri-methoxy-silane	Sigma-Aldrich, St. Louis, USA
<b>3.1.2 Consumables</b>	
Afa I	Invitrogen, Carlsbad, CA
Alkaline phosphatase-conjugated antibody	Promega, Madison, WI
Amphotericin B	Invitrogen, Carlsbad, CA
AnnexinV kit	Miltenyi Biotec, Bologna, Italy
Anti-AKT antibody	Cell Signaling Beverly, USA
Antibiotic/antimycotic	Gibco, Invitrogen, Paisley, UK
Anti-actin antibody	Sigma-Aldrich, St. Louis, USA
Anti-Erk1/2 antibody	Abcam, Cambridge, UK
Anti-DNMT1 antibody	Sigma-Aldrich, St. Louis, USA
Anti-IgG HRP antibody	GE Healthcare Life Sciences, Milan, Italy
Anti-LC3 antibody	Sigma-Aldrich, St. Louis, USA
Anti-p-AKT antibody	Santa Cruz, Heidelberg, Germany
Anti- p-Erk1/2 antibody	Cell Signaling Beverly, USA
Anti-p62/SQSTM1 antibody	Sigma-Aldrich, St. Louis, USA
Bafilomycin A1	Enzo Life Sciences, Lausen, Switzerland
BCA assay kit	Thermo Scientific, USA
BCIP/NTB Liquid Substrate System	Invitrogen, Paisley, UK
Bradford assay	Bio-Rad, Milan, Italy
BSA	Sigma-Aldrich, St. Louis, USA
DNA ladder 100 bp	Invitrogen, Paisley, UK
DNA ladder 50 bp	Invitrogen, Paisley, UK
dNTPs (100 mM)	Invitrogen, Paisley, UK

ExoSAP-IT kit	Affymatrix, Wycombe, UK
FBS	Gibco, Invitrogen, Paisley, UK
Fluorescent dye JC1	Invitrogen, Carlsbad, CA
GelRed	Biotium, Hayward, USA
HpaII	New England BioLabs, Ipswich, USA
Montage PCR centrifugal PCR purification filter	Millipore Corporation, Bedford, USA
Nitrocellulose Membrane	Hybond C, Amersham
Penicillin/Streptomycin (10 mg ml <sup>-1</sup> )	Invitrogen, Carlsbad, CA
PBS	Gibco, Invitrogen, Carlsbad, CA
Power SYBR Green PCR Master Mix	Applied Biosystems Philadelphia, USA
Propidium iodide	Invitrogen, Carlsbad, CA
Protease Inhibitor Cocktail	Sigma-Aldrich, St. Louis, USA
PureLink Genomic DNA kit	Invitrogen, Paisley, UK
Rapamycin	Santa Cruz Biotechnology, CA
RPMI	Gibco, Invitrogen, Paisley, UK
Random primers	Gibco, Invitrogen, Paisley, UK
REDTaq DNA Polymerase 0,05 U/μl	Sigma-Aldrich, St. Louis, USA
Ribonuclease H (2U/μl)	Invitrogen, Paisley, UK
Ribonuclease inhibitor	Invitrogen, Paisley, UK
RNase A	Invitrogen, Carlsbad, CA
Stoffel Kit for DD-PCR	Applied Biosystems Philadelphia, USA
SuperScript II Reverse Transcriptase 200 U/μl	Invitrogen, Paisley, UK
Taq DNA polymerase recombinant	Invitrogen, Carlsbad, CA
Thiazolyl Blue Tetrazolium Bromide	Sigma-Aldrich, St. Louis, USA
Total ROS/ Superoxide Detection Kit	Enzo Life Sciences, Lausen, Switzerland
Trypsin	Promega, Madison, WI



Trypsin-EDTA (0,05%)	Gibco, Invitrogen, Paisley, UK
TRI REAGENT	Sigma-Aldrich, St. Louis, USA
Western ImmunStar™ C™ Substrate Kit	Bio-Rad, Hercules, USA

### 3.1.3 Equipment

Balance	Gibertini Elettronica s.r.l., Novate, Italy
Burker counting chamber	Fortuna, Germany
Centrifuge Rotofix 32	Hettich Lab Technology, Tuttlingen
ChemiDoc System	Bio-Rad, Hercules, USA
CO <sub>2</sub> incubator	Sanyo Electric, Japan
FACSCanto apparatus	Biosciences, Franklin Lakes, NJ
Gel Chamber	Elettrofor, Borsea (Ro), Italy
Gel electrophoresis power supply	Elettrofor, Borsea (Ro), Italy
Glass plates Sequi-Gel	BioRad, Hercules, USA
Heater and magnetic stirrer	ALC International, Milan, Italy
Laminar flow cabinet, biowizard	Bicasa Spa, Bernareggio, Milan, Italy
Luminometre Multi Detection System	Promega, Milan, Italy
Nano-Acquity (Waters) LC system and Orbitrap Velos mass spectrometer	Thermo Electron Corp., San Jose, CA
Nanodrop spectrophotometer	Thermo Scientific, USA
Novablot equipment	Pharmacia, USA
pH meter	Crison Instrumentes, Barcelona, Spain
Phase contrast microscopy	Carl Zeiss, Oberkochen, Germany
Real Time PCR system 7300	Applied Biosystems, Almeida, USA g
Sequencing service	BMR Genomics Padova, Italy
Sonicator	Sonics & Materials, Newtown, USA

Spectrophotometer, DU-730	Beckman Coulter, Milan, Italy
Thermal Cycler	TECHNE, Bibby Scientific, Milan, Italy
Thermocycler T1 Plus	Biometria, Gottingen, Germany
Transilluminator Ultra-violet products	Cambrige, UK
Vortexer, Autovortex	Stuart Scientific, Redhill, UK
Water bath	Elettrofor, Borsea (Ro), Italy

### 3.1.4 Buffers and Solutions

All solution were prepared with ultrapure water:

Developing solution	3% Na <sub>2</sub> CO <sub>3</sub> , 200 µl Sodium thiosulfate (10 mg/ml), 1.5 ml Formaldehyde 37%
Fix stop solution	CH <sub>3</sub> COOH 10%
Lysis buffer	7 M Urea, 2 % CHAMPS, 1% IPG Buffer, 10 mM DTT, PMSF protease and phosphatases inhibitor cocktail 1X
Running buffer	Tris 0.6%, Glycine 2.88%, SDS 0.1%
Sample buffer	0.5 M Tris-HCl 12.5%, pH 6.8, 2% SDS, 10% glycerol, 5% β-mercaptoethanol, bromophenol blue 0.05%
Staining solution	0.1% AgNO <sub>3</sub> , 1.5 ml, Formaldehyde 37%
Stripping buffer	1 M Tris HCl pH 6.8, SDS 10%, β-mercaptoethanol 50 mM
TBE 10X	89 mM Tris-borate, 2 mM EDTA pH 8.3
TBS	NaCl 150 mM, Tris-HCl pH 7.4 100 mM

TBS-T	NaCl 150 mM, Tris-HCl pH 7.4 100 mM Tween-20 0.05%
Transfer buffer	Tris 0.29%, Glycine 1.44%, Methanol 20%

## 3.2 Methods

### 3.2.1 HDACis

JAHA and Homo-JAHA were synthesized as reported by Spencer et al., (2011) and dissolved at 6.5 mM concentration in dimethyl sulfoxide (DMSO) JAHA and Homo-JAHA, and SAHA at 3.8 mM as stock solutions.

### 3.2.2 Cell cultures and viability assay

MDA-MB231 breast tumor cells were maintained in RPMI 1640 medium plus 10% fetal bovine serum (FBS), 100 U/ml penicillin, 100 µg/ml streptomycin, and 2.5 mg/l amphotericin B (Invitrogen, Carlsbad, CA), at 37°C in a 5% CO<sub>2</sub> atmosphere. The cells were detached from flasks with 0.05% trypsin-EDTA, counted, and plated at the necessary density for treatment after achieving 60–80% confluency.

The assessment of in vitro cytotoxic activity was determined by an 3-(4,5-dimethylthiazol-2-yl)-2,5-diphenyltetrazolium bromide (MTT) assay (<http://www.molmeth.org/protocols/1VB7RPF>). Briefly, MDA-MB231 cells in exponential growth were plated at a concentration of 5500 cells/well in a 96-well plate and allowed to adhere overnight. Then, the cells were treated with 0.1, 1, 10, and 100 µM concentration of either drug or with the vehicle (DMSO) for 24, 48, and 72 h and observed under the phase-contrast microscope before processing for the viability assay. Different amounts of DMSO, equivalent to those diluting the drugs in the parallel experiments, were added to cells in the conditions of vehicle-only treatment. Fifteen microliters of MTT (final concentration, 0.75 mg/ml) was then added, and after incubation, 100 µl of SDS-containing solubilization buffer replaced the MTT-containing culture medium and dissolved the precipitated violet formazan crystals within metabolically viable cells. Absorbance of the dissolved dye was measured in an automated microplate reader at 550 nm. The cell viability ratio was determined as the ratio between treated cells and untreated controls. IC<sub>50</sub> was calculated with Prism 5.0 software (GraphPad, La Jolla, CA).

### 3.2.3 Apoptosis Assay

The possible onset of apoptosis was evaluated using the Annexin V-fluorescein isothiocyanate (FITC) kit (Miltenyi Biotec GmbH, Bergisch Gladbach, Germany) according to manufacturer's instructions. Briefly, plated cells were treated with 8.45  $\mu$ M JAHA for 5, 24, and 48 h. Then, attached and floating cells were collected and resuspended in 100  $\mu$ l of binding buffer  $1 \times 10^6$  cells, and 10  $\mu$ l of FITC-annexin V was added. After centrifugation and resuspension in 500  $\mu$ l of binding buffer 1X, propidium iodide was added immediately prior to flow cytometric analysis in a FACSCanto apparatus (BD Biosciences, Franklin Lakes, NJ). Data were represented as dot plots using Flowing software v.1.6.0., which discriminated normal cells (bottom left quadrant) from cells in early apoptosis (bottom right quadrant), cells in late apoptosis or early necrosis (top right quadrant), or cells undergoing necrosis (top left quadrant). Vehicle-treated cells were tested as parallel controls.

### 3.2.4 Cell Cycle Analysis

MDA-MB231 cells were seeded in six-well plates at a concentration of 88000 cells/well and allowed to adhere overnight and then treated with 8.45  $\mu$ M JAHA and harvested after 24 and 48 h of incubation. Cells were resuspended in 0.5% Triton X-100 in phosphate-buffered saline containing 0.5  $\mu$ g/ml RNase A, incubated at 37°C for 30 min, and then treated with propidium iodide at 4°C for 30 min in the dark. The cell cycle distribution was analyzed by flow cytometry in a FACSCanto apparatus and Weasel 3.0.1 software. Vehicle-treated cells were tested as parallel controls.

### 3.2.5 Evaluation of ROS Production

The production of ROS, such as hydrogen peroxide, peroxynitrite, hydroxyl radicals, nitric oxide, and peroxy radical, and of superoxide was checked using the Total ROS/Superoxide Detection Kit (Enzo Life Sciences, Lausen, Switzerland) according to the manufacturer's instructions. Briefly, attached and floating MDA-MB231 cells treated with 8.45  $\mu$ M JAHA were harvested after 24 and 48 h of incubation and resuspended in 500  $\mu$ l of ROS/Superoxide Detection Mix and incubated for 30 min at 37°C in the dark prior to flow cytometry assay for the green and orange fluorescence in a FACSCanto apparatus. Vehicle-treated cells were tested as parallel controls.

Positive (pyocyanin-treated) and negative (N-acetyl-L-cysteine-treated) controls were included in the analysis, and data were represented as dot plots using Flowing software v.1.6.0., which discriminate cells with increased total ROS production (top left quadrant), increased superoxide production (bottom right quadrant), and increased total ROS and superoxide production (top right quadrant). To assess the involvement of ROS production in the cytotoxic effect of JAHA, an MTT assay was performed as already reported on JAHA-treated cells incubated for 24 h in the presence of the antioxidant butylated hydroxytoluene (BHT) at 5, 10, 25, and 50  $\mu$ M final concentration.

### **3.2.6 Mitochondrial Membrane Potential (MMP) Assay**

Control and JAHA-treated cell preparations were stained with the fluorescent dye JC1 (Invitrogen) according to Cannino et al., (2008) and MMP was then checked by flow cytometry, according to Cossarizza and Salvioli, (2001). Essentially, control and JAHA-treated MDA-MB231 cells, both attached and floating, harvested after 24 and 48 h from treatment, were stained with JC1 (final concentration, 2.5  $\mu$ g/ml) for 10 min at 37°C, washed with phosphate-buffered saline (PBS), and analyzed for the green and orange fluorescence in a FACSCanto apparatus. Data were represented as dot plots using Flowing software v.1.6.0., which discriminate in the bottom quadrants the amount of cells that undergo loss of MMP.

### **3.2.7 Autophagy Assays**

AVOs, which are a hallmark of autophagy, were quantified by flow cytometry as reported by Jiang et al., (2009) and Chen et al., (2010). Essentially, control and JAHA-treated MDA-MB231 cells, both attached and floating, were harvested after 24 and 48 h of incubation and stained with acridine orange (final concentration, 100  $\mu$ g/ml) for 20 min in the dark and then analyzed in a FACSCanto flow cytometer. Data were represented as dot plots using Flowing software v.1.6.0., which discriminate cells with increased AVO accumulation in the top quadrants. In a parallel set of assays, as a negative control, untreated cells were incubated with bafilomycin A1 (Enzo Life Sciences), a macrolide antibiotic that inhibits the vacuolar type H<sup>+</sup>-ATPase of AVOs, at 200 nM final concentration for 30 min before acridine orange staining. To confirm this result JAHA-treated MDA-MB231 cells were incubated for 48 h with 1 nM rapamycin (Santa Cruz Biotechnology, CA), an antibiotic that increases autophagosome and autolysosome formation, and the reversion of JAHA-triggered cytotoxic

effect was monitored by an MTT assay, as previously reported. Control cells were tested in parallel.

### 3.2.8 Migration Assay

MDA-MB231 cells were plated on four 22 cm<sup>2</sup> culture plates at a concentration of 450.000 cells/cm<sup>2</sup>. After 24 hours of incubation at 37°C the culture plate was confluent. The cells were then washed with 1X PBS and scraped in the middle of the plate with the scratch machine thereby creating an artificial "wound" or denuded area, parallel to a straight line drawn with a permanent marker at the bottom of the culture dish. This created a "dark line area", useful to simplify motile cell evaluation, which was visible as a translucent, dark background under the microscope. Then, the PBS was removed and the appropriate medium was added to a volume of 5 ml. Experimental media were:

1. RPMI 1640;
2. RPMI 1640 supplemented with JAHA (RPMI 1640/JAHA) to a final concentration of 8.45 µM;
3. RPMI 1640 supplemented with hydroxyurea (RPMI 1640/H) to a final concentration of 2 mM;
4. RPMI 1640 supplemented with hydroxyurea to a final concentration of 2 mM and JAHA to a final concentration of 8.45 µM (RPMI 1640/H/JAHA).

MDA-MB231 cells were grown for 24 h, and at the end each five different areas of the plate were observed to determine the mean value and standard deviation of migrated cells into the denuded area. Pictures were taken with an AuxioCam MRc camera, which was connected to the microscope. RPMI 1640 was used as a negative control and reference value for the migration of cells treated with JAHA. The same media supplemented with 2 mM hydroxyurea, utilized to inhibit cell proliferation, were used to compare the obtained values to a cell growth-independent reference. Each set of experiment was performed in triplicate.

### 3.2.9 Total RNA Isolation

1x10<sup>6</sup> MDA-MB231 breast cancer cells were plated in 75 cm<sup>2</sup> flask and cultured in control conditions or with either JAHA or SAHA at 8.45 µM concentration for 18, 24 and 48 hours. RNA was extracted with TRI Reagent (Sigma). TRI Reagent is a quick and convenient reagent for use in the simultaneous isolation of RNA, DNA, and protein.

A single-step liquid phase separation results in the simultaneous isolation of RNA, DNA, and protein. This procedure is an improvement of the method reported by Chomczynski and Sacchi, (1987) for total RNA isolation. This product, a mixture of guanidine thiocyanate and phenol in a monophasic solution, effectively dissolves DNA, RNA, and protein on homogenization or lysis of tissue sample. Cells were isolated by centrifugation and then lysed in 1 ml of TRI Reagent by repeated pipetting (1 ml of the reagent is sufficient to lyse  $5 \times 10^6$  animal, plant, or yeast cells, or  $10^7$  bacterial cells). To ensure complete dissociation of nucleoprotein complexes, the samples were allowed to stand for 5 minutes at room temperature. After addition of 0.2 ml of chloroform per ml of TRI Reagent used, the samples were covered tightly, shaken vigorously for 15 seconds, and allowed to stand for 2-15 minutes at room temperature. The resulting mixture was centrifuged at 12,000 g for 15 minutes at 2-8°C. The centrifugation separates the mixture into 3 phases: a red organic phase (containing protein), an interphase (containing DNA), and a colorless upper aqueous phase (containing RNA). The aqueous phase was transferred into a fresh tube, 0.5 ml of 2-propanol per ml of TRI Reagent used in sample preparation was added and the sample was to stand for 5-10 minutes at room temperature, before centrifugation at 12,000 g for 10 minutes at 2-8°C. After removal of the supernatant, the RNA precipitate was washed by adding a minimum of 1 ml of 75% ethanol per 1 ml of TRI Reagent used in sample preparation, vortexing and then centrifuging at 7,500 g for 5 minutes at 2-8°C. The RNA pellet was dried for 5-10 minutes under a vacuum and finally an appropriate volume of RNase-free water (40 µl) was added and the RNA was solved by repeated up and down pipetting. The obtained RNA was quantified with a Nanodrop spectrophotometer (Thermo Scientific, USA) reading at  $\lambda=260$  nm and its purity determined from the ratio of readings at 260 and 280 nm respectively, and then was stored at -80°C until use. mRNA-enriched samples from total RNA preparations were obtained using Terminator™ 5'-Phosphate-Dependent Exonuclease, a processive 5'→3' exonuclease that digests RNA having a 5' monophosphate and is ineffective on RNA having a 5'-triphosphate, 5'-cap, or 5'-hydroxyl group. These enzymatic properties make Terminator Exonuclease ideal for producing mRNA-enriched samples from both eukaryotic and prokaryotic total RNA preparations by selectively digesting the ribosomal RNA (rRNA).

In a sterile (RNase-free) 0.5 ml tube, the following reaction components were mixed in ice:

- X µl RNase-free water
- 2 µl Terminator 10X Reaction Buffer A
- 0.5 µl RNase Inhibitor

- X µl total RNA sample (200 ng - 10 µg)
- 1 µl Terminator Exonuclease (1 U)

20 µl was the total reaction volume. The reaction was incubated at 30°C for 60 minutes in a thermocycler (with heated lid) and terminated with the addition of 1 µl of 100 mM EDTA (pH 8.0). The enriched mRNA was purified from excess EDTA, tRNA, 5S rRNA, and other small RNA species, by LiCl precipitation. Lithium chloride selectively precipitates large RNA such as mRNA, while small RNA such as tRNA, and nucleotides and salts (e.g., EDTA) remain in solution. One volume of 5 M LiCl solution was added to the sample mixed well and incubated in ice or at -20°C for 30 minutes. The RNA was pelleted by centrifugation in a microcentrifuge for 30 minutes at full speed at 4°C and, after careful removal of the supernatant which contains the tRNA, other small RNAs and nucleotides, washed with 70% ethanol to remove residual salt, and resuspended in RNase-free water or TE buffer. The success of the Terminator reaction was analyzed by denaturing agarose gel electrophoresis. The absence of 18S and 28S rRNA in the post-treatment sample indicates a successful reaction.

### 3.2.10 Genomic DNA isolation

The genomic DNA was purified from MDA-MB231 cells grown in control conditions or treated with 8.45 µM JAHA for 18, 30, and 48 h. To this purpose, we used the PureLink™ Genomic DNA Kit, which is based on the selective binding of DNA to silica-based membrane in the presence of chaotropic salt.

The following protocol was applied:

- to prepare cell lysate, growth medium was removed, and cells were harvested by trypsinization and resuspended in 200 µl PBS. Twenty µl Proteinase K and 20 µl RNase A were added to the sample. Each sample was mixed well by brief vortexing, and incubated at RT for 2 min. 200 µl PureLink™ Genomic Lysis/Binding Buffer were added and each sample was mixed well by vortexing to obtain a homogenous solution. The samples were incubated at 55°C for 10 min to promote protein digestion. Two hundreds µl of 96-100% ethanol were added to the lysate. Each sample was mixed well by vortexing for 5 seconds to yield a homogenous solution;
- to bind DNA, the obtained lysate was transferred in a PureLink™ Spin Column provided by the kit. The column was centrifuged at 10.000×g for 1 minute at RT. The collection



tube was discarded and the spin column was placed into a clean PureLink™ Collection Tube supplied with the kit;

- to wash DNA, 500 µl Wash Buffer 1 prepared with ethanol were added to the column. The column was centrifuged at RT at 10.000×g for 1 minute. The collection tube was discarded and the spin column was placed into a clean PureLink™ Collection Tube. 500 µl of Wash Buffer 2 prepared with ethanol were added to the column. The column was centrifuged at maximum speed for 3 minutes at RT and collection tube was discarded;
- to elute DNA the spin column was placed in a sterile 1.5 ml microcentrifuge tube. 50 µl of PureLink™ Genomic Elution Buffer were added to the column. The sample was incubated at RT for 1 minute and centrifuged at maximum speed for 1 minute at RT thus recovering the purified genomic DNA. To recover more DNA, a second elution step was performed using the same elution buffer volume as first elution in another sterile 1.5 ml microcentrifuge tube. Then the column was centrifuged at maximum speed for 1.5 min at RT. The tube contained purified DNA. The column was removed and discarded; the purified DNA was stored at -20°C.

Genomic DNA concentration was measured using a Nanodrop spectrophotometer (Thermo Scientific, USA).

### 3.2.11 Reverse Transcription Reaction

SuperScript™ II Reverse Transcriptase (RT) is an engineered version of M-MLV RT with reduced RNase H activity and increased thermal stability. The enzyme is purified to near homogeneity from *E. coli* containing the modified pol gene of Moloney Murine Leukemia Virus (Kotewicz et al., 1985; Gerard et al., 1986.). The enzyme can be used to synthesize first-strand cDNA at higher temperatures than conventional M-MLV RT, providing increased specificity, higher yields of cDNA, and more full-length product. It can generate cDNA up to 12.3 kb.

A 20 µl reaction volume was used for 250 ng of mRNA. The following components were mixed into a nuclease-free microcentrifuge tube:

- 2 µl (50 µM) random primers
- X µl 250 ng of mRNA
- 1 µl dNTP Mix (10 mM each)
- Sterile, distilled water to 12 µl

The mixture was heated to 65°C for 5 min and quickly chilled in ice. The contents of the tube were collected by brief centrifugation and added to:

- 4 µl 5X First-Strand Buffer
- 2 µl 0.1 M DTT
- 1 µl RNaseOUT™ (40 U/µl)

The mixture was incubated at 25°C for 2 min and then 1 µl (200 U) of SuperScript™ II RT was added and mixed by pipetting gently up and down. The tubes were incubated at 25°C for 10 min, then at 42°C for 50 min, and, at the end to inactivate the reaction, heated at 70°C for 15 min.

### 3.2.12 Conventional PCR reaction

For PCR amplification, the following reagents were mixed into a 0.5 ml PCR tube (20 µl was the total reaction volume) in the following order:

- 14.5 µl water
- 2 µl RED Taq PCR Reaction Buffer 10X
- 0.5 µl Forward Primer (100 pmoli/µl)
- 0.5 µl Reverse Primer (100 pmoli/µl)
- 1µl cDNA template
- 1µl RED Taq DNA Polymerase

Cycling parameters:

- Initialization step at 94°C for 2 minutes
  - Denature the template at 94°C for 1 minute
  - Anneal primers at 60°C for 1 minute
  - Extension at 72°C for 1 minute
  - Final elongation at 72°C for 5 minutes
- } 25, 30 or 35 cycles of amplification

The amplified DNA was loaded directly onto an 2% agarose gel after the PCR process.

## 3.2.13 Primer Sequences used for PCR amplification

Name	Amplicon Size (bp)	Ta (°C)	Forward Primer Reverse Primer
<i>PKCε</i>	249	60	5'- GATCAGAAGGTCCTGCAA-3' 5'-GTCGTCATGGAGGATGGACT-3'
<i>PKCι</i>	169	60	5'-TACGGCCAGGAGATAACAACC-3' 5'-TCGGAGCTCCCAACAATATC-3'
<i>ERGIC</i>	196	60	5'-GCCATGGAGTCTCTGGGATA-3' 5'-CCAAGTCTGAAACGACAGCA-3'
<i>LRCH1</i>	220	60	5'-GATTTCGGGAGTTGGAAGTGA-3' 5'-CTCCTGAGTTGGTGCTGTCA-3'
<i>RAD50</i>	215	60	5'-CTTGATATGCGAGGACGAT-3' 5'-CCAGAAGCTGGAAGTTACGC-3'
<i>MED25</i>	188	60	5'-CAGCGCCTATGAGTTTGTC-3' 5'-AGTATGGGGTGAGTTGCAG-3'
<i>NAALAD2</i>	229	60	5'-AAAAGGCTGGATTTGGAGGT-3' 5'-GGCGAAGAGATCAGTTTTGC-3'
<i>NTRK2</i>	181	60	5'-AGCATGAGCACATCGTCAAG-3' 5'-ATATGCAGCATCTGCGACTG-3'
<i>Brefeldine A</i>	231	60	5'-CGCCCTGTCTCTAAACTGC-3' 5'-CTGTCTGCGTTCATCAGCAT-3'
<i>VDUP1</i>	223	60	5'-TTGTTCTCCCTTCTGCCAT-3' 5'-AGGGTTGGGCATCTTGATCA-3'
<i>ID11</i>	206	60	5'-TTGGGCTGGATAAAACCCCT-3' 5'-ACACAGGCCTTTGTTGTTGT-3'
<i>Gelsolin</i>	270	60	5'-TGTGATCGAAGAGGTTCTTG-3' 5'-GACCAGTAATCATCATCCCA-3'
<i>Actin</i>	51	60	5'-AGG-CAC-CAG-GGC-GTG-AT-3' 5'-GCC-CAC-ATA-GGA-ATC-CTT-CTG-AC-3'
<i>GAPDH</i>	414	60	5'-CATGGAGGAGGCTGGGGCTC-3' 5'-CACTGACACGTTGGCAGTGG-3'

### 3.2.14 Differential Display- PCR

Differential display is a technique used to compare and identify changes in gene expression between cell samples. The RNA extracted from MDA-MB231 cells grown in control conditions or treated with 8.45  $\mu\text{M}$  of JAHA was amplified using arbitrary primer as reported by Sokolov and Prokop, (1994).

Their criteria used to design the primers for PCR amplification of the cDNAs were:

1. no stop codon was present in any possible reading frame in both directions;
2. the sequences had a minimal tendency to form internal loops;
3. the sequences included the most commonly employed codons in mammals;
4. there was a minimal overlap in sequences among primers;
5. the GC content should be 60-70%;
6. there was a minimal number of glycine codons so as to avoid over-representations of the collagens that are abundant in many mammalian tissues
7. primers were 13-mer or less.

Primers with arbitrary but fixed sequences were used for the PCR amplification in these combinations: BS52 + BS54, BS54 + BS55, BS57 + BS58, BS70 + BS73, BS76 + BS78.

BS52 CAAGCGAGGT	}	AB
BS54 AACGCGCAAC		
BS55 GTGGAAGCGT	}	BC
BS57 GGAAGCAGCT		
BS58 CAGTGAGCGT	}	DE
BS70 GAGCTATGGC		
BS73 CACAGTGAGC	}	FG
BS76 CTGGTCACAC		
BS78 AGCCTGTGTC	}	HI

For every samples the following reaction components were combined:

- 3  $\mu\text{l}$  Stoffel buffer 10X,
- 3  $\mu\text{l}$   $\text{MgCl}_2$  25 mM,
- 0.6  $\mu\text{l}$  dNTP mix (10 mM),
- 0.5  $\mu\text{l}$  (25 pmoli/ $\mu\text{l}$ ) forward primer,

- 0.5  $\mu\text{l}$  (25 pmoli/ $\mu\text{l}$ ) reverse primer,
- 0.36  $\mu\text{l}$  (10 U/ $\mu\text{l}$ ) AmpliTaq DNA Polymerase Stoffel Fragment (Applied Biosystems),
- 1  $\mu\text{l}$  cDNA,
- $\text{H}_2\text{O}$  up to a final volume of 30  $\mu\text{l}$ .

Cycling parameters:

- Initialization step at 94.5°C for 3 minutes
  - Denature the template at 94.5°C for 1 minute
  - Anneal primers at 34°C for 1 minute
  - Extension at 72°C for 1 minute
  - Final elongation at 72°C for 10 minutes
- } 45 cycles of amplification

The amplification products were examined by polyacrylamide gel electrophoresis and silver staining. To this purpose, a 6% non-denaturing polyacrylamide gel solution was prepared using the following mixture:

- 8.55 ml 40% acrylamide solution,
- 9 ml 2% N, N- methylene bis-acrylamide solution,
- 6 ml 10X TBE,
- $\text{H}_2\text{O}$  up to a final volume of 60 ml.

The mixture was subsequently degassed by the use of a vacuum pump.

The glass plates (Sequi-Gel, BioRad, USA) of the electrophoresis apparatus were treated with specific solutions as follows:

- the fixed glass plate with 1.5 ml silanisation solution,
- the mobile glass plate with a binding solution composed of 5  $\mu\text{l}$   $\gamma$ -methacryloxypropyltri-methoxy-silane, 5  $\mu\text{l}$   $\text{CH}_3\text{COOH}$  and 1 ml 95% ethanol.

In order to prepare the bottom layer of the gel, 10 ml of the 6% polyacrilamyde solution were mixed with 50  $\mu\text{l}$  TEMED and 50  $\mu\text{l}$  25% APS and poured over Whatman paper. The gel casting apparatus was assembled according to the manufacturer's manual allowing the bottom layer to soak in between the two plates by capillary forces.

Afterwards, the separation gel was prepared by combination of 40 ml of the 6% polyacrilamyde solution with 40  $\mu\text{l}$  TEMED and 40  $\mu\text{l}$  25% APS and carefully applied by a syringe. Immediately upon polymerization (45-60 min), the comb was removed; the upper (stacking) gel was prepared as described for the bottom layer and carefully applied to the

casting apparatus by a syringe and the gel comb was inserted. The gel was allowed to polymerize overnight at RT.

The next day, the gel comb was removed and the wells were carefully rinsed with 1X TBE to reduce bubble formation. Afterwards, 6 µl of PCR product were mixed with 0.6 µl of 10X gel loading solution and loaded. 100 or 50 bp DNA ladder (Sigma) were used as markers. Electrophoresis was performed at constant 2000 V and 55 W for 1 or 2 hours until the bromophenol blue bands run out of the gel.

For staining of the DNA bands the following solutions were prepared:

- Fix stop solution: 200 ml CH<sub>3</sub>COOH 10% and 1800 ml milliQ H<sub>2</sub>O up to a final volume of 2 l;
- Staining solution: 1 gr AgNO<sub>3</sub>, 1.5 ml Formaldehyde 37%, and milliQ H<sub>2</sub>O up to a final volume of 1 l;
- Developing solution: 30 gr Na<sub>2</sub>CO<sub>3</sub> in 1 l of milliQ H<sub>2</sub>O. This solution was stored at 4°C and immediately before use 1.5 ml of Formaldehyde 37%, and 200 µl Sodium thiosulfate (10 mg/ml) were added.

After the electrophoresis and the deassembling of the gel cassette, the gel fixed on the glass plate was subjected to the following treatments:

- fixation in agitation for 20 min in 1 l of Fix stop solution,
- three washings for 2 min in milliQ H<sub>2</sub>O,
- treatment with 1 l of Staining solution for about 30 min,
- washing for 10 sec in milliQ H<sub>2</sub>O,
- addition of 500 ml of Developing solution and shaking until some bands became visible (2-3 minutes). Addition of 500 ml of Developing solution for 2-3 min until all bands appear,
- addition of 1 l Fix stop solution to block the reaction,
- washing for at least 2 times with milliQ H<sub>2</sub>O and drying at RT prior to photography,
- bands of interest were cut out and stored at -20°C before to use.

To amplify the cDNA present in the excised bands, a PCR reaction was performed in the presence of Stoffel DNA polymerase and the specific primers used in DD-PCR, as described above. The obtained products were then subjected to various purification cycles using the kit described below, to obtain a single band observable after agarose gel electrophoresis. For this reason agarose (2 g) was dissolved in 100 ml Tris/Borate EDTA buffer 1X using TBE 10X (89 mM Tris-borate and 2 mM EDTA, pH 8.3) by heating in a microwave until boiling, this

solution was allowed to cool and ethidium bromide was added (0.5 µg/ml). Gel electrophoresis was carried out in a horizontal tank containing TBE buffer 1X and was run at 80 V for 1.5 h. Thermo Scientific 6X DNA Loading Dye was used to prepare DNA markers and samples for loading on agarose gel. It contains two different dyes (bromophenol blue and xylene cyanol) for visual tracking of DNA migration during electrophoresis. The 50 bp DNA Ladder (Invitrogen) was used for precise qualitative and approximate quantification of DNA mass. After the electrophoretic run, the DNA was checked under UV light.

Subsequently, to purify the PCR product from the gel we used the Montage<sup>TM</sup> PCR Centrifugal Filter Devices (MILLIPORE): it simplifies the purification of PCR products by allowing for concentration and removal of primers and unincorporated dNTPs prior to use of DNA in subsequent applications.

The following protocol was applied:

- 50 µl PCR reaction and 350 µl of distilled water were pipetted into sample reservoir to a final volume of 400 µl,
- the Montage PCR unit was spun at 1000xg for 15 min,
- the sample reservoir was placed upright into a clean vial and 20 µl of distilled water were added to the purple end of reservoir, avoiding to touch the membrane surface,
- to recover the purified DNA the reservoir was inverted into clean vial and spun at 1000xg for 2 min.

To remove any unconsumed dNTPs and primers remaining in the PCR product mixture, which could interfere with the sequencing reaction, the PCR products obtained by amplification were purified by ExoSAP-IT method that involves the use of two hydrolytic enzymes, Exonuclease I and Shrimp Alkaline Phosphatase, to remove the unwanted dNTPs and primers. In this case, 5 µl of PCR product and 2 µl of Exosap were mixed and incubated at 37°C for 15 min. Then, to inactivate Exosap the samples were heated to 80°C for 15 min. After that the PCR products were sequenced by the sequencing service of BMR Genomics (Padova, Italy).

### **3.2.15 Real Time Polymerase Chain Reaction**

Total RNA was extracted from control and treated MDA-MB231 cells and first-strand cDNA was synthesized as already reported mRNA expression levels were determined by quantitative real-time PCR, with Power SYBR Green PCR Master Mix (Applied Biosystems Philadelphia,

PA, USA) in a 7300 Real Time PCR system (Applied Biosystem). Actin was used as internal control.

PCR data obtained by the instrument software were automatically analysed by the Relative Quantification Study Software (Applied Biosystem ) and expressed as target/reference ratio.

The cycle conditions for real-time PCR were 95°C for 10 min, followed by 40 cycles of 95°C for 1 min, and 60°C for 1 min.

### 3.2.16 Methylation-Sensitive Restriction Endonucleases Multiplex-PCR

Genomic DNA was obtained from control and treated MDA-MB231 cells as already reported. The methylated CpG islands were detected by MeSAP-PCR, carried out according to Liang et al., (2002) with some modifications (Naselli et al., 2014). Briefly, DNA from MDA-MB231 breast cancer cells (2 µg) was digested in a total volume of 10 µl for at least 16 h, at 37°C, with 1 µl 10 U of *Afa* I restriction endonuclease (Invitrogen) (single digested DNA, SDD), 2 µl 10X Buffer T, 2 µl 0.1% BSA and steril water to 10 µl. The cleavage site of the enzyme is: (GT\*AC).

Then, one half of SDD digested was further treated with 0.5 µl 10 U *Hpa*II, a methylation-sensitive restriction endonuclease unable to cut DNA if methylated cytosine is present in its recognition site (CG\*GG) at 37°C for 16 h (double digested DNA, DDD), 1.2 µl Buffer 10X and sterile water to 12 µl. SDD and DDD were heat inactivated for 20 min at 65°C and separately amplified by Arbitrarily-Primed PCR using two subsequent amplification cycles, AP1-M and AP2-M, in a T1 Plus Thermocycler (Biometria, Gottingen, Germany). In the AP1-M (low stringency cycle), a permissive annealing temperature, a high salt and primer concentration were set to allow arbitrary primer annealing to the best matches in the template with the highest preference for all the genomic CpG sites since they are provided with a 3' tail complementary to these sites. The reproducibility of the reactions was ensured as all experiments were conducted using the same rates of buffer reaction.

PCR was performed in a total volume of 25 µl under the following conditions:

- 500 ng Genomic DNA
- 2.5 µl 21-mer arbitrary primer (5'-AACTGAAGCAGTGGCCTCGCG-3') 10 µM
- 2 µl dNTPs 0.2 mM
- 1.6 µl Taq DNA polymerase recombinant (Invitrogen) 0.8 U
- 2.5 µl Buffer 10X
- 2 µl MgCl<sub>2</sub> 50 mM



Cycle profile was:

A Cycle	94°C	5 min
4 Cycles at low stringency conditions	94°C	30 sec
	40°C	60 sec
	72°C	90 sec

AP2-M (high stringency cycle), runs immediately after AP1-M. Reaction mixture consisting of 75 µl of:

- 7.5 µl Buffer 10X
- 6 µl MgCl<sub>2</sub> 50 mM
- 2 µl dNTPs 0.2 mM
- 0.5 µl Taq DNA polymerase recombinant (Invitrogen) 2.5 U
- H<sub>2</sub>O up to a final volume of 75 µl.

was added to 25 µl of AP1-M mix, immediately before AP2-M cycle.

Cycle profile was:

A Cycle	94°C	60 sec
4 Cycles at low stringency conditions	60°C	60 sec
	72°C	2 min
	72°C	90sec

The amplified DNA was resolved by non-denaturing 6% acrylamide-bisacrylamide (29:1 ratio) gel electrophoresis prepared using the following mixture:

- 2.5 ml 10X TBE
- 5 ml 30% acrylamide-bisacrylamide (29:1 ratio)
- 600 µl APS 10%
- 11.3 µl TEMED
- H<sub>2</sub>O up to a final volume of 25 ml.

DNA fingerprinting was stained with Gel Red nucleic acid Gel Stain 3X submitted to densitometric scanning and analysed with the SigmaGel image analysis software (Jandel Scientific, San Rafael, CA, USA).

### 3.2.17 SDS-PAGE and western blotting analysis

1x10<sup>6</sup> MDA-MB231 breast cancer cells were plated in 75 cm<sup>2</sup> flask and treated with 8.45  $\mu$ M JAHA for 18, 24, and 48 h to detect LC3, p62/Sequestosome 1, and 18, 30, 48 h to detect Erk1/2, p-Erk1/2, Akt, p-Akt and DNMT1.

Cells were washed once in PBS, isolated by centrifugation and lysed in a lysis buffer containing 7 M Urea, 2% CHAMPS, 1% IPG Buffer, 10 mM DTT, PMSF protease and phosphatases inhibitor cocktail (Sigma) 1X. The lysates were centrifuged at 1.000 rpm for 1 min at 4°C. Protein concentrations were estimated by Bradford assay (Bio-Rad, Italy).

Twenty  $\mu$ g of proteins for LC3, p62/Sequestosome 1, Erk1/2, p-Erk1/2, Akt, p-Akt and 50  $\mu$ g of proteins for DNMT1 were denatured by boiling samples in 0.05% SDS and sample buffer [0.5 M Tris-HCl (12.5%), pH 6.8, (2%) SDS, (10%) glycerol, (5%)  $\beta$ -mercaptoethanol, bromophenol blue (0.05%)] for 3 min before electrophoresis. To detect LC3, p62/Sequestosome 1, Erk1/2, p-Erk1/2, Akt and p-Akt, proteins were subjected to 13% SDS-PAGE [Acrylamide (13%), Bis-Acrylamide (0.26%), Tris-HCl 1.5 M pH 8.8 (25%), SDS (0.1%), Ammonium persulphate (0.1%), Temed (0.04%)], with a 3% acrylamide upper gel [Tris-HCl 0.5 M pH 6.8 (50%), Acrylamide (3%), Bis-Acrylamide (0.08%), Ammonium persulphate (0.1%), SDS (0.1%), Temed (0.08%)]. To detect DNMT1, proteins were subjected to 10% SDS-PAGE [Acrylamide (10%), Bis-Acrylamide (0.2%), Tris-HCl 1.5 M pH 8.8 (25%), SDS (0.1%), Ammonium persulphate (0.1%), Temed (0.04%)], with a 3% upper gel [Tris-HCl 0.5 M pH 6.8 (50%), Acrylamide (3%), Bis-Acrylamide (0.08%), Ammonium persulphate (0.1%), SDS (0.1%), Temed (0.08%)]. Gel electrophoresis was carried out in a vertical tank containing running buffer [Tris (0.6%), Glycine (2.88%), SDS (0.1%)] and was run at 200 V for 3 h.

After electrophoresis, proteins were transferred to nitrocellulose membranes (Hybond C, Amersham) using a (Novablot equipment Pharmacia) in transfer buffer [Tris (0.29%), Glycine (1.44%), Methanol (20%)] at 200 mA for 1h. To detect DNMT1 the transfer was increased to 2 hours, for its higher molecular weight (183 kDa). The gels were stained for 30 min with 0.5% Coomassie Blue (LKB BROMMA) in 50% methanol and 10% acetic acid. Then the gel was treated with a destaining solution (50% methanol, 10% acetic acid), with 2 washes of 10 min each. A second solution (20% methanol, 10% acetic acid) was used for total destaining. The complete transfer was assessed using Ponceau red staining. The nitrocellulose filter was treated for two minutes with 3% TCA containing 0.2% Ponceau red, and then washed and destained with TBS-T [NaCl (150 mM), Tris-HCl pH 7.4 (100 mM) Tween-20 (0.05%)].

After 2 h of blocking with 5% non-fat dry milk in TBS-T, or in BSA, the membranes were incubated with the primary antibodies overnight at 4°C. The following antibodies were used: rabbit polyclonal anti-LC3 (L8918, Sigma, 1:1000 in 5% milk), anti-p62/SQSTM1 (P0068, Sigma, 1:1000 in 5% milk), anti-Erk1/2 rabbit (ab17942, Abcam, 1:500 in 5% milk), anti-AKT rabbit (9272, Cell Signaling, 1:750 in 5% BSA), anti-p-Erk1/2 rabbit (9101, Cell Signaling, 1:750 in 5% BSA), anti-p-AKT rabbit (SC-7985-R, Santa Cruz, 1:750 in 5% BSA) anti DNMT1 rabbit (SAB2106406, Sigma, 1:250 in 5% milk). After 5 washing with TBS-T for 5 min, for Erk1/2, p-Erk1/2, Akt, p-Akt and DNMT1 detection, the membranes were incubated with rabbit secondary antibody (anti-IgG HRP horseradish peroxidase-conjugated, NA934V, GE Healthcare Life Sciences, 1:2500 in TBS-T) for 60 min at room temperature. Then, after three washing: with TBS-T and two washings with TBS for 5 min each, the reaction was visualized in a Chemidoc XRS (Bio-Rad) after treating the membrane with the two development solutions provided by Western ImmunStar™ C™ Substrate Kit. For LC3 and p62/SQSTM1 detection, the membranes were incubated with secondary alkaline phosphatase-conjugated antirabbit IgG (Fc) antibody (S373B, Promega, Madison, WI), followed by incubation with 5-bromo-4-chloro-3'-indolyphosphate p-toluidine salt/nitro-blue tetrazolium chloride (BCIP/NBT) solution (Sigma).

The membranes were stripped with a stripping buffer (1 M Tris HCl pH 6.8, SDS 10%,  $\beta$ -mercaptoethanol 50 mM) for 30 min at 60°C. The data were appropriately normalized to actin by reprobing the filter with an antibody directed against actin (A5060, Sigma, 1:500 in 5% milk). Scanning densitometry of the bands were performed with the Quantity One software. Each Western experiment was performed in triplicate.

### 3.2.18 Liquid chromatography-tandem mass spectrometry analysis

$1 \times 10^6$  cells were plated in 75 cm<sup>2</sup> flasks, and allowed to adhere overnight. Then, the cells were treated with either JAHA or SAHA at 8.45  $\mu$ M concentration or with the vehicle (DMSO) for 18, 24, and 48 hours. Detached with 0.05% trypsin-EDTA and collected by brief centrifugation. The cellular pellet was dissolved in a solubilization buffer (0.1M Tris HCl pH 8, EGTA 25 mM, 4% SDS, protease inhibitors cocktail (Sigma) 1X. Then samples were sonicated, boiled for 3-5 min and clarified by centrifugation for 15 min at max speed after which the supernatant was collected. The proteins were precipitated using 5 volumes of cold acetone (-20°C), centrifuged at 13.000 rpm for 10 min at 4°C and resuspended in SDS 0.1% before sonication. The protein samples were quantified using BCA assay kit (Thermo Scientific) and 5  $\mu$ g of proteins were used for tryptic digestion and protein identification for

quantitative analysis whereas 24 µg for qualitative analysis. The solubilized proteins were digested overnight with sequencing grade modified trypsin (Promega, V5111, 0.01 µg per 1 µg of protein) and the reaction was quenched by adding 0.01% trifluoroacetic acid.

The peptidic mixtures were analyzed by LC-MS-MS/MS (liquid chromatography coupled to tandem mass spectrometry) using Nano-Acquity (Waters) LC system and Orbitrap Velos mass spectrometer (Thermo Electron Corp., San Jose, CA) (figure 3.1). Prior to the analysis, proteins were subjected to standard “in-solution digestion” procedure during which proteins were reduced with 100 mM DTT (for 30 min at 56°C), alkylated with 0.5 M iodoacetamide (45 min in dark room at room temperature) and digested overnight with trypsin (sequencing Grade Modified Trypsin, Promega V5111). The mixtures were applied to RP-18 precolumns (nanoACQUITY Symmetry® C18-Waters 186003514) using water containing 0.1% TFA as mobile phase and then transferred to nano-HPLC RP-18 column (nanoACQUITY BEH C18-Waters 186003545) using an acetonitrile gradient (0%-35% AcN in 180 minutes) in the presence of 0.05% formic acid with the flow-rate of 250 nl/min. Column outlet was directly coupled to the ion source of the spectrometer working in the regime of data dependent MS to MS/MS switch. A blank run ensuring lack of cross contamination from previous samples preceded each analysis. The acquired raw data were processed by Mascot Distiller followed by Mascot Search (Matrix Science, London, UK, on-site license) against Human database. Search parameters for precursor and product ions mass tolerance were 20 ppm and 0.6 Da, respectively, enzyme specificity: trypsin, missed cleavage sites allowed: 0, fixed modification of cysteine by carbamidomethylation and variable modification of methionine oxidation. Peptides with Mascot Score exceeding the threshold value corresponding to <5% False Positive Rate, calculated by Mascot procedure, and with the Mascot score above 30 were considered to be positively identified.

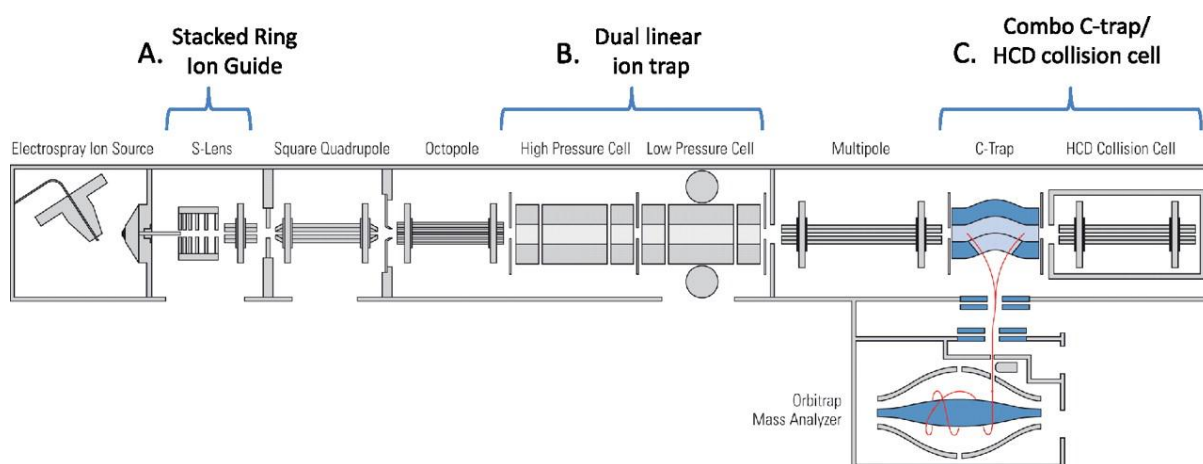


**Figure 3.1.** Schematic diagram of the LTQ Orbitrap Velos MS instrument with three new hardware implementations. A, the stacked ring ion guide (S-Lens) increases the ion flux from the electrospray ion source into the instrument by a factor 5–10. B, the dual linear ion trap design enables efficient trapping and activation in the high-pressure cell (left) and fast scanning and detection in the low pressure cell (right). C, the combo C-trap and HCD collision cell with an applied axial field with improved fragment ion extraction and trapping capabilities. (<http://planetorbitrap.com>)

### 3.2.19 Bioinformatic Analysis

The acquired MS/MS raw data files were processed to produce peak lists with Mascot Distiller software (version 2.2.1, Matrix Science). The resulting ion lists were searched using the Mascot search engine (version 2.2.03, Matrix Science) against a database comprising all human protein entries from the Sprot (540.732 sequences) and their reversed versions.

#### Mascot

Mascot is a popular web-based tool from Matrix Science for performing rapid, accurate, online MS analysis of peptides and proteins that supports 3 kinds of analyses:

- Peptide Mass Fingerprinting (PMF)
- Sequence (tag) querying
- MS/MS Ion searches

The search parameters were as follows: enzyme specificity, trypsin, variable modifications, oxidation (M) and protein mass, unrestricted. The peptide and fragment ion mass tolerances used were 20 ppm and 0.6 Da respectively. Peptides with Mascot score exceeding the threshold value corresponding to <5% false positive rate (figure 3.2), calculated by Mascot

procedure, were considered to be positively identified. At least two peptides for protein with score above the threshold were required for identification.

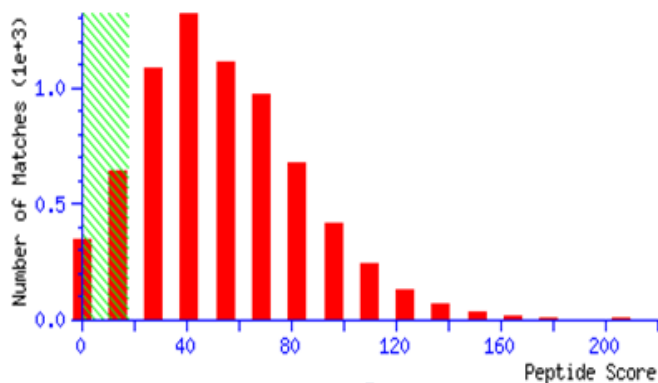


**Figure 3.2.** Peptide score distribution. Ions score is  $-10 \log(P)$ , where P is the probability that the observed match is a random event. Individual ions scores  $>18$  indicate identity or extensive homology ( $p < 0.05$ ).

### Program for qualitative proteomic analysis MScan

This is a program designed for the analysis of qualitative data, operating on the basis of files generated by the database system Mascot containing a list of peptides and proteins identified in the samples (<http://www.proteom.ibb.waw.pl>). The statistical significance of peptide identifications was assessed estimating the  $q$ -value for each peptide spectrum match (PSMs) in the data set. Only PSMs with  $q$ -values of  $\leq 0.01$  and proteins represented by at least two peptides identified were regarded as confidently. Proteins identified by a subset of peptides were excluded from analysis, and proteins matching the same set of peptides were clustered into single groups. Mscan software remove the sequence not selected and the random sequence (RS) using a FDR. The program is also responsible for the preparation of data for quantitative analysis (figure 3.3).

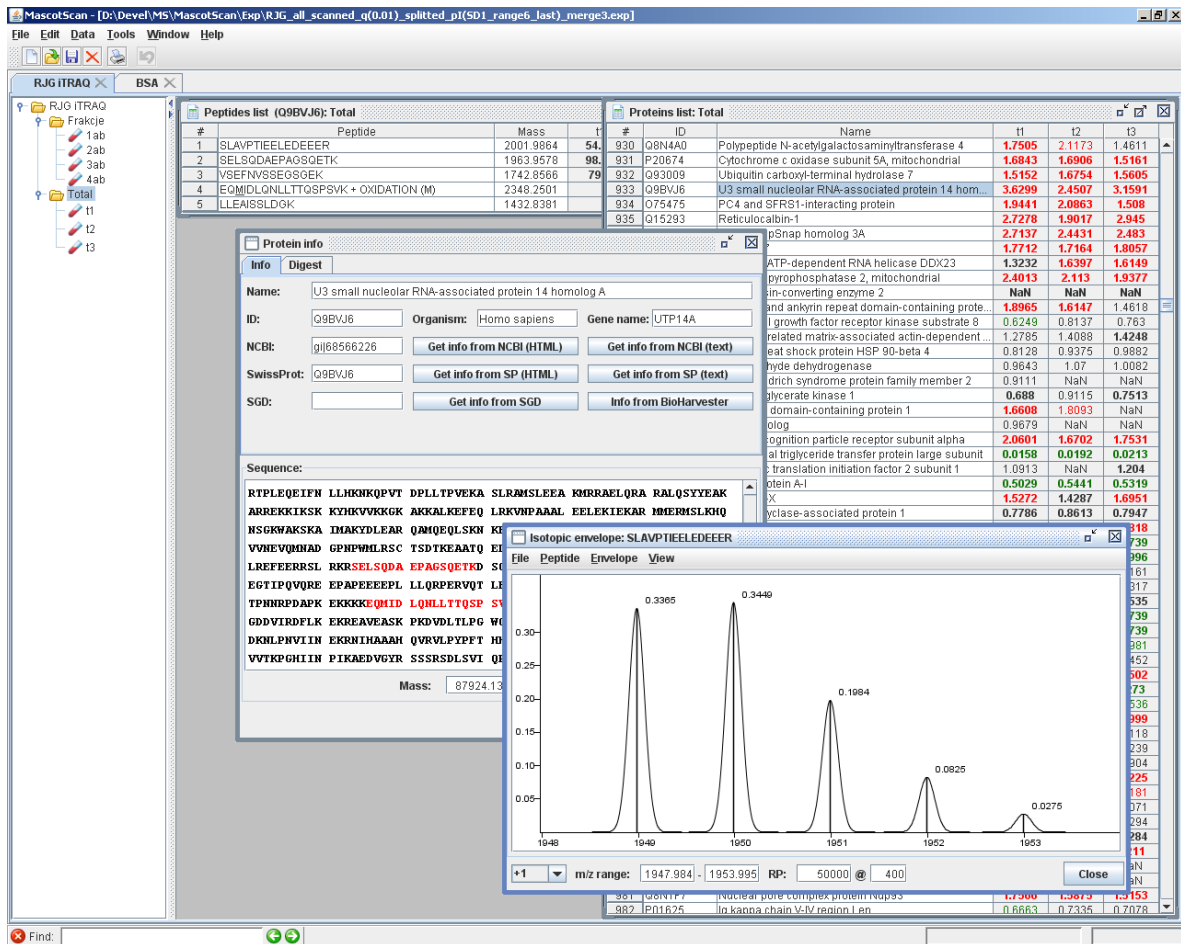


Figure 3.3. Example of Mascot analysis.

The basic functions of the program were:

- Divide the sample into groups reflecting different experimental conditions, of the list of peptides and proteins identified.
- Access at the Mascot informations and more information on additional parameters such as (theoretical retention time, isoelectric point, hydrophobicity, isotopic pattern) and proteins informations such as (coverage degree, theoretical distribution of peptides with proteolytic enzyme selected).
- Control of technical quality measurement in the spectrometer based on the parameters of distributions of the masses, retention times and the isoelectric points of the peptides.
- Standardisation of timing waveforms chromatographic samples, aimed at reducing the adverse effects of instability in the parameters of the HPLC system.

- Estimation of the percentage of false positive identification of peptides and determination of  $q$ -value (being a measure of the reliability of the identification peptides) based on the type of database search target/decoy.
- Elimination from the resulting set of proteins and peptides that do not meet user-defined criteria for the reliability of identification, prevalence in the studied samples, the error of weight derogation from the expected retention time and theoretical isoelectric point and a number of other parameters.
- Reduced redundancy by combining the results of the identification of a group of proteins (clustering) sequences having substantial homology.
- Ability to interface with generally available databases to obtain additional information about the identified proteins and download their sequences by directly supporting the database of NCBI, SwissProt and SGD.

### **Program for quantitative proteomic analysis**

To perform the quantitative analysis a MSparky software tool for quantitative proteomic analysis was used. Starting from the raw data, MSparky was able to calculate the relative intensities of reporter ions from a specific identified tandem mass spectrum. Protein intensities resulted from the average of the single reporter ion intensities, obtained for each peptide associated to a specific protein. The program is based on the representation of LC-MS data in the form of two-dimensional maps and models of theoretical spectra of peptide ions.

The basic functions of the program were:

- Visualization of high-quality two-dimensional representation of the LC-MS analysis of multiple samples simultaneously (figure 3.4).
- Automatic search for the position of the mass spectra of peptides in the mass spectra of the solid test samples. The position of the peptides is based on the degree of fit of theoretical models of spectra to the experimental data. As a result of the search algorithm to each peptide is assigned a quantitative parameter defined as the volume of the fitted model.
- Automatic or manual verification of the results.
- Processing (normalization) and visualization of the numerical value of the expression.



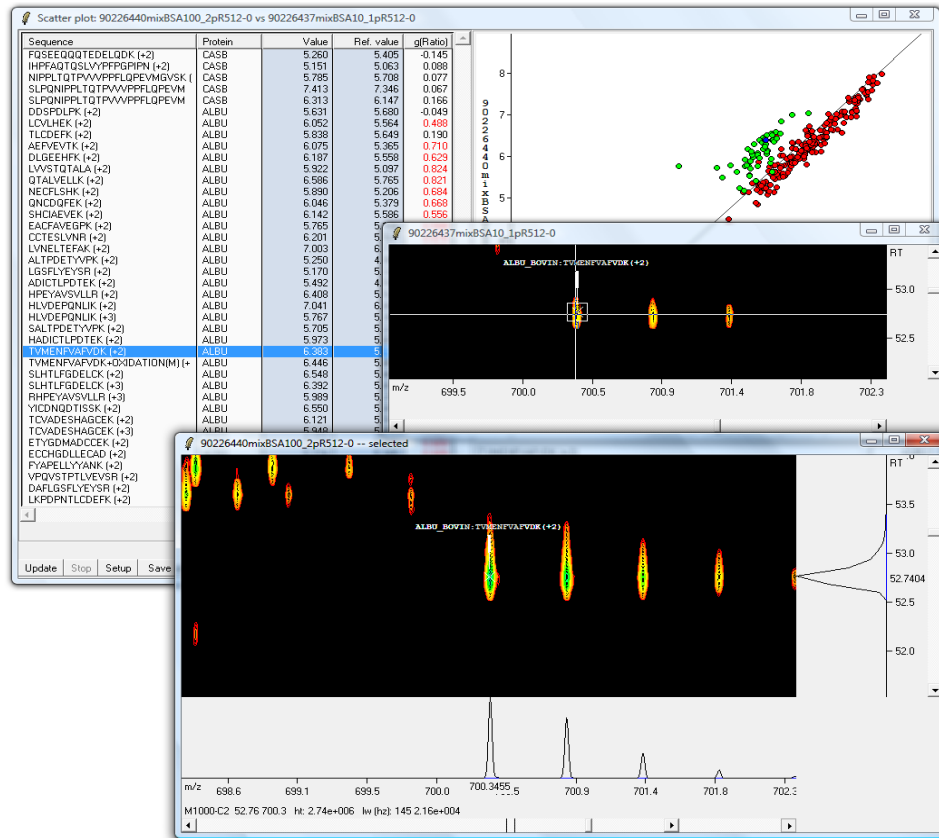


Figure 3.4. Example of MSparky analysis.

The Diffprot program allows the statistical analysis of quantitative data from proteomic experiments performed without isotopic labeling or iTRAQ-labeling method. The tool is particularly well-suited to the analysis of data from a small number of samples and exhibits a high resistance to errors that may result from incorrect identification of peptides.

The basic functions of the program were:

- Determination of protein concentration ratios in the compared groups of samples based on quantitative measurements of peptides.
- Determination of the statistical significance of protein concentration ratios using non-parametric permutation test, which determines the distribution of the test statistics at the truth of the null hypothesis based on random changes in assignments of samples to groups and peptides to proteins. Resulting  $p$ -value are corrected for multiple testing to control the FDR (*False Discovery Rate*).
- Normalization of quantitative values derived from separate measurements using a linear scale.

- Elimination from the data set of selected peptides that do not meet the criteria of the quality or intensity of the identification of the observed peaks and the proteins represented by too few peptides. It is also possible to exclude from the analysis of proteins selected by the user (e.g. Known contaminating proteins).
- Grouping of proteins with a high degree of commonality of peptides.

It is possible to obtain from the analysis with this software a list of proteins that appear to be differentially expressed in the control and treated. For each was calculated R value (the control and treated intensities ratio).  $0 < R \text{ value} < 1$  down-regulation (control/treated ratio) or  $1 < R \text{ value} < +\infty$  up-regulation (control/treated ratio). Another parameter, F give information about the fold changing. Data were displayed as the mean  $\pm$  SE of independent triplicate experiments. Q-values less than 0.05 were assigned as statistically significant.

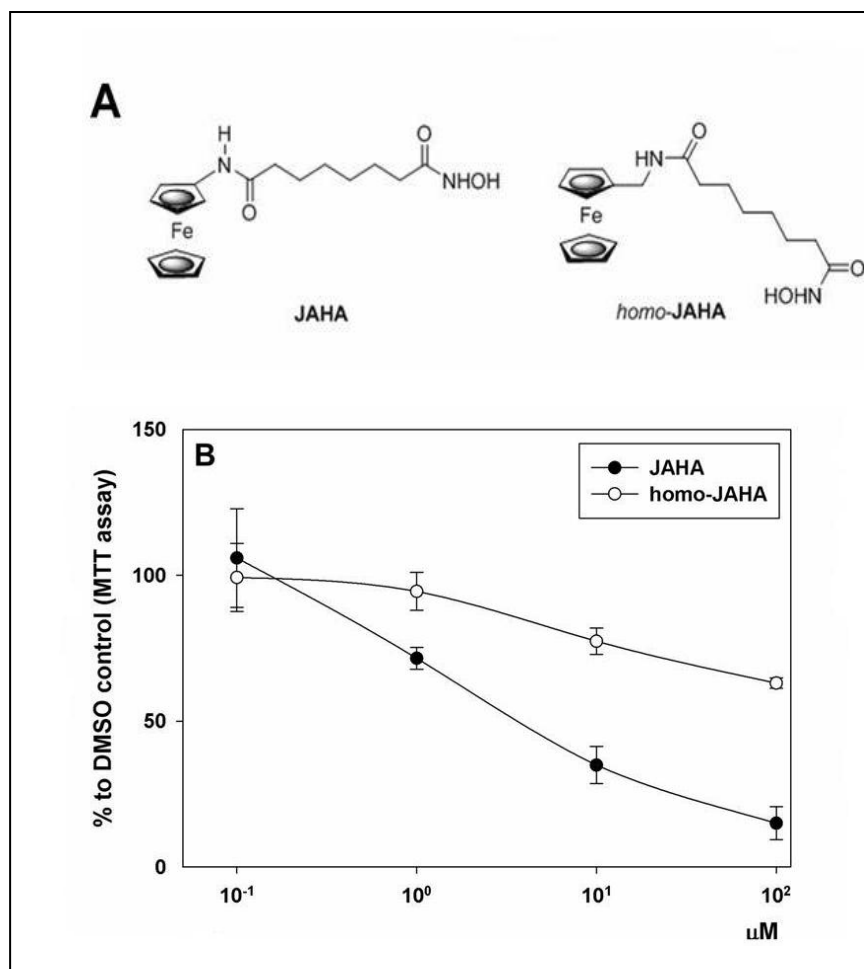
### **3.2.20 Statistical Analysis**

Statistical analysis was applied using the Microsoft Office Programme Excel 2007. The average mean value with the respective standard deviation for each set of triplicate experiments was plotted in a graph for the final evaluation. Results are given as mean  $\pm$  SD. Data were analyzed using software-assisted analysis of variance (Sigma Stat v.2; SPSS, Chicago, IL, USA) and  $p < 0.05$  was taken as the minimal level of statistical significance.

## 4. Results

### 4.1 Effect of JAHA and homo-JAHA treatment on cell viability/proliferation

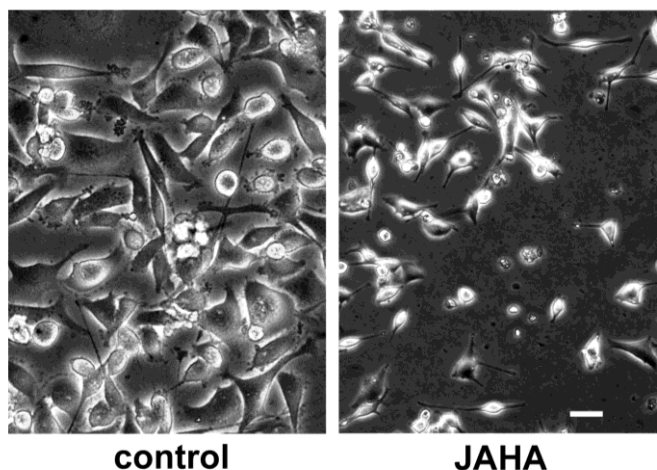
In a first set of experiments, we checked the effect of dose- and time-dependent incubation with JAHA and homo-JAHA (figure 4.1) on MDA-MB231 cell viability via MTT assay. As shown in Figure 1B, when cells were exposed for 72 h to JAHA, this compound caused death in a concentration dependent manner with an  $IC_{50}=8.45 \mu\text{M}$ , and such concentration was chosen for all of the subsequent biochemical experiments. On the other hand, after 72 h of treatment, homo-JAHA at the highest concentration used (100  $\mu\text{M}$ ) reduced cell viability only to  $63 \pm 1.8\%$ . The same concentration of either JAHA and homo-JAHA determined a decrease of cell viability to  $83.9 \pm 5.1$  and  $83.15 \pm 9.7\%$  at 24 h of incubation and  $66.4 \pm 6.7$  and  $61.54 \pm 2.09\%$ , respectively. We showed that JAHA is more active than homo-JAHA, for this reason we used only JAHA for the subsequent experiments.



**Figure 4.1.** JAHAs and their effect of 72 h of incubation on the viability of MDA-MB231 cells. (A) Structure of JAHA and homo-JAHA. (B) Dose-response curves for JAHA and homo-JAHA from triplicate MTT assays. The results are expressed as means  $\pm$  SEMs.

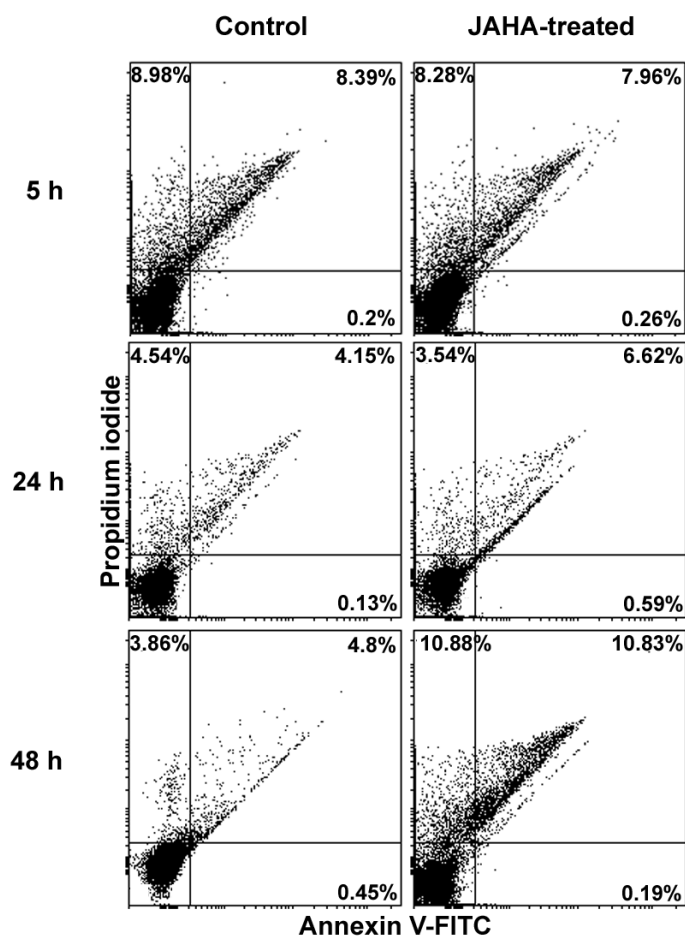
## 4.2 JAHA-induced non-apoptotic death on MDA-MB231 cells

Phase-contrast microscopical observation of MDA-MB231 cells treated with 8.45  $\mu\text{M}$  JAHA showed visible effects of cell death such as decreased cell number and the presence of rounded and floating cells, with respect to the firmly spread control cell preparations (figure 4.2).



**Figure 4.2.** Representative phase contrast micrographs of control and 8.45  $\mu\text{M}$  JAHA-treated cells showing changes in cell number and morphology after exposure to JAHA. Bar=10  $\mu\text{M}$ .

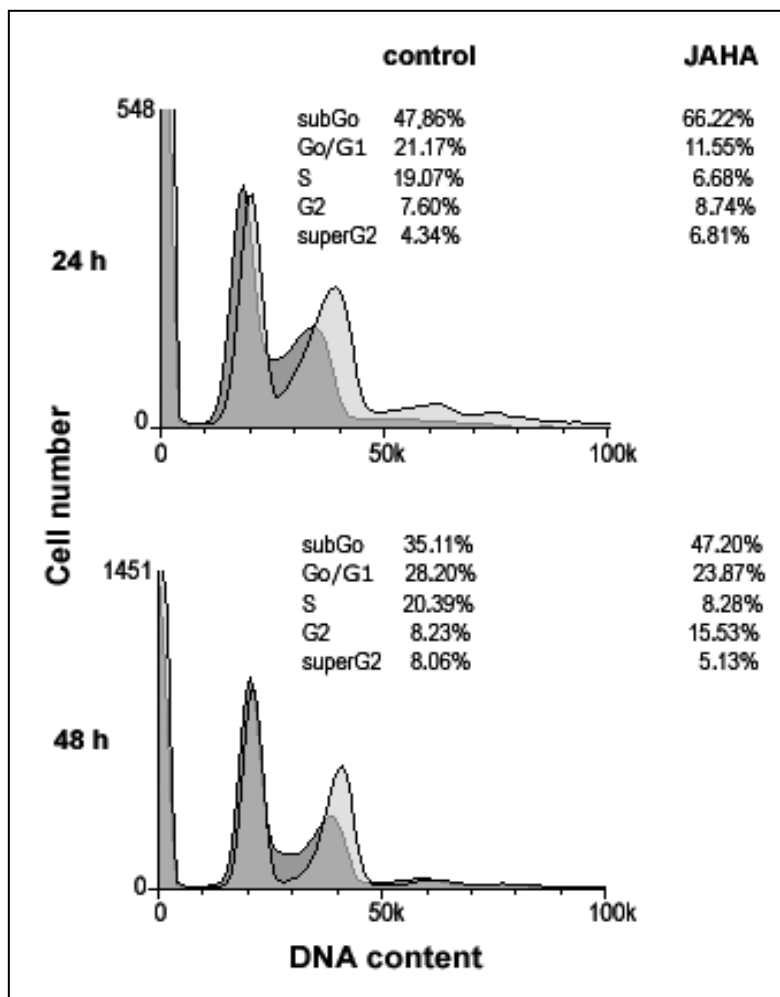
Therefore, we performed a set of experiments aimed to get more detailed data on the molecular mechanism of JAHA-induced toxicity on MDA-MB231 cells. First, samples of control and JAHA-treated cells were submitted to annexin V/FITC/propidium iodide (PI) staining and flow cytometric measurement to investigate the effect of JAHA on phosphatidylserine externalization, as a hallmark of induction of apoptosis, after short-term (5 h), and longer term (24 and 48 h) treatments. As shown in figure 4.3, JAHA treatment appeared to elicit a non apoptotic cytotoxic effect as indicated by the increase of the percentage of necrotic cells in both top quadrants at 48 h of exposure and the almost total absence of apoptotic annexin+/PI- cells in the bottom right quadrant at all times of investigation.



**Figure 4.3.** Flow cytometric analysis of control and JAHA-treated MDA-MB231 cells stained with annexin V-FITC and PI for detection of phosphatidylserine externalization after 5, 24 and 48 h-exposure. The percentage indicated in the four quadrants in each frame is referred to necrotic annexin<sup>-</sup>/PI<sup>+</sup> and annexin<sup>+</sup>/PI<sup>+</sup> cells (both top quadrants), apoptotic annexin<sup>+</sup>/PI<sup>-</sup> cells (bottom right quadrant) and normal annexin<sup>-</sup>/PI<sup>-</sup> cells (bottom left quadrant). Upon treatment, apoptotic cells never accounted for more than 0.59% of the cell population, whereas the percentage of necrotic cells showed an increase at long-term exposure.

### 4.3 Alterations of MDA-MB231 cell cycle cells after JAHA treatment

In order to check which kind of perturbation was induced by JAHA treatment on MDA-MB231 cell cycle, cells treated with JAHA for 24 and 48 h were stained with PI and subjected to flow cytometric analysis of the distribution of cell cycle phases. Figure 4.4 shows that, if compared to controls, exposure to JAHA was linked with a higher percentage of cells in the subG<sub>0</sub> fraction (66.22 and 47.20% vs. 47.86 and 35.11%, respectively, at 24 and 48 h), consistent with an increase of damaged and fragmented cells due to compound toxicity more prominent at earlier times, a pronounced decrease of the S phase fraction (6.68 and 8.28% vs 19.07 and 20.39%, respectively, at 24 and 48 h) and also of the 24 h G<sub>0</sub>/G<sub>1</sub> phase fraction (11.55 vs. 21.17%). Noteworthy, flow cytometric analysis also showed an increase of the 48 h G<sub>2</sub> phase fraction (15.53 vs 8.23%), indicative of the acquisition of the inability to proceed through the G<sub>2</sub>/M transition upon prolonged incubation.

**Figure 4.4.**

DNA profiles of control (darker in the background) and JAHA-treated (lighter superimposed) MDA-MB231 cells after 24 and 48 h of exposure. Cell cycle distribution is reported in the annexed tables for both cell samples.

#### 4.4 JAHA-induced decrease of MMP in MDA-MB231 cells

To detect variations of MMP after exposure to JAHA, we used the JC1 probe that is selectively uptaken into mitochondria, undergoing a fluorescence emission shift from green (~529 nm) to red (~590 nm) in the case of intact MMP, whereas in the case of mitochondrial depolarization, a decrease in the red/green fluorescence intensity ratio can be observed. As shown in figure 4.5, flow cytometry analysis puts in evidence the time-dependent loss of the MMP in JAHA-treated cells, the percentage of low red-emitting cells (bottom quadrants) being about 9% after 24 h of exposure and increasing up to about 36% at 48 h of incubation, versus 2 and 5% of control cells, respectively.

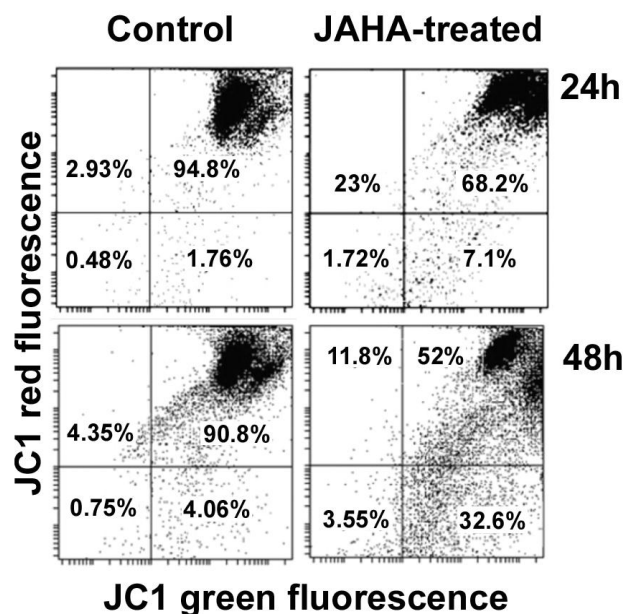


**Figure 4.5.** Analysis of MMP in control and JAHA-treated MDA-MB231 cells. Flow cytometric analysis of control and JAHA-treated MDA-MB231 cells stained with JC1 after 24 and 48 h-exposure. The percentages indicated in the bottom quadrants in each frame are referred to low red-emitting cells that underwent to dissipation of MMP.

## 4.5 JAHA-induced increase in reactive oxygen species production in MDA-MB231 cells

The ability of JAHA to affect mitochondrial metabolism was also assessed through evaluation of ROS production using a commercial kit, which differentiates between total ROS and superoxide. As shown in figure 4.6 A, exposure to JAHA determined an early 3-fold increase of total intracellular ROS within 24 h of incubation; on the other hand, such upregulation of total ROS was not recorded at 48 h of treatment. In addition, although the superoxide-positive fraction of MDA-MB231 cells treated with JAHA for 48 h was higher than that of controls (19.69 vs. 4.05%), the value was consistently less than half of that obtained with the pyocyanin-treated sample as positive control, thereby indicating that the observed upregulation of superoxide ion was not significant (data not shown). To check whether the observed ROS up-regulation could be involved, at least in part, in the onset of JAHA-triggered cytotoxicity, MDA-MB231 cells were coincubated with 8.45  $\mu$ M JAHA and the phenolic antioxidant BHT at increasing concentrations. The results shown in figure 4.6 B demonstrate that the co-treatment was capable of reversing the decrease in cell number

recorded with JAHA-only treatment, with 25 and 50  $\mu\text{M}$  BHT concentrations, respectively, inducing a comparable and more pronounced cell growth than that of the untreated control.

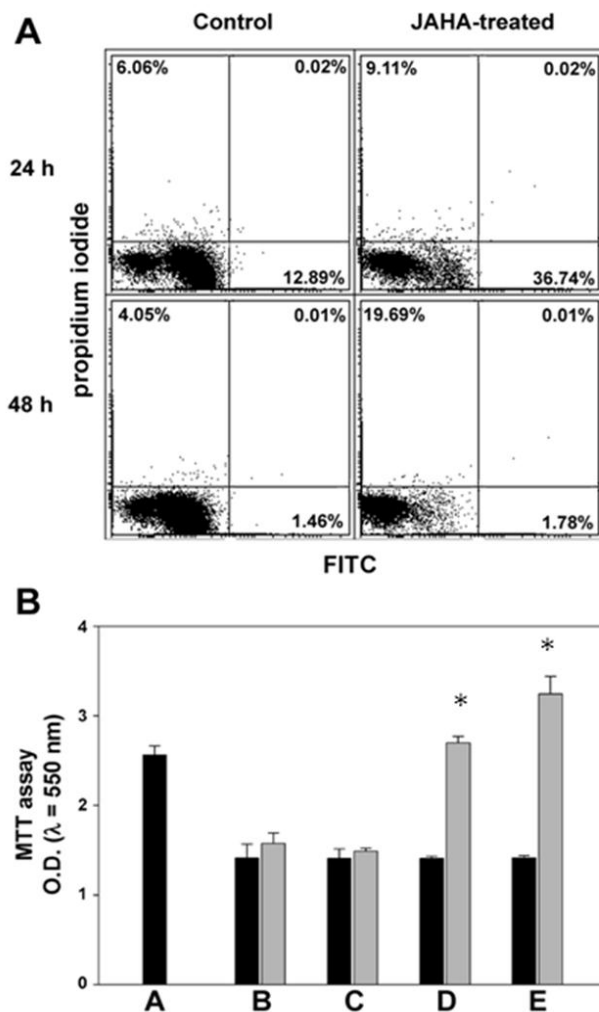


**Figure 4.6.** Effect of JAHA treatment on ROS production by MDA-MB231 cells and its involvement in the cytotoxic effect. A) Flow cytometric analysis of control and JAHA-treated MDA-MB231 cells stained with two color ROS detection reagents, after 24 and 48 h-exposure. The percentage indicated in the four quadrants in each frame is referred to superoxide only overproducing cells (top left quadrant), total ROS overproducing cells (bottom right quadrant) and total ROS/superoxide overproducing cells (top right quadrant). Upon treatment, MDA-MB231 cells undergo a threefold up-regulation of total ROS within 24 h of exposure. The up-regulation of superoxide ion recorded at 48 h is not significant, the value being less than half of that of pyocyanin-treated sample, used as positive control (data not shown). B) MTT assay of control (A) and JAHA-treated (B-E, black bars) MDA-MB231 cells assayed in parallel with cells co-incubated with 8.45  $\mu\text{M}$  JAHA and BHT at 5, 10, 25 and 50  $\mu\text{M}$  concentrations (B-E, grey bars). The culture was grown for 24 h and the

assay was made in triplicate. The results are expressed as mean  $\pm$  s.e.m. \* indicates  $p < 0.05$ . BHT at 25 and 50  $\mu\text{M}$  concentrations induced a reversal of the cytotoxic effect exerted by JAHA.

## 4.6 Autophagy inhibition in MDA-MB231 breast cancer cells treated with JAHA

We checked whether JAHA determined a modification in the amount of autolysosomes, a hallmark of autophagy, through staining with acridine orange, a cell-permeable fluorescent dye that can be sequestered by acidic compartments after uptake and protonation. Figure 4.7 shows that JAHA-treated cells underwent a consistent reduction of AVO accumulation between 24 and 48 h of exposure and that such a decrease was comparable to that observed when cells were incubated with 200 nM bafilomycin A1, a well-known inhibitor of



autolysosome maturation, (Yamamoto et al., 2008) as a negative control. Autophagy modulation by JAHA treatment was also monitored via molecular markers through immunoblot analysis.

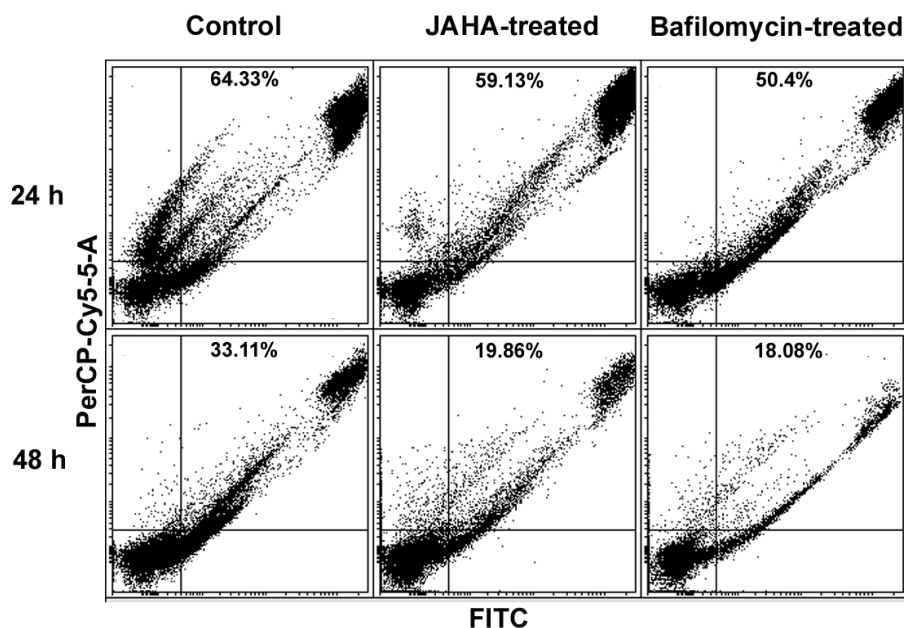


**Figure 4.7.** Effect of JAHA treatment on AVO accumulation in MDA-MB231 cells. Flow cytometric analysis of control, JAHA, and bafilomycin A1-treated MDA-MB231 cells stained with acridine orange, after 24 and 48 h-exposure. The percentage indicated is referred to AVO-positive cells. JAHA treatment induced a consistent reduction of AVO accumulation between 24 and 48 h of exposure, comparable to that observed when cells were incubated with autophagy-inhibitor bafilomycin A1.

In particular, we checked (i) the conversion of microtubule-associated protein light chain 3 (LC3) from its cytosolic form (LC3-I) to its autophagosome-associated lipidated form (LC3-II), which differs for its lower molecular mass and can be discriminated through SDS-PAGE, (Mizushima et al., 2007) and (ii) the changes in the accumulation levels of p62/SQSTM1, a receptor for ubiquitinated proteins that selectively delivers them into the autophagosome and is known to be a specific degradation substrate for autophagy. After the Western blot, the densitometry of the immunostained bands was performed with the ImageJ software. The immunoblot in Figure 4.8 A shows that LC3-II was decreased in MDA-MB231 cells after 48 h of exposure to JAHA. In particular, figure 4.8 B, C reports the densitometric analyses referred to the LC3-II/LC3-I ratio and also to the LC3-II band only, as suggested by the advice of Mizushima and Yoshimori, (2007). In both cases, although the difference between control and exposed cells was not evident at 24 h, apart from a faint decrease of the band intensity ratio, the increase of the duration of incubation with JAHA up to 48 h resulted in a reduction of both the LC3-II/LC3-I ratio and the intensity of LC3-II band down to about 52

and 71%, respectively, thus confirming the flow cytometric data. Further evidence of JAHA-induced autophagy down-regulation was also given by the immunoquantitation of p62/SQSTM1. In fact, as shown in figure 4.8 D the p62/SQSTM1 amount in JAHA-treated cells normalized for that of actin increased by about 50% after 48 h of incubation, whereas it remained constant at 24 h of culture.

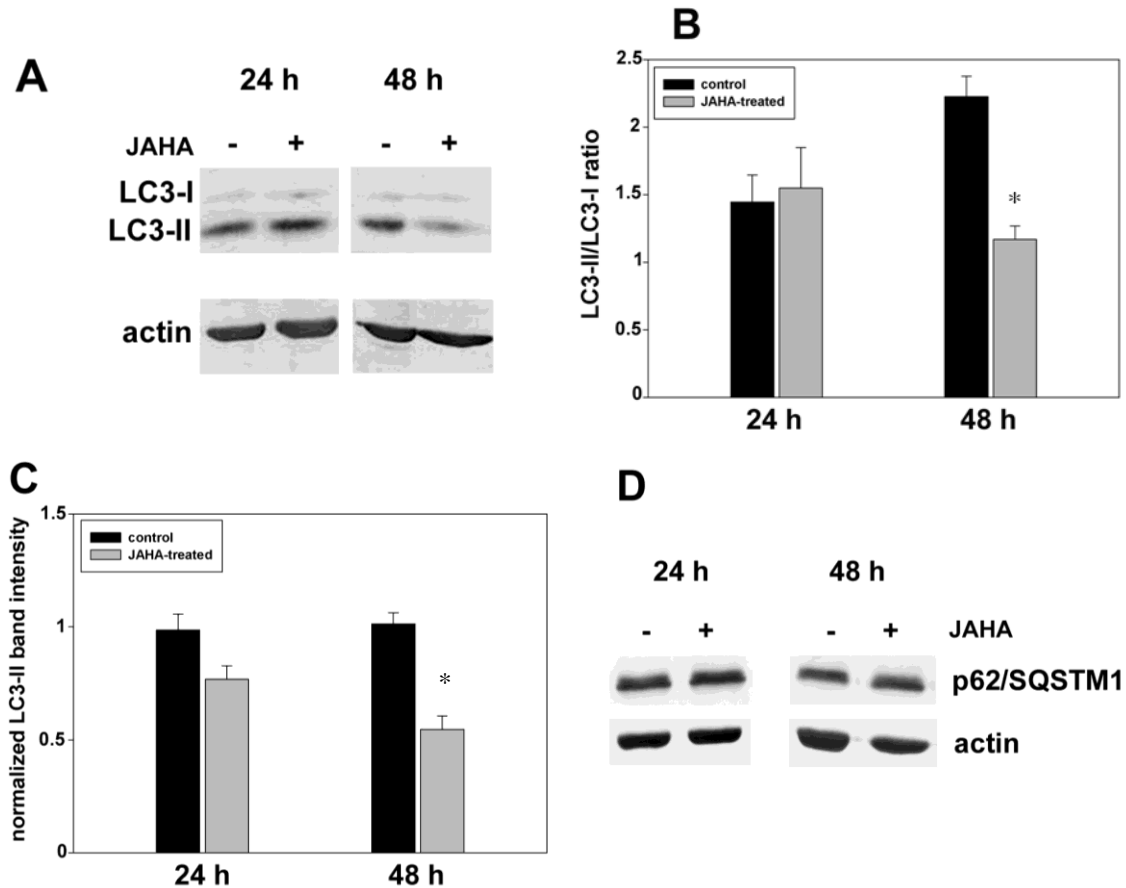


**Figure 4.8.** Effect of JAHA treatment for 24 and 48 h on autophagosome formation in MDA-MB231 cells. A) SDS-PAGE and Western blotting for LC3-I and -II of whole-cell lysates of samples grown in control conditions or exposed to 8.45  $\mu$ M JAHA for 24 and 48 h. Beta-actin was used as loading control. B) and C) Histograms showing the LC3-II/LC3-I ratio (B) and the normalized LC3-II band intensity (C) of control (black bars) and JAHA-treated (grey bars) MDA-MB231 cells after 24 and 48 h of culture. The results are expressed as mean  $\pm$  s.e.m. of triplicate experiments. \* indicates  $p < 0.05$ . D) SDS-PAGE and Western blotting for p62/SQSTM1 of whole-cell lysates of samples grown in control conditions or exposed to 8.45  $\mu$ M JAHA for 24 and 48 h. Beta-actin was used as loading control.

Interestingly, when we evaluated the amount of LC3-I, LC3-II, and p62/SQSTM1 after shorter term JAHA treatment, that is, at 18 h from cell plating, we found an increase of the LC3-II/LC3-I ratio by about 62% and a reduction of p62/SQSTM1 down to about 20% (figure 4.9), consistent with an early autophagy induction, which is then followed by an arrest of the

autophagic flux over 24-48 h of treatment. To check whether inhibition of the autophagic process could account, at least in part, for the observed JAHA-triggered lethal effect on MDA-MB231 cells, cells were coincubated with 8.45  $\mu$ M JAHA and increasing concentrations of rapamycin (sirolimus), an antibiotic acting as autophagy promoter via inhibition of the mammalian target of rapamycin (mTOR), a serine-threonine kinase that plays a key role in regulating fundamental cellular activities, such as growth, proliferation, cytoskeletal architecture, transcription, and translation. When MDA-MB231 cells were coincubated with 8.45  $\mu$ M JAHA and 1 nM rapamycin, by analogy with BHT treatment, we found that also this cotreatment was capable of reversing the JAHA triggered decrease in cell number figure 4.10, thereby revealing autophagy inhibition as a further aspect, supplementary to early ROS production, involved in the cytotoxic effect exerted by the HDACi under study on MDA-MB231 breast tumor cells.

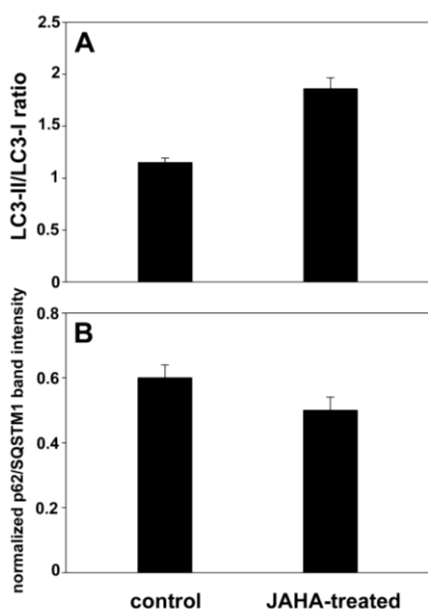
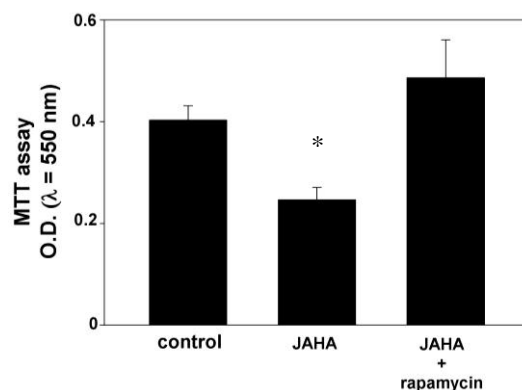


**Figure 4.9.** Effect of JAHA treatment for 18 h on autophagosome formation in MDA-MB231 cells. Histograms showing the LC3-II/LC3-I ratio (A) and the normalized p62/SQSTM1 band intensity (B) of control and JAHA-treated cells.

**Figure 4.10.** Effect of rapamycin co-treatment on JAHA-induced cytotoxicity on MDA-MB231 cells. MTT assay of control, JAHA-treated and JAHA/rapamycin co-treated MDA-MB231 cells. The culture was grown for 48 h and the assay was made in triplicate. The results are expressed as mean  $\pm$  s.e.m. \* indicates  $p < 0.05$ . Rapamycin at 1 nM concentration induced a reversal of the cytotoxic effect exerted by JAHA.



## 4.7 Inability of JAHA to affect MDA-MB231 cell motile behaviour

A wound assay was set up and performed, to evaluate the effects of migration on MDA-MB231 breast cancer cells treated with JAHA. Cultures were grown to a confluency of 80-90%. A wound was created using the scratch machine (figure 4.11). The migration of the cells treated with JAHA into the denuded area of the artificial wound was evaluated. The migrating cells were distinguishable from non-migrating cells and showed directional change towards the denuded area.

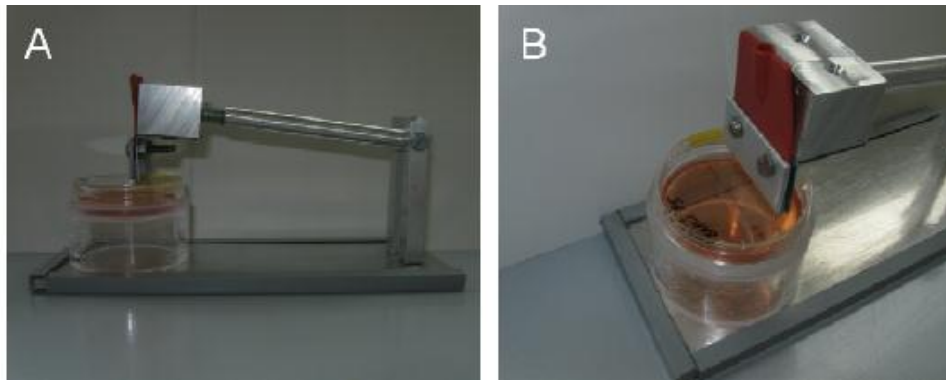


**Figure 4.11.** The scratch machine. A) The scratch machine is shown with an adjusted cell dish. B) Head of the scratch machine is shown to visualise the scraper.

MDA-MB231 cells cultured with RPMI/H medium were assessed for migration by comparison to migrated cells cultured in control medium, (figures 4.12) where proliferation was inhibited by hydroxyurea.

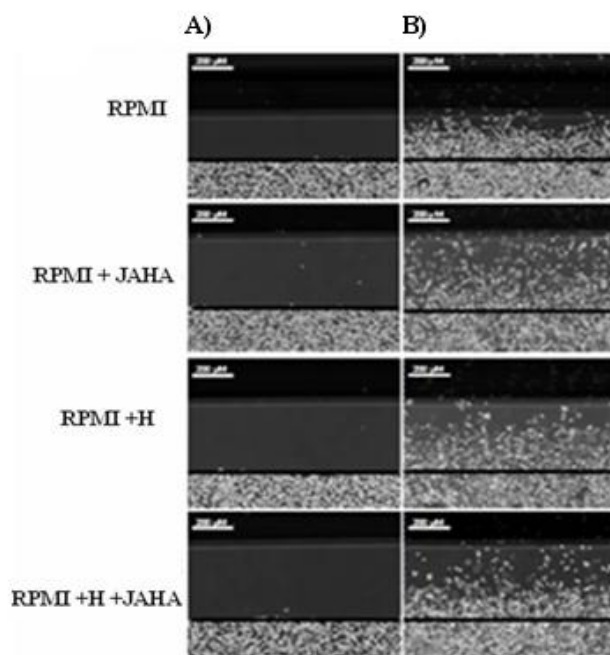


**Figure 4.12.** The migration Assay before and after incubation of scraped MDA-MB231 cells in the respective media. A) Scraping of MDA-MB231 for the migration assay using a line drawn underneath the culture dish to simplify scraping. B) MDA-MB231 cells after 24 h of incubation in RPMI, RPMI/JAHA, RPMI/H, RPMI/H/JAHA. The results shown were performed in triplicates. Bar=200  $\mu$ M.

For the evaluation of the wound assay, the migrating MDA-MB231 cells were counted and statistical analysis was applied using the Microsoft Office Programme Excel 2007. Since the migration assay was performed in triplicates, a mean value of all counted areas, five in total, for each of the three plates was taken (tables 4.1-4.4). In addition, the standard deviation was calculated for every culture dish. The probability (p) value was calculated for comparison of the RPMI and the RPMI supplemented with JAHA to evaluate the statistical significance observed amongst the migrating MDA-MB231 cells stimulated by the respective media. For the final evaluation, the averaged mean value with the respective standard deviation was plotted in a graph (figure 4.13).

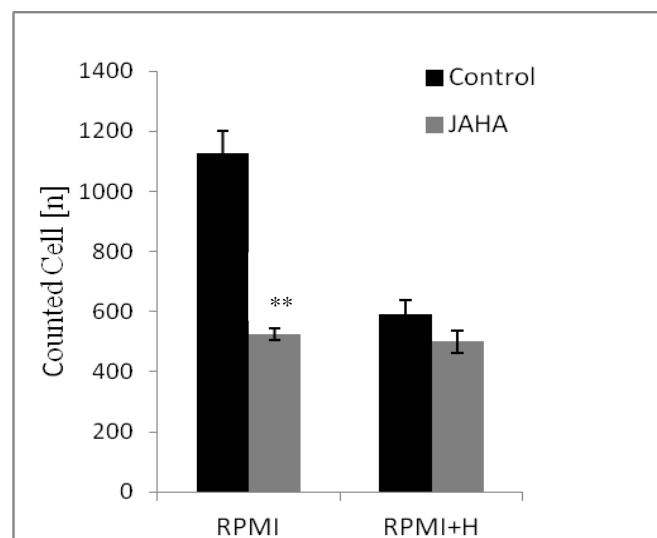


**Figure 4.13.** Evaluation of the migration assay. The histogram shows the total number of migrated MDA-MB231 cells cultured in RPMI medium supplemented with JAHA compared to cells grown in plain medium. (control). Proliferation effects were excluded by the addition of 2 mM hydroxyurea. The result was evaluated from triplicate assays. \*\* indicates  $p < 0.01$ .

In this case we observed that JAHA had no effect on the motile behaviour of MDA-MB231 cells but influence only the proliferation of this cell line, the data are shown in the tables below. These data were obtained in collaboration with Prof. Tobiasch of the University of Applied Sciences of Bonn-Rhein-Sieg, in Germany.

<b>RPMI</b>							
<b>Number of count area</b>	<b>1</b>	<b>2</b>	<b>3</b>	<b>4</b>	<b>5</b>	<b>Mean value</b>	<b>Standard deviation</b>
<b>Plate 1</b>	1216	1043	1149	1237	1231	1175,2	81,79364278
<b>Plate 2</b>	1048	1220	1065	1000	1100	1086,6	82,8118349
<b>Plate 3</b>	1500	1024	1030	1012	1031	1119,4	212,8962188
<b>Total</b>						<b>1127,066667</b>	<b>75,39989955</b>

**Table 4.1.** Statistical data of a migration assay performed with MDA-MB231 cells stimulated with control RPMI medium. This experiment was performed in triplicate.

<b>RPMI+JAHA</b>							
<b>Number of count area</b>	<b>1</b>	<b>2</b>	<b>3</b>	<b>4</b>	<b>5</b>	<b>Mean value</b>	<b>Standard deviation</b>
<b>Plate 1</b>	478	571	590	585	579	560,6	46,71509392
<b>Plate 2</b>	473	475	500	353	377	435,6	65,86956809
<b>Plate 3</b>	589	602	534	570	596	578,2	27,48090246
<b>Total</b>						<b>524,8</b>	<b>19,19434661</b>

**Table 4.2.** Statistical data of a migration assay performed with MDA-MB231 cells stimulated with control RPMI medium supplemented with 8.45  $\mu$ M of JAHA. This assay was performed in triplicate.

<b>RPMI+H+JAHA</b>							
<b>Number of count area</b>	<b>1</b>	<b>2</b>	<b>3</b>	<b>4</b>	<b>5</b>	<b>Mean value</b>	<b>Standard deviation</b>
<b>Plate 1</b>	519	397	394	470	615	479	92,36611933
<b>Plate 2</b>	392	369	392	414	400	393,4	16,33401359
<b>Plate 3</b>	543	665	680	637	615	628	53,73081053
<b>Total</b>						<b>500,1333333</b>	<b>38,01773404</b>

**Table 4.3.** Statistical data of a migration assay performed with MDA-MB231 cells stimulated with control RPMI medium supplemented with 8.45  $\mu$ M of JAHA and with 2 mM of H-hydroxy urea. This assay was performed in triplicate.

<b>RPMI+H</b>							
<b>Number of count area</b>	<b>1</b>	<b>2</b>	<b>3</b>	<b>4</b>	<b>5</b>	<b>Mean value</b>	<b>Standard deviation</b>
<b>Plate 1</b>	637	474	645	700	412	573,6	123,6216001
<b>Plate 2</b>	578	526	608	499	505	543,2	47,74620404
<b>Plate 3</b>	670	725	637	620	663	663	40,0562105
<b>Total</b>						<b>593,2666667</b>	<b>46,18691382</b>

**Table 4.4.** Statistical data of a migration assay performed with MDA-MB231 cells stimulated with control RPMI medium supplemented with 2 mM of H-hydroxy urea. This assay was performed in triplicate.

## 4.8 Effect of JAHA on ERK and AKT signaling pathways

Activation of ERK is known to regulate cell proliferation (McCubrey et al., 2007). Therefore, we investigated whether JAHA reduced cell viability by altering cell survival pathway. We assessed the expression of total and phosphorylated ERK1/2 proteins. In MDA-MB231 breast cancer cells treated with 8.45  $\mu$ M of JAHA decreases the phosphorylation of ERK1/2 at Thr 202 and Ty 204 at 18, 30 h of the treatment and increases the total ERK1/2 level at 48 h as shown in figures 4.14-4.15.

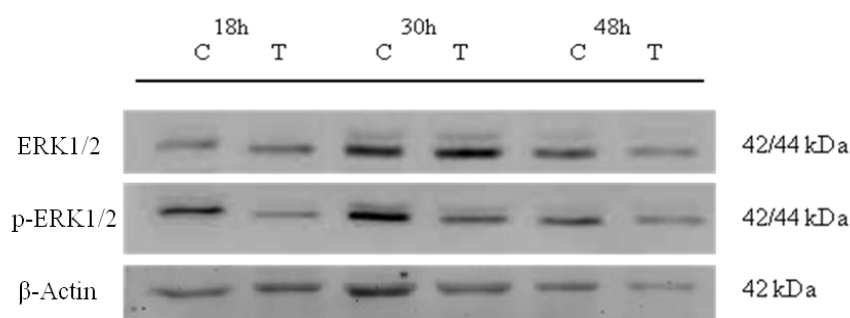


**Figure 4.14.** JAHA blocks the activation of p-ERK1/2 at early times. Different total cell lysates were prepared and Western Blot analysis was performed for ERK1/2 and p-ERK1/2 signaling proteins in control and 8.45  $\mu$ M JAHA-treated cells cultured for 18, 30 and 48 h. Beta-actin was used as loading control.

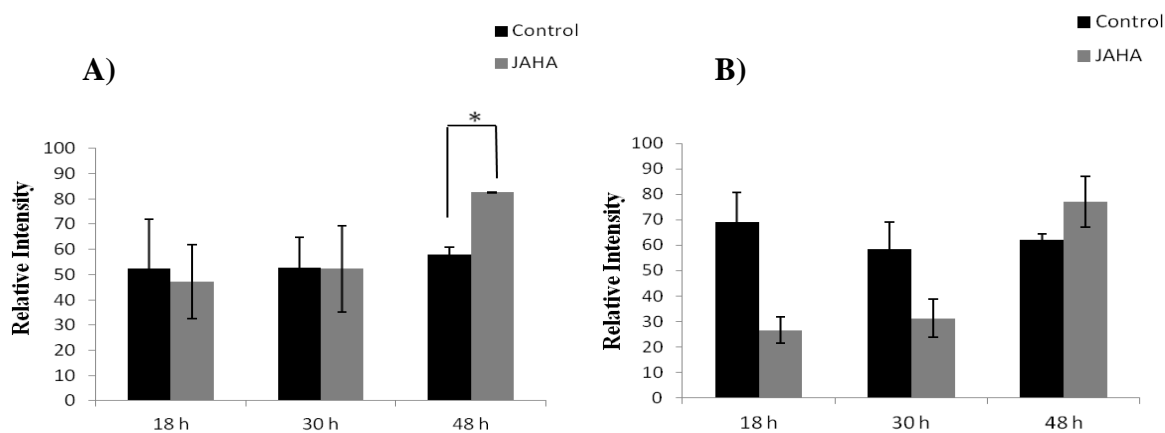


**Figure 4.15** JAHA effect on A) ERK1/2 and B) p-ERK1/2 levels in MDA-MB231 cells incubated either in the absence (control) or in the presence of 8.45  $\mu$ M JAHA for 18, 30 and 48 h. The data of the densitometric analysis are expressed as mean  $\pm$  s.e.m. of triplicate experiments. \* indicates  $p < 0.05$  for JAHA treatment compared to control.

We also assessed the effects of JAHA on cell survival signaling pathway regulated by Akt. A reduced of total Akt in 8.45  $\mu$ M JAHA-treated MDA-MB231 cells after 30 hours was observed while no significant change in the AKT phosphorylated expression at Ser 473 was noticed in figures 4.16-4.17. (These data were obtained in collaboration with Prof. Maria Carmela Roccheri, Dr. Roberto Chiarelli and Dr. Liana Bosco of Department STEBICEF of the University of Palermo).

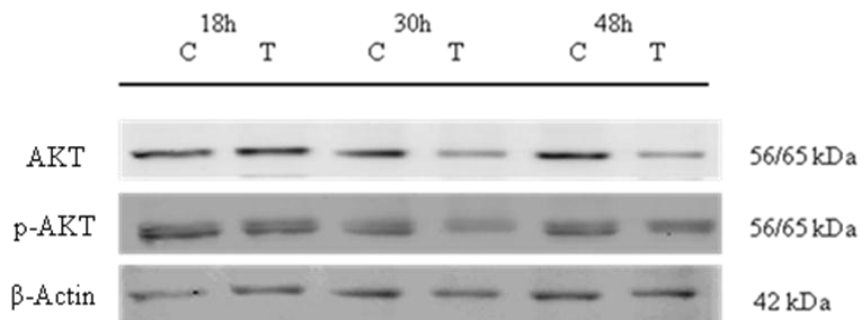


**Figure 4.16.** Different total cell lysates were prepared and Western Blot analysis was performed for AKT and p-AKT signaling proteins in control and 8.45  $\mu$ M JAHA-treated cells cultured with for 18, 30 and 48 h. Beta-actin was used as loading control.

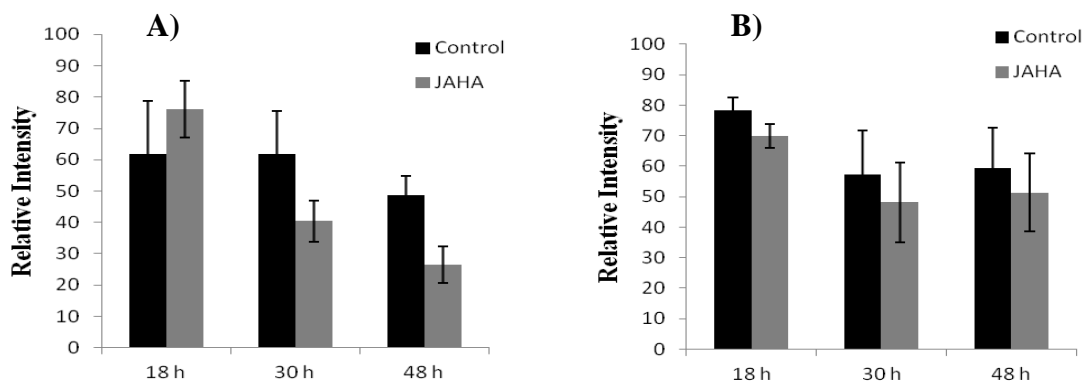


**Figure 4.17.** JAHA effect on A) AKT and B) p-AKT levels in MDA-MB231 cells incubated either in the absence (control) or in the presence of 8.45  $\mu$ M JAHA for 18, 30 and 48 h. The data of the densitometric analysis are expressed as mean  $\pm$  s.e.m. of triplicate experiments. The densitometry analysis was performed by Quantity One software.



## 4.9 JAHA influence on DNMT1 protein expression in MDA-MB231 cells

The observed inhibition of DNMT1 activity by JAHA may be due to a reduction of its expression. We investigated this effect in MDA-MB232 cells treated with 8.45  $\mu\text{M}$  of JAHA compared to control at 18, 30, 48 hours by Western blot analysis, (figure 4.18). JAHA down-regulated DNA (cytosine-5-)-methyltransferase 1 (DNMT1) after 18 h and until 48 h of the treatment.

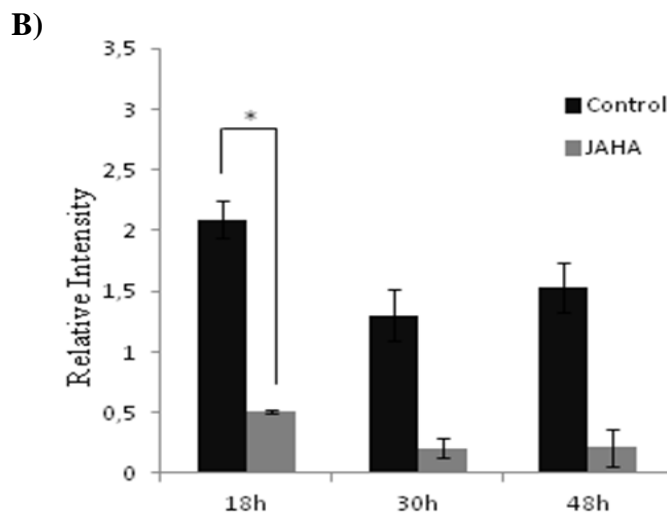
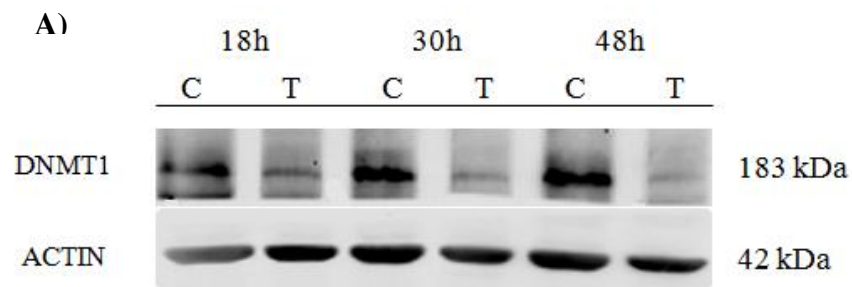
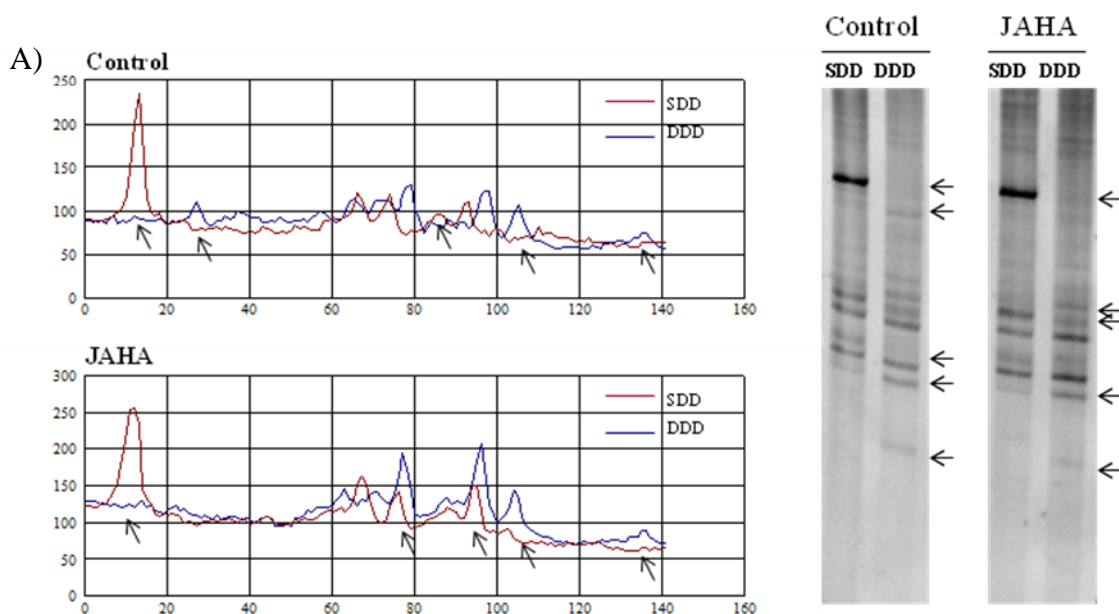


**Figure 4.18.** A) Different total cell lysates were prepared from JAHA-treated (8.45  $\mu\text{M}$ ) and untreated proliferating MDA-MB231 cells cultured for 18, 30, 48 h and submitted to Western blot analysis of DNMT1 protein. Beta-actin was used as loading control.

B) Densitometric analysis of DNMT1 expression by Quantity One software. The data are expressed as mean  $\pm$  s.e.m. of triplicate experiments. \* indicates  $p < 0.05$  for JAHA treatment compared to control.

## 4.10 Epigenetic effects of JAHA on genomic methylation status in MDA-MB231 cells

Histone deacetylase inhibitors (HDACi) have been actively explored as a new generation of chemotherapeutics for cancers, generally known as epigenetic therapeutics. Recent findings indicate that several types of HDACi repress angiogenesis, a process essential for tumor metabolism and progression. Changes in genome methylation may be one of the mechanism through which HDACi act as gene expression regulators. The effect of JAHA on DNA methylation patterns in the breast cancer cell line was therefore investigated. In particular, DNA isolated from MDA-MB231 cells grown for 18, 30 and 48 h, either in the absence or in the presence of 8.45  $\mu\text{M}$  JAHA was analysed by MeSAP-PCR, to investigate changes induced by the HDACi on global methylation status of genomic DNA. In accordance with this method, genomic DNA samples are digested with methylation-insensitive restriction enzyme (SDD) followed by methylation-sensitive restriction enzymes (DDD). Comparison of the products from PCR amplification using a no-specific primer allows screening for DDD from either control or JAHA-treated MDA-MB231 cells and the results are reported in figure 4.19. The examination of the PCR fragments differences revealed that treatment with 8.45  $\mu\text{M}$  JAHA was effective in modifying the global DNA methylation pattern, as shown by the different number, intensity and size of the bands in the matched samples compared with untreated MDA-MB231 cells after 48 h. It is worth mentioning that MeSAP-PCR gives no indication of the genomic region affected by methylation/demethylation by an external agent.



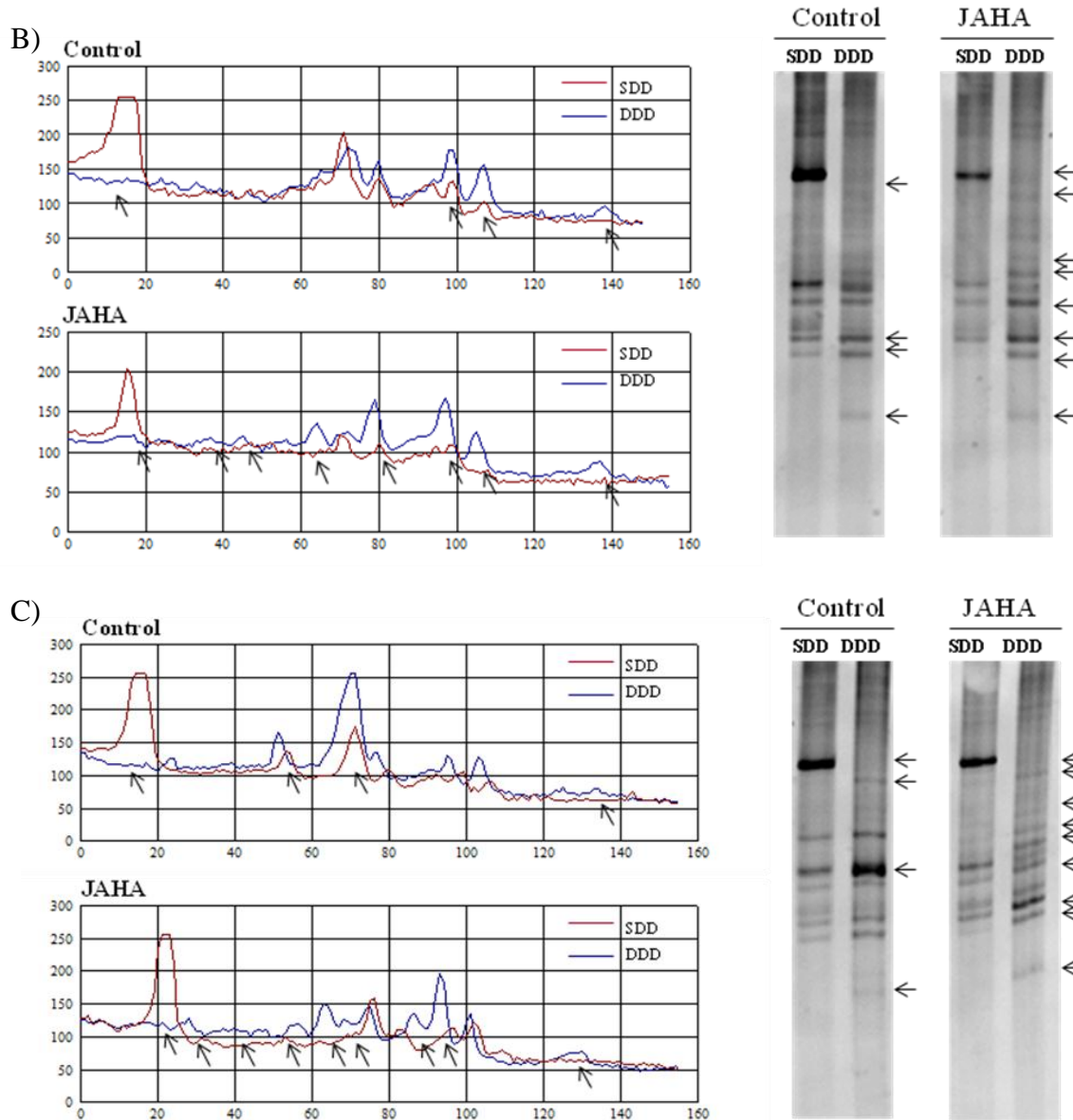


**Figure 4.19.** Methylation-sensitive arbitrarily-primed fingerprintings (right) and relevant densitometry profiles (left) of the matched SDD and DDD pairs from either untreated or JAHA-treated MDA-MB231 cells cultured for A) 18 h, B) 30 h, C) 48 h. PCR was performed using an arbitrary primer after 16h-restriction enzyme digestion with 5X excess of AfaI (single-digested DNA, SDD) or AfaI + HpaII (double-digested DNA, DDD). Matching SDD and DDD fingerprinting, differences in appeared/disappeared or increased/decreased bands (indicated by arrows) were counted as semiquantitative evidences of different genomewide methylation status. The images are representative of three independent experiments and were obtained by SigmaGel Software support.

The difference in the DNA methylation pattern between single-digested DNA (SDD) and double-digested DNA (DDD) shows us that the second enzyme was able to cut a major number of unmethylated CpG-contained sites; then, it is possible to deduce that to the increasing of the variation of genomic methylation pattern, corresponds a decreasing of the genomewide DNA-methylation status in an inversely-proportional manner.

Finally, the data here reported show an evident hypomethylation of the DNA after 48 h of treatment with JAHA (figure 4.20). These data were obtained in collaboration with Prof. Fabio Caradonna of Department STEBICEF of the University of Palermo.

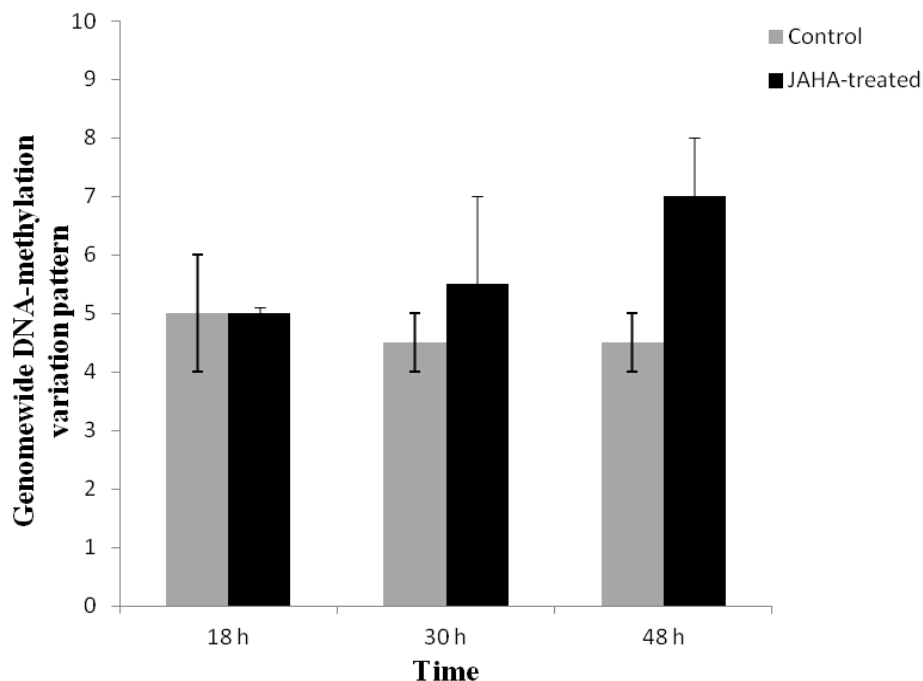


**Figure 4.20.** Variation of the genomic methylation pattern in control and JAHA-treated cells. In the ordinate the pattern refers to the total number of different bands between the treated and control samples at different times. The assay was performed in triplicate.

#### 4.11 Differentially-Expressed Genes in MDA-MB231 cell treated with JAHA

To search for differentially-expressed genes in MDA-MB231 cells treated at 18, 24, 48 h with JAHA 8.45  $\mu$ M, DD-PCR was performed on enriched mRNA samples isolated from control and treated cell preparations, in the presence of primer combinations as listed previously in Materials and Methods section. After polyacrylamide gel electrophoresis and silver stain, several bands appeared differently expressed in either control and treated sample, and they were cut from the gel (figure 4.21).

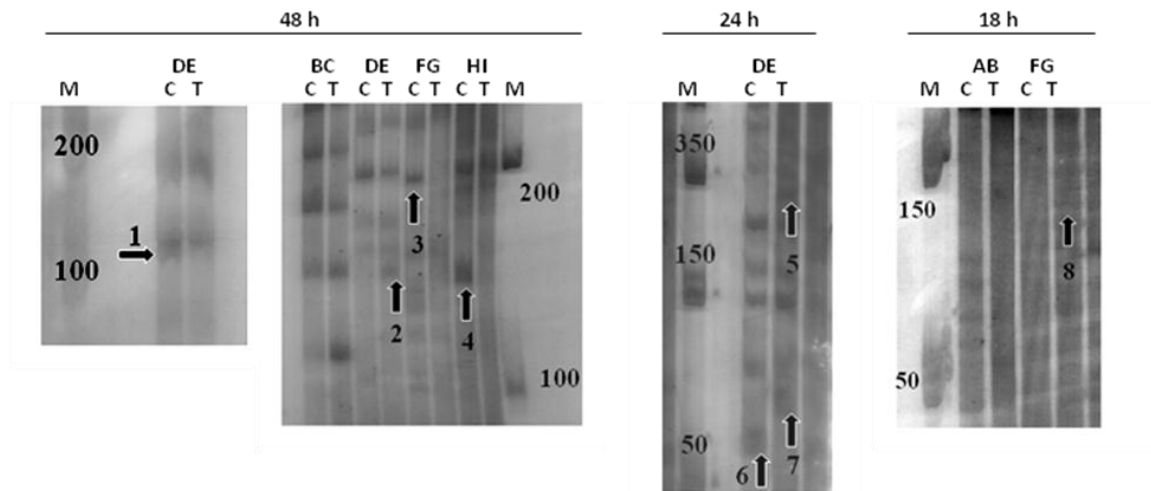


**Figure 4.21.** 6% polyacrylamide gel of cDNA preparations from MDA-MB231 cells cultured with (T) and without (C) JAHA at different time (18, 24, 48 h). AB, BC, DE, FG, and HI indicate the different primer pairs as listed previously. M=100 bp DNA marker (Invitrogen) for 48 h gels and M=50 bp DNA marker (Invitrogen) for 24 and 18 h gels. The arrows indicate the differentially-displayed bands that have been identified by silver stain.

The eight bands, indicated in the figure with arrows were submitted to further analysis. To this purpose, the cDNA contained in the bands was purified, re-amplified until purity and adequate yield, and then the material was submitted to sequencing. The analysis by FASTA showed homology for band 2 with a portion of cDNA of Brefeldine A-Inhibited guanine nucleotide-exchange protein 3 (acc. nr. NM\_020340.3), Protein kinase C epsilon (acc. nr. NM\_005400.2), Mediator of RNA Polymerase II transcription subunit 25 (acc. nr. NM\_030973.3) and ER-Golgi intermediated compartment 2 KDa protein (acc. nr. NM\_016570.2); for band 4 with a portion of cDNA of Protein kinase C iota (acc. nr. NM\_002740.5), for band 5 with a portion of cDNA of Inactive\_N-acetylated-alpha-linked acidic peptidasi-like protein 2 (acc. nr. NM\_207015.2) and neurotrophic tyrosine kinase, receptor, type 2 (acc. nr. NM\_001018064.1) for band 7 with a portion of cDNA of DNA repair protein (acc. nr. NM\_005732.3), and for band 8 with a portion of Leucina-Rich-Repeat and calponin homology domain containing protein 1 (acc. nr. NM\_001164211.1). No sequence identified for 1, 3, 6 bands (table 4.5).

Gel bands	Gene name	Gene reference
<b>1</b> (cDNA 48h)	No seq.	
<b>2</b> (cDNA 48h)	Brefeldine A-Inhibited guanine nucleotide-exchange protein 3 <i>PKCε</i> (Protein kinase C epsilon) <i>MED25</i> (Mediator of RNA Polymerase II trascription subunit 25) <i>Ergic2</i> (ER-Golgi intermediated compartment 2KDa protein)	NM_020340.3 NM_005400.2 NM_030973.3 NM_016570.2
<b>3</b> (cDNA 48h)	No seq.	
<b>4</b> (cDNA 48h)	<i>PKCι</i> (Protein kinase C iota)	NM_002740.5
<b>5</b> (cDNA 24h)	<i>NAALAD2</i> (Inactive_N-acetylated-alpha-linked acidic peptidasi-like protein 2) <i>NTRK2</i> (neurotrophic tyrosine kinase, receptor, type 2)	NM_207015.2 NM_001018064.1
<b>6</b> (cDNA 24h)	No seq.	
<b>7</b> (cDNA 24h)	<i>Rad50</i> (DNA repair protein)	NM_005732.3
<b>8</b> (cDNA 18h)	<i>Lrch1</i> (Leucina-Rich-Repeat and calponin homology domain containing protein 1)	NM_001164211.1

**Table 4.5** FASTA analysis of cDNAs that showed homology with the sequences obtained for the different bands extracted from DD gel.

NCBI has a tool for aligning two sequences provided by the user. The tool is called BLAST 2 Sequences, which uses the chosen BLAST algorithm to align sequences as if they were found in a database search. This can be helpful for observing differences between two sequences, however, it still performs local alignments, not global alignments (data showed in the table 4.6).

Gene name	Score	E-value	Identity	Gaps
<i>ERGIC</i>	37.4 bits (40)	4.5	23/25 (92%)	0%
<i>PKCε</i>	35.6 bits (38)	9.9	19/19 (100%)	0%
<i>Brefeldin-A</i>	37.4 bits (40)	4.5	28/30 (92%)	0%
<i>PKCι</i>	30.2 bits (15)	114	21/21 (100%)	0%
<i>MED25</i>	35.6 bits (38)	5.4	25/25 (100%)	0%
<i>RAD50</i>	39.2 bits (42)	0.87	23/24 (96%)	0%
<i>NAALAD2</i>	37.4 bits (40)	4.9	25/28 (89%)	0%
<i>NTRK2</i>	37.4 bits (40)	4.9	25/28 (89%)	0%
<i>LRCH1</i>	37.4 bits (40)	4.9	22/23 (96%)	0%

**Table 4.6.** Alignment statistics for match. High E values make sense because short sequences were analyzed.

Since DD-PCR may give false positive data, experiments were carried out to confirm the data obtained. To this purpose, first semiquantitative PCR assays were performed on cDNA preparations obtained from control and JAHA-treated MDA-MB231 cells in the presence of primers specific for LRCH1, RAD 50, ERGIC 2, Inactive N-acetylated alpha-linked acid dipeptidase like-2, Protein kinase iota, NTRK2, Brefeldine A-Inhibited guanine nucleotide-exchange protein 3, Protein kinase epsilon and MED 25, designed using Primer 3 online software (<http://primer3.wi.mit.edu>). In order to put in evidence the possible presence/absence of amplification bands between control and treated samples, thereby confirming the DD-PCR data, the cDNAs were submitted to a lower number (i.e 25-35 cycles) of amplification. *GAPDH* was used as a control. The amplified DNA was loaded directly into an agarose gel after the PCR process. As shown in figure 4.22, data from this first approach indicated that JAHA at 8.45  $\mu$ M concentration induced the expression of *NTRK2* and *RAD 50* genes in MDA-MB231 breast cancer cells after 48 and 24 h of treatment, respectively, whereas expression of *Protein Kinase ε* was restrained after 48 h of treatment.

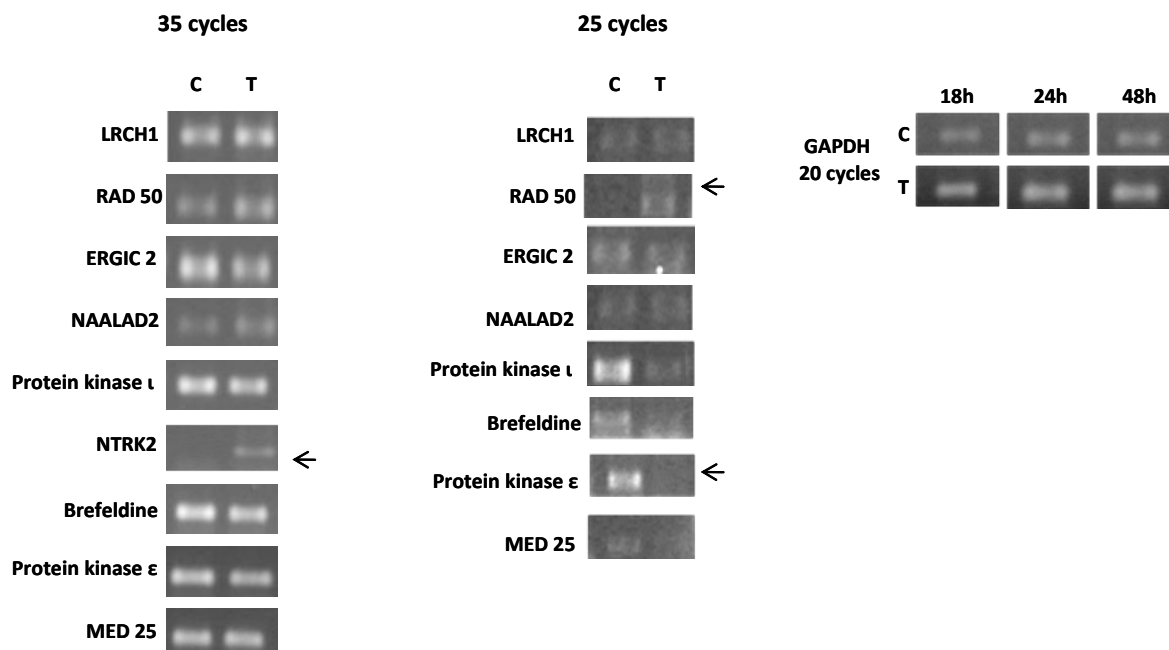


**Figure 4.22.** JAHA influence gene expression in human breast cancer cells. Total RNA isolated from MDA-MB231 cells treated with DMSO (C), or JAHA (T) at 8.45  $\mu$ M for 18, 24 and 48 h, was reverse transcribed and subjected to 35 and 25 cycles of PCR amplifications with primers specific for: *LRCH1* (cDNA 18h), *RAD 50* (cDNA 24h), *ERGIC 2* (cDNA 48h), *N-acetylated alpha-linked acid dipeptidase like-2* (cDNA 24h), *Protein kinase iota* (cDNA 48h), *NTRK2* (cDNA 24h), *Brefeldine A-Inhibited guanine nucleotide-exchange protein 3* (cDNA 48h), *Protein kinase epsilon* (cDNA 48h), *MED 25* (cDNA 48h). PCR of *glyceraldehyde-3-phosphate dehydrogenase (GAPDH)* was included and served as a loading control. The panel shows the amplified PCR products (220 bp for *LRCH1*, 215 bp for *RAD50*, 196 bp for *ERGIC*, 229 for *NAALAD2*, 169 bp for *PKC $\iota$* , 181 bp for *NTRK2*, 231 bp for *Brefeldine A*, 249 bp for *PKC $\epsilon$* , 188 for *MED25* and 414 bp for *GAPDH*). The arrows indicate the differentially expressed genes, i.e. *NTRK2* and *RAD50* (prominently up-regulated by JAHA) and *Protein Kinase  $\epsilon$*  (prominently down-regulated by JAHA).

Second, Real Time PCR assays were carried out in order to extend the validation, if applicable, of the DD-PCR results. Only the expression of *Brefeldine A*, *Protein kinase epsilon*, *Protein kinase iota*, *ERGIC 2*, *MED 25* and *RAD50* in control and treated samples was examined.

This technique utilizes the fluorophore, Sybr Green, which intercalates in a nonspecific manner into the DNA double helix, that is formed during the PCR. Sybr Green when excited emits a green light whose intensity is proportional to the concentration of amplified DNA. In particular the number of the PCR cycle when Sybr Green starts to emit fluorescence is proportional to the original amount of cDNA in each sample. As shown in figure 4.23, JAHA at 8.45  $\mu$ M concentration induced the expression of *RAD 50* genes after 24 h of the treatment in MDA-MB231 breast cancer cells, while reduced the expression of *Protein Kinase  $\epsilon$*  after 48 h of treatment. No difference was observed for the other genes studied.



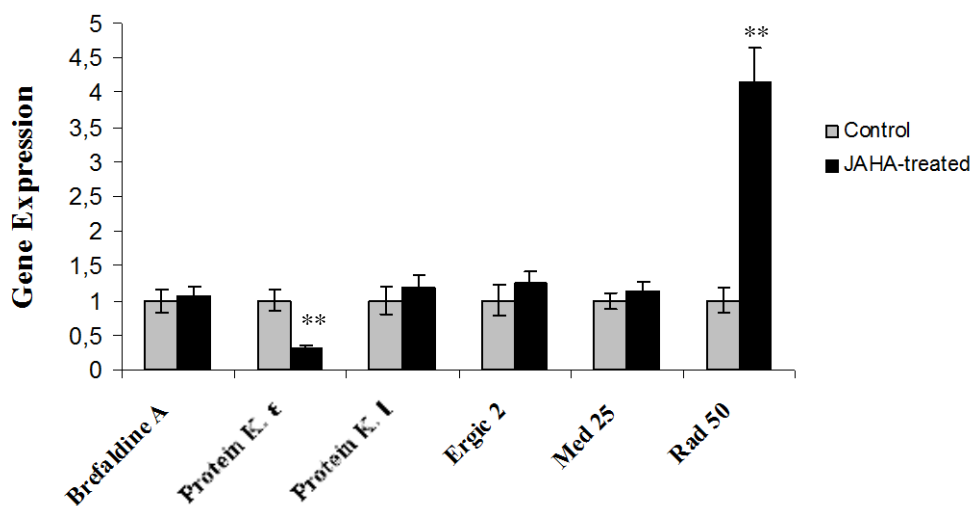


**Figure 4.23.** Gene expression (arbitrarily units) levels in MDA-MB231 cells, control and treated with 8.45  $\mu$ M JAHA, assayed through Real time PCR with  $\beta$ -actin used as an internal control. Values are the mean  $\pm$  s.e.m. of two quadruplicate experiments. \* indicates  $p < 0.05$ , \*\* indicates  $p < 0.01$  for JAHA treatment compared to control.

The same approach was applied to cells treated with SAHA at the same dosage (8.45  $\mu$ M) and at the same time of exposure (24 h for *RAD50* and at 48 h for the other genes). This was aimed to check differences and/or similarities in the gene signatures associated to the exposure of cells to the two closely-related HDACis. The data obtained show a clear reduction in the expression levels of *genes PKε*, *Brefeldine A*, *PKI* and *Ergic 2* while no significant change in the expression levels of *Med 25* and *Rad 50* (figure 4.24).

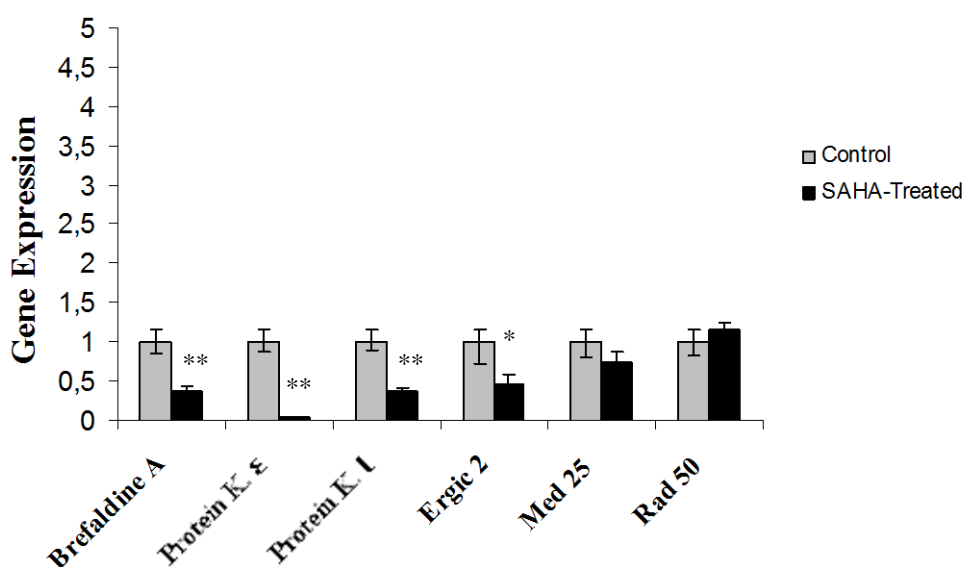


**Figure 4.24.** Gene expression (arbitrarily units) levels in MDA-MB231 cell, control and treated with 8.45  $\mu$ M SAHA, assayed through Real time PCR with  $\beta$ -actin used as an internal control. Values are the mean  $\pm$  s.e.m. of two quadruplicate experiments. \* indicates  $p < 0.05$ , \*\* indicates  $p < 0.01$  for JAHA treatment compared to control.

Literature data (Huang et al., 2000) have previously reported that SAHA treatment to MDA-MB231 cells was able up-regulate a number of genes associated with differentiation and/or growth inhibition. These genes encode for *gelsolin*, *isopentenyl-diphosphate delta isomerase (IDI1)*, and *1,25-dihydroxyvitamin D-3 up-regulated protein 1 (VDUP1)*. Induction of these genes may contribute to SAHA-mediated pro-differentiating and antiproliferative effects. In order to extend the comparative evaluation of the molecular effects of SAHA and JAHA molecules on MDA-MB231 cells, we checked the effects of JAHA on the expression levels of the same genes identified as up-regulated in SAHA-treated cells.

The results obtained show a similarity of action of SAHA and JAHA on the expression levels of the gene examined (figure 4.25).

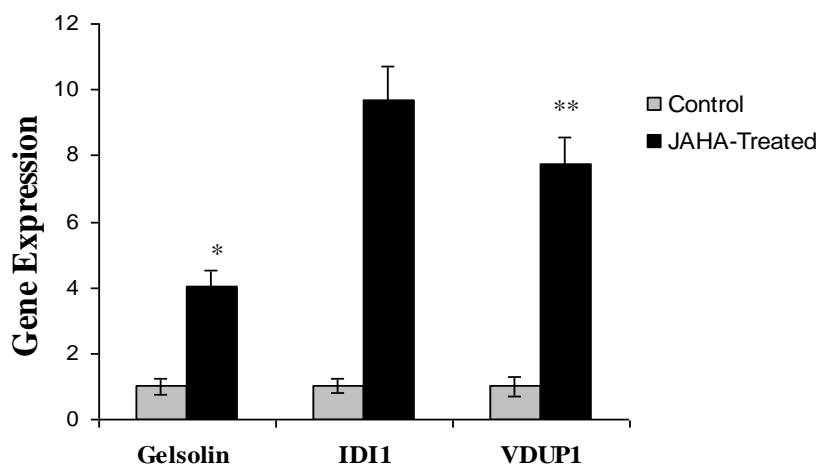


**Figure 4.25.** Gene expression (arbitrarily units) levels in MDA-MB231 cells, control and treated for 48 h with 8.45  $\mu$ M JAHA, assayed through Real time PCR with  $\beta$ -actin used as an internal control. Values are the mean  $\pm$  s.e.m of two quadruplicate experiments.\* indicates  $p < 0.05$ , \*\* indicates  $p < 0.01$  for JAHA treatment compared to control.

## 4.12 Differentially-Expressed Proteins in MDA-MB231 cell treated with HDACis

In order to expand the search of JAHA-associated signatures to the protein level, proteomic analysis were performed and showed a differential expression of eleven proteins (six, one and four associated to 18, 24 and 48 h of treatment with JAHA at 8.45  $\mu$ M, respectively). Of the six proteins associated to 18 h-treatment, four were down-regulated (i.e. AHNAK protein, high mobility group protein B2, Cystatin-B, High mobility group protein B1) and two were up-regulated (i.e. Ribosome-binding protein 1, Glutaredoxin-1) in treated samples compared to controls. A single up-regulated protein (i.e. Hematological and neurological Expressed 1

protein) was found in cells treated with JAHA for 24 hours, and four up-regulated proteins in cells treated with JAHA for 48 hours (i.e. prelamin-A/C, Ribosome-binding protein, Sulfiredoxin-1, Histone H1) (tables 4.7-4.9).

<i>cod.</i>	<i>Protein</i>	<i>qvalue</i>	<i>ratio</i>	<i>fold change</i>	<i>peptides</i>
<b>Q09666</b>	Neuroblast differentiation-associated protein AHNAK	0.00079	1.35	1.35	276
<b>P26583</b>	High mobility group protein B2	0.00158	2.44	2.44	12
<b>P04080</b>	Cystatin-B	0.02422	2.94	2.94	7
<b>Q9P2E9</b>	Ribosome-binding protein 1	0.02587	0.61	1.64	22
<b>P09429</b>	High mobility group protein B1	0.08112	2.70	2.70	11
<b>P35754</b>	Glutaredoxin-1	0.08978	0.48	2.09	5

**Table 4.7.** Proteomic analysis of proteins differentially expressed in MDA-MB231 cells cultured in control conditions and treated with JAHA at 8.45  $\mu$ M concentration for 18 h.

<i>cod.</i>	<i>Protein</i>	<i>qvalue</i>	<i>ratio</i>	<i>fold change</i>	<i>peptides</i>
<b>Q9UK76</b>	Hematological and neurological expressed 1 protein	0.02226	0.44	2.26	10

**Table 4.8.** Proteomic analysis of proteins differentially expressed in MDA-MB231 cells cultured in control conditions and treated with JAHA at 8.45  $\mu$ M concentration for 24 h.

<i>cod.</i>	<i>protein</i>	<i>Qvalue</i>	<i>ratio</i>	<i>fold change</i>	<i>peptides</i>
<b>P02545</b>	Prelamin-A/C	0.00075	0.5	2.00	36
<b>Q9P2E9</b>	Ribosome-binding protein 1	0.01057	0.42	2.36	24
<b>Q9BYN0</b>	Sulfiredoxin-1	0.04155	0.12	8.55	3
<b>P07305</b>	Histone H1	0.04578	0.20	5.05	6

**Table 4.9.** Proteomic analysis of proteins differentially expressed in MDA-MB231 cells cultured in control conditions and treated with JAHA at 8.45  $\mu$ M concentration for 48 h.

Twenty-two proteins appeared to be differentially expressed in cells treated with SAHA at the same concentration of JAHA (sixteen, five and one respectively associated to 18, 24 and 48 h-treatment). Of the sixteen proteins identified at 18 h-treatment, six were down-regulated (i.e. Reticulocalbin-1, Microtubule-associated protein 1B, Caprin-1, spectrin alpha chain non-erythrocytic 1 Integrin beta-1, Myristoylated alanine-rich C-kinase substrate) whereas the other ones were up-regulated in the treated samples (i.e. Histone H1.0, neuroblast differentiation-associated protein AHNAK, Hematological and neurological Expressed protein 1, Reticulocalbin-1, Nucleolar and coiled-body phosphoprotein 1, nucleolin,

Eukaryotic translation initiation factor 4H, 78 kDa glucose-regulated protein, Histidine triad nucleotide-binding protein 2 mitochondrial Na(+)/H(+) exchange regulatory cofactor NHE-RF1, non-erythrocytic spectrin alpha chain 1 Integrin beta-1, Heterogeneous nuclear ribonucleoproteins A2/B1). Of the five proteins associated to 24 h-treatment, two were down-regulated (i.e. neuroblast differentiation-associated protein AHNAK, Nicotinamide phosphoribosyltransferase) and three were up-regulated (i.e. Na(+)/H(+) exchange regulatory cofactor NHE-RF1, Histone H1, 78 kDa glucose-regulated protein). Finally, a single protein was identified down-regulated (neuroblast differentiation-associated protein AHNAK) in the samples treated for 48 h (figure 4.10-4.12).

<i>cod.</i>	<i>Protein</i>	<i>qvalue</i>	<i>ratio</i>	<i>fold change</i>	<i>peptides</i>
P07305	Histone H1.0	0.00035	0.11	9.03	6
Q09666	Neuroblast differentiation-associated protein	0.00035	1.41	1.41	257
Q9UK76	Hematological and neurological expressed 1 protein	0.00280	0.47	2.13	10
Q15293	Reticulocalbin-1	0.00469	2.60	2.60	13
Q14978	Nucleolar and coiled-body phosphoprotein 1	0.00489	0.54	1.85	17
P19338	Nucleolin	0.00545	0.51	1.96	28
Q15056	Eukaryotic translation initiation factor 4H	0.00559	0.49	2.04	7
P46821	Microtubule-associated protein 1B	0.01389	2.03	2.03	14
Q14444	Caprin-1	0.01565	1.75	1.75	11
P11021	78 kDa glucose-regulated protein	0.01623	0.64	1.56	35
Q9BX68	Histidine triad nucleotide-binding protein 2, mitochondrial	0.01679	0.20	4.97	3
O14745	Na(+)/H(+) exchange regulatory cofactor NHE-RF1	0.01776	0.37	2.71	4
Q13813	Spectrin alpha chain, non-erythrocytic 1	0.01849	1.51	1.51	36
P05556	Integrin beta-1	0.01877	1.67	1.67	10
P22626	Heterogeneous nuclear ribonucleoproteins A2/B1	0.02038	0.55	1.81	14
P29966	Myristoylated alanine-rich C-kinase substrate	0.05348	1.98	1.98	10

**Table 4.10.** Proteomic analysis of proteins differentially expressed in MDA-MB231 cells cultured in control conditions and treated with SAHA at 8.45  $\mu$ M concentration for 18 h.

<i>cod.</i>	<i>Protein</i>	<i>qvalue</i>	<i>ratio</i>	<i>fold change</i>	<i>peptides</i>
Q09666	Neuroblast differentiation-associated protein	0.00072	1.53	1.53	267
O14745	Na(+)/H(+) exchange regulatory cofactor NHE-RF1	0.00502	0.26	3.79	4
P07305	Histone H1.0	0.01815	0.54	1.85	6
P11021	78 kDa glucose-regulated protein	0.03586	0.55	1.83	35
P43490	Nicotinamide phosphoribosyltransferase	0.05941	3.04	3.04	9

**Table 4.11.** Proteomic analysis of proteins differentially expressed in MDA-MB231 cells cultured in control conditions and treated with SAHA at 8.45  $\mu$ M concentration for 24 h.

---

<i>cod.</i>	<i>Protein</i>	<i>qvalue</i>	<i>ratio</i>	<i>fold change</i>	<i>peptides</i>
Q09666	Neuroblast differentiation-associated protein	0.08576	2.26	2.26	254

---

**Table 4.12.** Proteomic analysis of proteins differentially expressed in MDA-MB231 cells cultured in control conditions and treated with SAHA at 8.45  $\mu$ M concentration for 48 h.

## 5. Discussion

Breast tumour is a widely-spread neoplastic histotype accounting for about 20% of all cancers in women; about 15% of breast cancers are triple-negative and the lack of receptors for estrogens, progesterone and epidermal growth factor makes neoplastic cells highly aggressive and endowed with a higher malignant potential than other breast tumour subtypes (Gluz, et al., 2009). Since the pharmacological options for treating triple-negative tumours are limited, there has been great interest in testing novel drugs or analogues of pre-existing drugs counteracting triple-negative cell growth, which, on the other hand, necessitate of a comprehensive biological characterization. SAHA is an archetypal HDACi whose effect on triple-negative MDA-MB231 breast cancer cells, the model system used in the present study, has been previously tested. In fact, Huang et al., (2000) and Xu et al., (2005) demonstrated that SAHA affected cell cycle progression and induced polyploidy, the onset of apoptosis and also the up-regulation of several proliferation inhibiting- and differentiation promoting-genes, as assessed through DD-PCR assays. The role of SAHA in triggering ROS production and dissipating MMP was reported in other cell model systems, e.g. leukemia and colon carcinoma cells, although such events have been always associated to the promotion of apoptosis or autophagy by the HDACi (Dai et al., 2005; Portanova et al., 2008; Li et al., 2010). In addition, SAHA was proven to enhance autophagy also in other neoplastic cytotypes, such as hepatocellular carcinoma, chondrosarcoma and glioblastoma cells. (Yamamoto et al., 1998; Gammoh et al., 2005; Liu et al., 2010).

In the present study, we have tested the cytotoxic effect on triple-negative MDA-MB231 cells of two ferrocene-containing SAHA analogues, JAHA and homo-JAHA, already validated for their *in vitro* extensive inhibitory activity on class I HDACs, although to a lesser degree for HDAC8, and class IIb HDAC6 (Spencer et al., 2011). The MTT viability assay demonstrated that if exposure to MDA-MB231 cells was prolonged to 72 h, JAHA exhibited an  $IC_{50}$  of 8.45  $\mu$ M whereas homo-JAHA, which differs from JAHA for the presence of an additional methylene spacer, induced a maximum lowering of cell number down to about 63% only. Shorter term treatments of cells with JAHA, i.e. 24 and 48h, determined cell number reduction down to about only 84 and 66%, respectively (data not shown). The individuation of a cytotoxic effect exerted by JAHA on triple-negative cancer cells prompted a more detailed analysis of its mechanism of action, in particular focusing on cell cycle perturbation, and the possible onset of apoptosis and/or autophagy, coupled to ROS over-production and/or MMP dissipation.

Flow cytometric analysis of cell cycle phases produced similar data to those obtained on MCF-7 cells, (Spencer et al., 2011) which are shared with other HDACi (e.g. SAHA, trichostatin, apicidin, psammaplin A), i.e. a perturbation of S phase entry and a delay at G<sub>2</sub>/M transition, (Ueda et al., 2007; Ahn et al., 2008; Yamamoto et al., 2008; Noh et al., 2009; Knutson et al., 2012) although in our model system we did not observe apoptotic cell death as with the other HDACi cited, this being a distinctive feature of JAHA. The most intriguing results on JAHA mechanism of action regard its ability to induce early ROS production and subsequent MMP dissipation and autophagy inhibition, and the reversion of the cytotoxic effect obtained by co-treatment with either anti-oxidant or autophagy-promoter compound.

It is well-known that ROS are generated by mitochondria where a multiplicity of producing sources exist and where also ROS detoxifying systems are actively operating; therefore, the net intracellular amount of ROS derives from the imbalance of ROS production, removal and extra-mitochondrial release (Andreyev et al., 2005). It can be hypothesized that JAHA treatment induces an oxidative stress due to mitochondrial defence failure, such as structural impairment and/or loss of matrix solutes (e.g. glutathione) through the permeability transition pores. On the other hand, initial ROS production may induce the onset of a “vicious cycle” (Andreyev et al., 2005) i.e. a further exacerbation of ROS formation due to the activation of additional ROS-generating sites within the mitochondria, which might be directly responsible of the following MMP collapse as already reported in other cell model systems (Abramov et al., 2007; Rogalska et al., 2008) and may be restrained in the presence of the anti-oxidant BHT.

Autophagy, i.e. the formation of double membrane-autophagosomes sequestering cytoplasmic material which is digested due to subsequent fusion of the vesicles with the lysosomes, plays a complex role in breast cancer. In fact, some authors consider autophagy as a tumour suppressor mechanism leading to cell death, whereas other literature data strongly support the concept that this process is necessary to provide energy and basic elements allowing tumour cells survive under conditions of metabolic stress, due to oxygen and nutrient shortage and rapid proliferative rate (Armstrong et al., 2010). A number of published papers suggest that autophagy rate in MDA-MB231 cells is constitutively elevated, thereby playing a likely pro-survival role. For example, it is acknowledged that inhibition of autophagy sensitizes MDA-MB231 cells to the lethal effects of chemical or physical agents (e.g. sulforaphane and capsaicin treatment, or ionizing radiations), and that MDA-MB231 cells are resistant to rapamycin effects, probably due to their elevated phospholipase D activity that leads to the formation of phosphatidic acid, a lipid involved in autophagosome formation (Chen et al.,

2003; Chang et al., 2007; Apel et al., 2008; Choi et al., 2010; Kanematsu et al., 2010; Moreau et al., 2012). The data here presented clearly indicate that JAHA can be included in the list of those molecules that trigger autophagy inhibition and deprive cells of such protective mechanism, which can be restored upon rapamycin co-incubation, addressing them to death. It is known that mitochondria play a central and complex role in autophagy. Recently, Okamoto, (2011) reported that MMP plays a role in autophagy regulation, and that defective mitochondria may impair the autophagic flux and vice versa through a protein kinase A-dependent mechanism. In addition, Kathiria et al., (2012) demonstrated that ROS up-regulation following mitochondrial membrane depolarization led to autophagy inhibition in human intestinal epithelial cells, and Karantza-Wadsworth et al., (2007) proposed that in cases of defective autophagy breast tumour cells lose the ability to adapt to metabolic stress, produce insufficient ATP and accumulate damaged mitochondria with excessive ROS. In light of such evidence, we cannot exclude the occurrence of an interplay between the early ROS increase, MMP collapse and autophagy down-regulation in JAHA-treated MDA-MB231 cells, although further studies will be required to confirm this hypothesis. Importantly, Rao et al., (2012) reported the superior anti-cancer activity of co-treating triple-negative breast cancer cells and xenografts with the pan-HDACi panobinostat and the autophagy inhibitor chloroquine; therefore, the possible clinical utilization of the sole JAHA, an HDACi possessing an intrinsic autophagy-inhibiting activity, appears to be worth-investigating. Noteworthy, the time-course study of JAHA effect on the control of the autophagic flux in MDA-MB231 cells revealed a biphasic trend of the biological progress, whose molecular basis will deserve further and more detailed investigation.

HDACis also negatively control angiogenesis, metastasis, and invasion by down-regulating the expression of (hypoxia inducible factor) *HIF-1 $\alpha$*  (Fath et al., 2006; Qian et al., 2006), matrix metallo-proteinases *MMP-2* and *MMP-9* (Kim et al., 2004; Liu et al., 2003), chemokine (*C-X-C motif*) receptor 4 (*CXCR4*) (Qian et al., 2006) endothelial nitric oxide synthase (*e-NOS*) (Rossig et al., 2002) and up-regulating the expression of angiostatic protein ADAMTS1 (Chou et al., 2008). To investigate the influence of JAHA on cell migration and proliferation, an experimental “scratch assay” was designed in this study, to test the motile behaviour of MDA-MB231 breast cancer cells cultured in the presence of 8.45  $\mu$ M JAHA for 24 hour. To distinguish whether proliferation or migration was increased, 2 mM hydroxurea was used as a control in combination with JAHA to inhibit cell proliferation (Clay et al., 2001). Our preliminary data indicate that JAHA does not influence cell migration.



Recent study demonstrated also that multi-platform classification of breast cancers is based on genomic sequencing, gene expression profiling, and proteomics. For this reason in this study we wanted to evaluate some molecular aspects of the effects exerted by JAHA on MDA-MB231 breast cancer cells.

The results obtained by differential display PCR and confirmed by Real Time-PCR assay showed that the NTRK2, BDNF/NT-3 growth factors receptor was upregulated in treated cells. BDNF is a nerve growth factor (NGF) like neurotrophin 3 (NT3), and neurotrophin 4/5 (NT-4/5). These factors are known especially for their roles in the development and maintenance of the nervous system, where they stimulate the survival, differentiation and neuronal plasticity. Their activity is mediated by tyrosine kinase receptors (TRK) specific for each neurotrophin (Knüsel et al., 1994). Currently, these receptors are considered potential targets for cancer treatment, in particular for breast cancer cells negative for the estrogen receptor, such as TNBC. Literature data show that BDNF and NT4/5 are both expressed and secreted by cells in breast cancer and they have been shown to directly contribute to the progression of mammary carcinogenesis through an autocrine "loop" of apoptosis inhibition that is achieved through TrkB-specific receptors (Yang et al., 2012). It is conceivable that the increase of NTRK2 expression level following treatment of cells with JAHA represents a defense cellular response against the cytotoxic effect which is, however, unable to re-establish the viability of MDA-MB231 cells exposed to the HDACi.

Our data confirm also the down-regulation of the expression of the gene coding for PKC $\epsilon$  and the up-regulation of that coding for Rad 50 in cells treated with JAHA at 8.45  $\mu$ M concentration. PKC $\epsilon$  is a phospholipid-dependent serine/threonine kinase regulated by DAG and PS but does not require Ca<sup>2+</sup> for activation which plays an essential role in the regulation of various cellular processes linked to the involvement of cytoskeletal proteins, such as adhesion, motility, cell cycle, growth and the regulation of neuronal ion channels. This protein is also involved in the immune response, in the invasion of cancer cells and in the regulation of apoptosis. During cytokinesis, it forms a complex with YWHAB (Tyrosine 3-monooxygenase Tryptophan 5-monooxygenase Activation Protein, Beta Polypeptide) (<http://www.genenames.org>), important for the division of the mother cell into two daughter cells, and facilitates the abscission with a mechanism that may involve the regulation of RhoA factor (Sauter et al., 2008). PKC $\epsilon$  is over-expressed in epithelial tumors including those of the breast (Pal et al., 2013). It is known that the down-regulation of this protein alters the oncogenic pathway of NF- $\kappa$ B in breast cancer cells bringing them to apoptotic death (Körner et al., 2013). Rad 50 protein contains a long internal coiled-coil domain that folds back on itself,

bringing the N- and C-termini together to form a globular ABC ATPase head domain. Rad 50 can dimerize both through its head domain and through a zinc-binding dimerization motif at the opposite end of the coiled-coil known as the “zinc-hook” (Hopfner et al., 2002). RAD 50 forms a complex with MRE11 and NBS1 (also known as Xrs2 in yeast). This MRN complex (MRX complex in yeast) binds to broken DNA ends and displays numerous enzymatic activities that are required for double-strand break repair by nonhomologous end-joining or homologous recombination. Gene knockout studies of the mouse homolog of Rad 50 suggest that it is essential for cell growth and viability.

Subsequently, we wanted to assess whether the effect induced by JAHA in this cell line is comparable to that induced by its analogue. The data obtained show that SAHA is able to induce a down-regulation of a higher number of analysed genes than JAHA, in particular of *Ergic 2* (ER-Golgi intermediated compartment 2KDa protein), protein kinase C iota (*PKC $\iota$* ), Protein kinase C  $\epsilon$  (*PKC $\epsilon$* ) and *Brefeldine a-Inhibited guanine nucleotide-exchange protein 3* except *MED25* (mediator of RNA Polymerase II transcription subunit25) which encodes a component of the complex transcriptional coactivator defined with the name of mediator complex and *Rad 50*.

*PKC $\iota$*  is a calcium-independent serine/threonine protein kinase and does not require phosphatidylserine, diacylglycerol (DAG) for activation. It plays a protective role against apoptotic stimuli, is involved in the activation of NF- $\kappa$ B in cell survival, differentiation and polarity, and contributes to the regulation of dynamics of the microtubules in the early secretory pathway. An over-expression of *PKC $\iota$*  was found in a "subset" of breast cancer. The depletion of *PKC $\iota$*  in breast cancer cell lines in which the gene is over-expressed increases the number of senescent cells. In this case in the absence of a response to DNA damage induced by p21 and aurora kinase VX-680 inhibitor, senescence is likely to be triggered by defects in the mitosis process. This function, however, seems to be limited to tumor cells (Paget et al., 2012).

ERGIC 2, also called PTX1, plays a possible role in the chaperone protein transport between the rough endoplasmic reticulum and the Golgi apparatus. The protein contains two hydrophobic transmembrane domains that help to anchor the molecule on the ER membrane, its large luminal domain is addressed within the ER lumen while the amino and carboxy-termini are facing the cytosol. ERGIC2, *Erv41p* homolog in yeast, forms a complex with two other proteins, *hErv46* (*Ergic3* homologous in mammalian) and ERGIC32 (also known as ERGIC1), acting as a "shuttle" for protein trafficking between ER and Golgi (Žak et al., 2012). These ERGIC also seem to interact with several proteins, such as otoferlin, SNARE

(syntaxin 5, syntaxin 17, syntaxin 18, rBet1, Sec22) and small GTPases, such as Rab1 and Rab2 (Appenzeller-Herzog et al., 2006; Muppirala et al., 2011). Therefore, it can play an important role in cellular functions in addition to acting as a shuttle for the trafficking of proteins. ERGIC2 is a ubiquitously expressed nuclear protein that appears to be downregulated in prostate cancer (Kwok et al., 2001). There is no data in the literature in relation to breast cancer, and therefore the result obtained in this work represents the first experimental evidence of ERGIC2 as molecular marker activity of the HDACi JAHA in TNBC cells.

Brefeldine A-Inhibited guanine nucleotide-exchange protein 3 is involved in regulating vesicular transport in the Golgi apparatus by promoting the activation of ARF1/ARF5/ARF6. The only data related to its involvement in mammary tumorigenesis, concern the activation of the estrogen/estrogen receptor  $\alpha$  pathway in estrogen receptor-positive cells (Kim et al., 2009).

It is known that by Differential Display PCR, some authors had identified molecular targets associated with differentiation and/or growth inhibition in human breast cancer cells treated with SAHA. These genes were *ID11*, *VDUP1* and *gelsolin* (Lili et al., 2000).

ID11 is an enzyme important for isoprenoid biosynthesis and the prenylation of proteins (Hahn et al., 1996). Post-translational modification by prenylation is important for the function of certain proteins, such as the ras p21/ras p21-like small GTP-binding proteins. Ras proteins have been shown to regulate cell growth, differentiation, and apoptosis (Olson et al., 2000). For instance, during TPA induced differentiation of hematopoietic leukemia cell lines, ras p21 is activated (Katagiri et al., 1994), and ras p21/ras p21-like G proteins are markedly induced (Adachi 1992), suggesting potential roles of ras proteins in cell differentiation.

VDUP1 was first reported as a novel protein up-regulated by 1,25-dihydroxyvitamin D-3 in HL60 cells (Chen et al., 1994). Later, the rat VDUP1 homologue was found to be down-regulated in N-methyl-N-nitrosourea (MNU)-induced rat mammary tumors (Young et al., 1996), and up-regulated in a cell line derived from MNU-induced rat mammary tumor after treatment with 1,25-dihydroxyvitamin D3, which also inhibited cell growth (Yang et al., 1998). VDUP1 recently was found to be identical to the thioredoxin-binding protein-2 (TBP-2), which acts as a negative regulator of thioredoxin (TRX) function and expression (Nishiyama et al., 1999).

TRX is a disulfide oxidoreductase, originally discovered as an adult T-cell leukemia-derived factor from T-lymphotropic virus type I transformed lymphocytes (Tagaya et al., 1989). TRX is overexpressed in some human tumor cells (Fujii et al., 1991; Berggren et al., 1996), and has

cell growth stimulating effects (Wakasugi et al., 1990; Gasdaska et al., 1995). Moreover, TRX increases colony formation in soft agarose when transfected into human breast cancer cells; whereas, a TRX dominant-negative mutant inhibits tumor cell growth (Gallegos et al., 1996). Thus, it is plausible that down-regulation of TRX expression and function by VDUP1 might contribute to the pro-differentiating and antiproliferative effects of 1,25-dihydroxyvitamin D3 observed in promyelocytic leukemia cells and MNU-induced rat mammary tumor cells (Chen et al., 1994; Yang et al., 1998), and the antiproliferative and potential pro-differentiating effects of SAHA on human breast cancer cells.

Another differentiation-associated gene, *gelsolin*, also was induced drastically by SAHA. Gelsolin, an actin-regulatory protein, is down-regulated in a variety of cancer cells (Tanaka et al., 1995; Mielnicki et al., 1999), and up-regulated in differentiated keratinocytes (Schwartz et al., 1994; Olsen et al., 1995) and in cancer cells when induced to differentiate (Dieffenbach et al., 1989). Interestingly, as *ID1*, *gelsolin* also is up-regulated in human promyelocytic leukemia HL60 cells when induced to differentiate by phorbol myristate acetate (Kwiatkowski et al., 1988). As a candidate tumor suppressor, *gelsolin*, when reintroduced into cancer cells, greatly reduces the colony-forming ability and in vivo tumorigenicity of cancer cells (Tanaka et al., 1995; Tanaka et al., 1999). In this work we demonstrate that the SAHA-homologue JAHA is capable to induce the same up-regulation of these genes as reported for SAHA by Huang et al., (2000).

Taken the results from gene expression experiments together, it appears that JAHA, although sharing some common features with SAHA has a more restricted effect, at least under the experimental conditions tested.

JAHA does not only influence gene expression but also protein accumulation, as shown by proteomic analyses aimed to evaluate the different effect induced by the two HDACis JAHA and SAHA on MDA-MB231 cells. Also in this case the first one appears to have a more limited and discriminative effect on up and down-regulation of the protein products. Following treatment with JAHA we observed an up-regulation of Ribosomal binding protein-1, the glutaredoxin-1 and sulfiredoxin-1 which can be tentatively interpreted as an attempt of cells to counteract the HDACi-induced stress in the intracellular redox homeostasis of the endoplasmic reticulum to the accumulation of misfolded proteins (Li et al., 2013; Tsai et al., 2013). Furthermore, the late accumulation of pre-laminae A/C is symptomatic of an inhibition of the post-translational prenylation processes in the endoplasmic reticulum, by analogy with published data regarding the effect of the anti-tumor R115777 molecule (Kelland et al., 2001). The down-regulation of protein Histone H1.0, Hematological and neurological expressed-1

and AHNAK is a common aspect between JAHA and SAHA, but given the scarcity of data on the biological activity of these proteins it is not possible to hypothesize the effect of the specific cellular modulation of their expression.

As already mentioned, the types of proteins differentially accumulated after the treatment with SAHA appear to be more numerous and varied, and they primarily include the scaffold protein NHE-RF1, which is down-regulated together with Microtubule-Associated protein-1B, the  $\alpha$  chain of non-erythrocyte spectrin and integrin  $\beta$ 1, whereas other proteins, such as intranuclear Nucleolar and coiled-body phosphoprotein 1 and Eukaryotic translation initiation factor 4H, nucleolin and HnRNP A2/B1, were found to be up-regulated. Probably, such up-regulation attempts to establish a "drug resistance" (Hu et al., 2011; Han et al., 2014), together with the over-expression of Histidine triad nucleotide-binding protein 2, which is an AMP-lysine hydrolase that acts as a mitochondrial "apoptotic sensitizer" (Martin et al., 2006). Regarding the proteins with membrane localization, we observed the increase of the accumulation of GRP78, a stress-induced chaperonin of the endoplasmic reticulum (Niforou et al., 2014). Regarding the cytoplasmic proteins, after 24 h of treatment we observed the down-regulation of the anti-apoptotic protein Myristoylated alanine-rich C kinase substrate, and the Nicotinamide phosphoribosyltransferase, which reduces the proportion of intracellular NAD<sup>+</sup>, and is involved in the process of cell death (Tan et al., 2013), whereas the down-regulation of Caprin-1 may be involved in cell cycle arrest at the G<sub>1</sub> phase (Wang et al., 2005). Finally, SAHA suppressed the expression of reticulocalbin as reported in Tong et al., (2008).

Basal-like tumors are often characterized by frequent mutations in the PI3K-AKT pathway and elevated expression of phospho-AKT as reported in Cancer Genome Atlas Network, (2012). Akt, plays a critical role in controlling survival and apoptosis (Burgering et al., 1995; Franke et al., 1995; Franke et al., 1997). This protein kinase is activated by insulin and various growth and survival factors to function in a wortmannin-sensitive pathway involving PI3 kinase (Burgering et al., 1995; Franke et al., 1995). Akt is activated by phospholipid binding and the activation is due to phosphorylation at Thr308 by PDK1 (Cross et al., 1995) and within the carboxy terminus at Ser473. The PI3K/AKT/mTOR pathway plays a key regulatory function in cell survival, proliferation, migration, metabolism, angiogenesis, and apoptosis. This pathway is constitutively activated in various malignancies, including breast cancer (Hernandez-Aya et al., 2011). The PI3K pathway is up-regulated in basal-like carcinomas, as shown by a significantly increased activation of downstream targets, AKT and mTOR (Marty et al., 2008). López-Knowles et al., (2010) found that PI3K pathway activation

was significantly associated with ER/PR negative status, high tumor grade, and a “basal-like” phenotype, where 92% of tumors had an altered PI3K/AKT pathway (López-Knowles et al., 2010). Also Raf/mitogen-activated protein kinase (MAPK) kinase 1/2 (MEK1/2)/extracellular signal-regulated kinase 1/2 (ERK1/2) pathway is frequently dysregulated in neoplastic transformation (Dent et al., 2005; Valerie et al., 2007). The Ras/Raf/MEK/ERK cascade couples signals from cell surface receptors to transcription factors, which regulate gene expression. Furthermore, this cascade also regulates the activity of many proteins involved in apoptosis. This pathway is often activated in certain tumors by chromosomal translocations such as BCR-ABL, mutations in cytokine receptors or over-expression of wild type or mutated receptors, e.g. EGFR. The Raf/MEK/ERK pathway also has profound effects on the regulation of apoptosis via the post-translational phosphorylation of apoptotic regulatory molecules including Bad, Bim, Mcl-1, caspase 9 and, more controversially, Bcl-2. This pathway has diverse effects which can regulate cell cycle progression, apoptosis or differentiation (Steelman et al., 2004). ERK1 and ERK2 are 44 and 42-kDa MAPKs, respectively, and exhibit a high homology in the protein level. Both these isoforms appear inactive in quiescent cells, but upon cell stimulation their activity elevates rapidly. Activation of ERKs requires phosphorylation of two regulatory residues, threonine and tyrosine, that reside in a TEY phosphorylation motif 1 (Payne et al., 1991; Canagarajah et al., 1997). This phosphorylation seems to be mediated solely by its upstream activators MAPK/ERK kinases (MEK), (Seger et al., 1992), which phosphorylate both regulatory residues of ERK. However, the activity of ERK in stimulated cells is regulated not only by MEK, but also by the action of various phosphatases, which remove phosphates from either the Thr alone, Tyr alone, or both residues, to render the ERK inactive (Gopalbhai et al., 1998). ERKs appear to be important regulatory molecules, which by themselves can phosphorylate regulatory targets in the cytosol, phosphorylate substrates in the nucleus or transmit the signal to the MAPKAPK level. Treatment with HDACis of multiple tumor types has resulted in potent inhibition of Akt and Erk pathways. For this reason, we evaluated the effect of JAHA on the two survival proliferative pathways, and the data showed that JAHA is able to induce a significant alteration on ERK pathway.

A recent study suggested that DNA methylation in colon cancer cells and in NIH 3T3 cells may be regulated by ERK activity (Lu et al., 2007). To determine if JAHA might be exerting effects on DNA methylation through ERK, we first examined the effect of JAHA on ERK activity, as assessed by modulation of ERK phosphorylation status. Our results show that ERK phosphorylation was completely inhibited by exposure to JAHA, whereas the total

levels of ERK protein were affected only in 48 h. By contrast, there were no consistent effects by the HDACi on the levels of phospho-AKT. These results raised the possibility that the HDACi might be regulating DNA methylation and gene expression through ERK. We therefore tested this hypothesis by examining the effect of JAHA treatment on DNMT1 protein accumulation and demonstrated that the HDACi, which inhibited ERK activity, also down-regulated DNMT1. Down-regulation of DNMT1 resulted in demethylation of global DNA after about 48 h of exposure, suggesting that some genes, like those acting as tumor suppressor, could be expressed after such epigenetic change and cause cell cycle arrest and apoptosis. These data confirm the model supported by Sibaji et al., (2011) in which they described how HDACis inhibit ERK activation through a direct inhibitory effect on ERK phosphorylation, and that this event modulates negatively DNMT1 protein levels. DNMT1 down-regulation influences the methylation status of the DNA. Furthermore, in light of the evidence that DNA demethylation can regulate diverse cellular processes in normal and malignant cells, we can hypothesize that JAHA may influence gene expression also in a manner alternative to that of histone acetylation which may have prominent and broad implications.

## 6. Conclusion

In conclusion, two different SAHA analogues, JAHA and homo-JAHA, obtained by manipulation of SAHA aryl cap and assayed for their inhibitory action on purified HDACs, (Spencer et al., 2011) have been tested for their ability to restrain survival of a TNBC cell line *in vitro*. Of the two compounds, only JAHA exhibited a remarkable activity on MDA-MB231 cell viability and growth with an  $IC_{50}$  of 8.45  $\mu$ M at 72 h. This indicates that the additional methylene spacer present in homo-JAHA, which in the *in tube* assay exhibited a similar profile to that of JAHA for HDACs except HDAC6 and -8, affects its activity in a cellular environment, and underlines the importance of a detailed biological characterization of promising bioinorganic probes for HDACs on specific cell model systems.

Thus, JAHA, a ferrocene-derivative of SAHA, provides a fascinating tool for studying the interactions of bioorganometallic agents in breast cancer (Osella et al., 2005; Spencer et al., 2012). The results from biological and molecular assays of JAHA activity highlight the clear involvement of oxidative damage of autophagy inhibition in cytotoxicity expanding the list of autophagy-regulating drugs and also giving an additional example of the role played by autophagy inhibition in breast cancer cell death; its involvement in the molecular and biochemical pathways and the possible epigenetic effect on the DNA methylation status.

For all this reason the future prospective will be to test this compound *in vivo* situation (animals and human trials) to confirm this data and to hope that JAHA become a promising anticancer drug for prevention and/or therapy of “aggressive” breast carcinoma.



## **7. Future work**

The future work will be focussed on the confirmation of the modality of cell death as analysed by flow cytometry. To this purpose, we will perform Western blot analyses to evaluate the level of expression of some apoptotic markers as indicators of increased cell death after the treatment. Moreover, we will carry on further assays to confirm the DNA methylation state in MDA-MB231 cell line, both control and treated with JAHA, by immunostaining of 5-methylcytosine in metaphasic chromosomes and, at gene level, by Methylation Sensitive Restriction Endonuclease-PCR.

An interesting aspect to be checked, related to the possible genotoxicity of JAHA, is the evaluation of chromosomal damage. To this purpose, it will be possible to perform the micronuclei test which is simple and quick, but alone is not sufficient to distinguish between broken or whole chromosome loss. To determine more precisely the presence of whole chromosomes with their centromeres in micronuclei it will be necessary to use the technique of FISH hybridization with centromeric DNA as probes (Becker et al., 1990) according to the protocol of Antonacci et al., (1995). In addition, the test of sister chromatid exchanges (SCE) will be performed to analyze the chromosomal damage induced on cell lines treated with JAHA, in parallel with the Comet assay, a sensitive method, qualitative and quantitative, useful to detect single and double strand breaks in the DNA molecule, alkali-labile sites and incisions caused by the activities of nucleotide excision repair.

---

## References

- Abedin, M.J., Wang, D., McDonnell, M.A., Lehmann, U., Kelekar, A. (2007). Autophagy delays apoptotic death in breast cancer cell following DNA damage. *Cell Death And Differentiation* 14: 500-10.
- Abramov, A.Y., Scorziello, A., Duchen, M.R. (2007). Three distinct mechanisms generate oxygen free radicals in neurons and contribute to cell death during anoxia and reoxygenation. *J. Neurosci.* 27: 1129-1138.
- Adachi, M., Ryo, R., Yoshida, A., Sugano, W., Yasunaga, M., Saigo, K., Yamaguchi, N., Sato, T., Sano, K. (1992). Induction of smg p21/rap1A p21/krev-1 p21 gene expression during phorbol ester-induced differentiation of a human megakaryocytic leukemia cell line. *Oncogene* 7: 323-329.
- Adams, R.H., Alitalo, K. (2007). Molecular regulation of angiogenesis and lymphangiogenesis. *Nat. Rev. Mol. Cell Biol.* 8: 464-78.
- Ahn, M.Y., Jung, J.H., Na, Y.J., Kim, H.S. (2008). A natural histone deacetylase inhibitor, Psammaplin A, induces cell cycle arrest and apoptosis in human endometrial cancer cells. *Gynecol. Oncol.* 108: 27-33.
- Anders, C.K., Carey, L.A. (2009). Biology, metastatic patterns and treatment of patients with triple-negative breast cancer. *Clinical Breast Cancer* 9: S73-S81.
- Andreyev, A.Y., Kushnareva, Y.E., Starkov, A.A. (2005). Mitochondrial metabolism of reactive oxygen species. *Biochemistry (Mosc)* 70: 200-214.
- Apel, A., Herr, I., Schwarz, H., Rodemann, H.P., Mayer, A. (2008). Blocked autophagy sensitizes resistant carcinoma cells to radiation therapy. *Cancer Res.* 68: 1485-1494.
- Appenzeller-Herzog, C., Hauri, H.P. (2006). The er-golgi intermediate compartment (ergic): In search of its identity and function. *J. Cell Sci.* 119: 2173-2183.
- Armstrong, L.J., Gorski, S.M. (2010). Breast cancer and autophagy. In *Breast cancer: causes, diagnosis and treatment*. Nova Science Publishers 53-88.
- Beckers, T., Berkhardt, C., Wieland, H., Gimminich, P., Ciossek, T., Maier, T., Sanders, K. (2007). Distinct pharmacological properties of second generation HDAC inhibitors with the benzamide or hydroxamate head group. *Int. J. Cancer* 121(5): 1138-1148.
- Berggren, M., Gallegos, A., Gasdaska, J.R., Gasdaska, P.Y., Warneke, J., Powis, G. (1996). Thioredoxin and thioredoxin reductase gene expression in human tumors and cell lines, and the effects of serum stimulation and hypoxia. *Anticancer Res.* 16: 3459-3466.
- Bolden, J., Peart, M., Johnstone, R. (2006). Anticancer activities of histone deacetylase inhibitors. *Nat. Rev. Drug Discov.* 5: 769-84.
- Buggy, J.J., Sideris, M.L., Mak, P., Lorimer, D.D., McIntosh, B. Clark, J.M. (2000). Cloning and characterization of a novel human histone deacetylase, HDAC8. *Biochem. J.* 350: 199-205.

- Burgering, B.M. Coffey, P.J. (1995). Protein kinase B (c-Akt) in phosphatidylinositol-3-OH kinase signal transduction. *Nature* 376: 599-602.
- Butler, L.M., Zhou, X., Xu, W.S. (2002). The histone deacetylase inhibitor SAHA arrests cancer cell growth, up-regulates thioredoxin-binding protein-2, and down-regulates thioredoxin. *Proc. Natl. Acad. Sci. U S A.* 99: 11700-11705
- Canagarajah, B.J., Khokhlatchev, A., Cobb, M.H., Goldsmith, E.J. (1997). Activation mechanism of the MAP kinase ERK2 by dual phosphorylation. *Cell* 90: 859-869.
- Cancer Genome Atlas Network. (2012). Comprehensive molecular portraits of human breast tumours. *Nature* 490: 61-70.
- Candido, E.P., Reeves, R., Davie, J.R. (1978). Sodium butyrate inhibits histone deacetylation in cultured cells. *Cell* 14 (1): 105-113.
- Cannino, G., Ferruggia, E., Luparello, C., Rinaldi, A.M. (2008). Effects of cadmium chloride on some mitochondria-related activity and gene expression of human MDA-MB231 breast tumor cells. *J. Inorg. Biochem.* 102: 1668-1676.
- Carew, J.S., Medina, E.C., Esquivel, J.A. (2010). 2nd, Mahalingam D, Swords R, Kelly K, Zhang H, Huang P, Mita AC, Mita MM, Giles FJ, Nawrocki ST. Autophagy inhibition enhances vorinostat-induced apoptosis via ubiquitinated protein accumulation. *J. Cell Mol. Med.* 14: 2448-59.
- Chang, S.B., Miron, P., Miron, A., Iglehart, J.D. (2007). Rapamycin inhibits proliferation of estrogen-receptor-positive breast cancer cells. *J. Surg. Res.* 138: 37-44.
- Chen, Y., Azad, M.B., Gibson, S.B. (2010). Methods for detecting autophagy and determining autophagy-induced cell death. *Can. J. Physiol. Pharmacol.* 88: 285-295.
- Chen, K.S., DeLuca, H.F. (1994). Isolation and characterization of a novel cDNA from HL-60 cells treated with 1,25-dihydroxyvitamin D-3. *Biochim. Biophys. Acta* 1219: 26-32.
- Chen, Y., Zheng, Y., Foster, D.A. (2003). Phospholipase D confers rapamycin resistance in human breast cancer cells. *Oncogene* 22: 3937-3942.
- Choi, C.H., Jung, Y.K., Oh, S.H. (2010). Autophagy induction by capsaicin in malignant human breast cells is modulated by p38 and extracellular signal-regulated mitogen-activated protein kinases and retards cell death by suppressing endoplasmic reticulum stress-mediated apoptosis. *Mol. Pharmacol.* 78: 114-125.
- Chomczynski, P., Sacchi, N. (1987). Single-step method of RNA isolation by acid guanidinium thiocyanate-phenol-chloroform extraction. *Anal Biochem* 162: 156-9.
- Chou, C.W. Chen, C.C. (2008). HDAC inhibition upregulates the expression of angiostatic ADAMTS1. *FEBS Lett* 582: 4059-65.
- Clay, C.E., Namen, A.M., Atsumi, G., Trimboli, A.J., Fonteh, A.N., High, K.P., Chilton, F.H. (2001). Magnitude of peroxisome proliferator-activated receptor-gamma activation is associated with important and seemingly opposite biological responses in breast cancer cells. *J. Investig Med.* 49 (5): 413-20.

- Condorelli, F., Gnemmi, I., Vallario, A., Genazzani, A.A., Canonico, P.L. (2008). Inhibitors of histone deacetylase (HDAC) restore the p53 pathway in neuroblastoma cells. *Br. J. Pharmacol* 153: 657-68.
- Cory, S., Adams, J.M. (2002). The Bcl2 family: regulators of the cellular life-or-death switch. *Nat. Rev. Cancer* 2: 647-56.
- Cossarizza, A., Salvioli, S. (2001). Flow cytometric analysis of mitochondrial membrane potential using JC-1. *Curr. Prot. Cytom.* Chapter 9: 14.1-14.7.
- Cousens, L.S., Gallwitz, D., Alberts, B.M. (1979). Different accessibilities in chromatin to histone acetylase. *J. Biol. Chem.* 254 (5): 1716-23.
- Crighton, D., Wilkinson, S., O'Prey, J., Syed, N., Smith, P., Harrison, P.R., Gasco, M., Garrone, O., Crook, T., Ryan, K.M. (2006). DRAM, a p53-induced modulator of autophagy, is critical for apoptosis. *Cell* 126: 121-34.
- Cross, D.A., Alessi, D.R., Cohen, P., Andjelkovich, M., Hemmings, B.A. (1995). Inhibition of glycogen synthase kinase-3 by insulin mediated by protein kinase B. *Nature* 378: 785-9.
- Dai, Y., Rahmani, M., Dent, P., Grant, S. (2005). Blockade of histone deacetylase inhibitor-induced RelA/p65 acetylation and NF-kappaB activation potentiates apoptosis in leukemia cells through a process mediated by oxidative damage, XIAP downregulation, and c-Jun N-terminal kinase 1 activation. *Mol. Cell. Biol.* 25: 5429-5444.
- Dent, P. (2005). MAP kinase pathways in the control of hepatocyte growth, metabolism and survival. *Signaling Pathways in Liver Diseases*, Springer Press 19: 223-38.
- Dickinson, M., Johnstone, R.W., Prince, H.M. (2010). Histone deacetylase inhibitors: potential targets responsible for their anti-cancer effect. *Invest. New Drugs* 28 Suppl. 1, S3-S20.
- Dieffenbach, C.W., SenGupta, D.N., Krause, D., Sawzak, D., Silverman, R.H. (1989). Cloning of murine gelsolin and its regulation during differentiation of embryonal carcinoma cells. *J. Biol. Chem.* 264: 13281-13288.
- Dokmanovic, M., Marks, P.A. (2005). Prospects: histone deacetylase inhibitors. *J. Cell Biochem.* 96: 293-304.
- Drummond, D.C., Noble, C.O., Kirpotin, D.B., Guo, Z., Scott, G.K., Benz, C.C. (2005). Clinical development of histone deacetylase inhibitors as anticancer agents. *Annu. Rev. Pharmacol Toxicol* 45: 495-528.
- Eads, C.A., Danenberg, K.D., Kawakami, K., Saltz, L.B., Danenberg, P.V., Laird, P.W. (1999). CpG island hypermethylation in human colorectal tumors is not associated with DNA methyltransferase overexpression. *Cancer Res.* 59(10): 2302-2306.
- Egger, G., Liang, G., Aparicio, A., Jones, P.A. (2004). Epigenetics in human disease and prospects for epigenetic therapy. *Nature Review* 429: 457-463.
- Fath, D.M., Kong, X., Liang, D., Lin, Z., Chou, A., Jiang, Y., Fang, J., Caro, J., Sang, N. (2006). Histone deacetylase inhibitors repress the transactivation potential of hypoxia-

- inducible factors independently of direct acetylation of HIF- $\alpha$ . *J. Biol. Chem.* 281: 13612-9.
- Fenrick, R., Hiebert, S.W. Role of histone deacetylases in acute leukemia. (1998). *J. Cell Biochem. Suppl.* 30-31: 194-202.
  - Finnin, M.S., Donigian, J.R., Cohen, A., Richon, V.M., Rifkind, R.A., Marks, P.A., Breslow, R. Pavletich, N.P. (1999). Structures of a histone deacetylase homologue bound to the TSA and SAHA inhibitors. *Nature* 401: 188-193.
  - Fischle, W., Dequiedt, F., Hendzel, M.J., Guenther, M.G., Lazar, M.A., Voelter, W., Verdin, E. (2002). Enzymatic activity associated with class II HDACs is dependent on a multiprotein complex containing HDAC3 and SMRT/N-CoR. *Mol. Cell.* 9: 45-57.
  - Franke, T.F., Yang, S.I., Chan, T.O., Datta, K., Kazlauskas A., Morrison D.K., Kaplan D.R., Tsichlis P.N. (1995). The protein kinase encoded by the Akt proto-oncogene is a target of the PDGF-activated phosphatidylinositol 3-kinase. *Cell* 81: 727-36.
  - Franke, T.F., Kaplan, D.R., Cantley, L.C. (1997). PI3K: downstream AKT ion blocks apoptosis. *Cell* 88: 435-7.
  - Fujii, S., Nanbu, Y., Nonogaki, H., Konishi, I., Mori, T., Masutani, H., Yodoi, J. (1991). Coexpression of adult T-cell leukemia-derived factor, a human thioredoxin homologue, and human papillomavirus DNA in neoplastic cervical squamous epithelium. *Cancer* 68: 1583-1591.
  - Gallegos, A., Gasdaska, J.R., Taylor, C.W., Paine-Murrieta, G.D., Goodman, D., Gasdaska, P.Y., Berggren, M., Briehl, M.M., Powis, G. (1996). Transfection with human thioredoxin increases cell proliferation and a dominantnegative mutant thioredoxin reverses the transformed phenotype of human breast cancer cells. *Cancer Res.* 56: 5765-5770.
  - Gammoh, N., Lam, D., Puente, C., Ganley, I., Marks, P.A., Jiang, X. (2010). Role of autophagy in histone deacetylase inhibitor-induced apoptotic and nonapoptotic cell death. *Proc. Natl. Acad. Sci. USA* 109: 6561-6565.
  - Gasdaska, J.R., Berggren, M., Powis, G. (1995). Cell growth stimulation by the redox protein thioredoxin occurs by a novel helper mechanism. *Cell Growth Differ.* 6: 1643-1650.
  - Gerard, G.F., D'Alessio, J.M., Kotewicz, M.L., Noon, M.C. (1986). Influence on stability in *Escherichia coli* of the carboxy-terminal structure of cloned Moloney murine leukemia virus reverse transcriptase. *DNA* 5(4): 271-9.
  - Glaser, K., Li, J., Aakre, M., Morgan, D., Sheppard, G., Stewart, K., Pollock, J., Lee, P., O'Connor, C.Z., Anderson, S.N., Mussatto, D.J., Wegner, C.W., Moses, H.L. (2002). Transforming growth factor b mimetics: discovery of 7-[4-(4-cyanophenyl)phenoxy]-heptanohydroxamic acid, a biaryl hydroxamate inhibitor of histone deacetylase. *Mol. Cancer Ther.* 1: 759-68.
  - Glaser, K.B., Li, J., Staver, M.J., Wei, R.Q., Albert, D.H., Davidsen, S.K. (2003). Role of class I and class II histone deacetylases in carcinoma cells using siRNA. *Biochem. Biophys Res. Commun.* 310: 529-36.

- Glaser, K.B. (2007). HDAC inhibitors: Clinical update and mechanism based potential. *Biochem. Pharmacol.* 74: 659-671.
- Gluz, O., Liedtke, C., Gottschalk, N., Pusztai, L., Nitz, U., Harbeck, N. (2009). Triple-negative breast cancer-current status and future directions. *Ann. Oncol.* 20: 1913-1927.
- Gopalbhai, K., Meloche, S. (1998). Repression of mitogen-activated protein kinases ERK1/ERK2 activity by a protein tyrosine phosphatase in rat fibroblasts transformed by upstream oncoproteins. *J. Cell. Physiol.* 174: 35-47.
- Gui, C.Y., Ngo, L., Xu, W.S., Richon, V.M., Marks, P.A. (1999). Histone deacetylase (HDAC) inhibitor activation of p21WAF1 involves changes in promoter-associated proteins, including HDAC1. *Proc. Natl. Acad. Sci. USA* 101: 1241-46.
- Hahn, C.K., Ross, K.N., Warrington, I.M., Mazitschek, R., Kanegai, C.M., Wright, R.D., Kung, A.L., Golub, T.R., Stegmaier, K. (2008). Expression-based screening identifies the combination of histone deacetylase inhibitors and retinoids for neuroblastoma differentiation. *Proc. Natl. Acad. Sci. USA* 105 (28): 9751-6.
- Han, J., Tang, F.M., Pu, D., Xu, D., Wang, T., Li, W. (2014). Mechanisms underlying regulation of cell cycle and apoptosis by hnRNP B1 in human lung adenocarcinoma A549 cells. *Tumori* 100 (1): 102-11.
- Hahn, F.M., Xuan, J.W., Chambers, A.F., Poulter, C.D. (1996). Human isopentenyl diphosphate: dimethylallyl diphosphate isomerase: overproduction, purification, and characterization. *Arch. Biochem. Biophys.* 332: 30-34.
- Harms, K.L., Chen, X. (2007). Histone deacetylase 2 modulates p53 transcriptional activities through regulation of p3-DNA binding activity. *Cancer Res.* 67: 3145-52.
- Hashimshony, T., Zhang, J., Keshet, I., Bustin, M., Cedar, H. (2003). The role of DNA methylation in setting up chromatin structure during development. *Nat. Genet.* 34 (2): 187-192.
- Hernandez-Aya, L.F., Gonzalez-Angulo, A.M. (2011). Targeting the phosphatidylinositol 3-kinase signaling pathway in breast cancer. *Oncologist* 16: 404-414.
- Hideshima, T., Bradner, J.E., Wong, J., Chauhan, D., Richardson, P., Schreiber, S.L., Anderson, K.C. (2005). Small-molecule inhibition of proteasome and aggresome function induces synergistic antitumor activity in multiple myeloma. *Proc. Natl. Acad. Sci. USA* 102: 8567-72.
- Hopfner, K.P., Craig, L., Moncalian, G., Zinkel, R.A., Usui, T., Owen, B.A., Karcher, A., Henderson, B., Bodmer, J.L., McMurra, C.T., Carney, J.P., Petrini, J.H., Tainer, J.A. (2002). The Rad50 zinc-hook is a structure joining Mre11 complexes in DNA recombination and repair. *Nature* 418 (6897): 562-6.
- Hsiao, Y.H., Chou, M.C., Fowler, C., Mason, J.T. Man, Y. (2010). Breast cancer heterogeneity: mechanisms, proofs, and implications. *J. Cancer* 1: 6-13.
- Hu, J., Lin, M., Liu, T., Li, J., Chen, B., Chen, Y. (2011). DIGE-based proteomic analysis identifies nucleophosmin/B23 and nucleolin C23 as over-expressed proteins in relapsed/refractory. *Leukemia research* 35 (8): 1087-92.

- Huang, L., Pardee, A.B. (2000). Suberoylanilide hydroxamic acid as a potential therapeutic agent for human breast cancer treatment. *Mol. Med.* 6: 849-866.
- Hubbert C., Guardiola, A., Shao, R., Kawaguchi, Y., Ito, A., Nixon, A., Yoshida, M., Wang, X.F., Yao, T.P. (2002). HDAC6 is a microtubule-associated deacetylase. *Nature* 417: 455-8.
- Iwata, A., Riley, B.E., Johnston, J.A., Kopito, R.R. (2005). HDAC6 and microtubules are required for autophagic degradation of aggregated huntingtin. *J. Biol. Chem.* 280: 40282-92.
- Jenuwein, T., Allis, C.D. (2001). Translating the histone code. *Science, Review* 293: 1074-1080.
- Jiang, H., White, E.J., Conrad, C., Gomez-Manzano, C., Fueyo, J. (2009). Autophagy pathways in glioblastoma. *Methods Enzymol.* 453: 273-286.
- Johnstone, R.W. (2002). Histone-deacetylase inhibitors: novel drugs for the treatment of cancer. *Nature Reviews Drug Discovery* 1: 287-299.
- Johnstone, R.W., Licht, J.D. (2003). Histone deacetylase inhibitors in cancer therapy: is transcription the primary target? *Cancer Cell* 4: 13-8.
- Johnstone, R.W., Prince, H.M. (2007). Histone deacetylase inhibitors in cancer therapy. *Expert Opin Investig Drugs* 16: 659-678.
- Johnstone, R.W., Ruefli, A.A., Lowe, S.W. (2002). Apoptosis: a link between cancer genetics and chemotherapy. *Cell* 108: 153-64.
- Kabeya, Y., Mizushima, N., Ueno, T., Yamamoto, A., Kirisako, T., Noda, T., Kominami E., Ohsumi, Y., Yoshimori, T. (2000). LC3, a mammalian homologue of yeast Apg8p, is localized in autophagosome membranes after processing. *EMBO J* 19: 5720-8.
- Kanematsu, S., Uehara, N., Miki, H., Yoshizawa, K., Kawanaka, A., Yuri, T., Tsubura, A. (2010). Autophagy inhibition enhances sulforaphane-induced apoptosis in human breast cancer cells. *Anticancer Res.* 30: 3381-3390.
- Karantza-Wadsworth, V., Patel, S., Kravchuk, O., Chen, G., Mathew, R., Jin, S., White, E. (2007). Autophagy mitigates metabolic stress and genome damage in mammary tumorigenesis. *Genes Dev.* 21: 1621-1635.
- Kassam, F., Enright, K., Dent, R., Dranitsaris, G., Myers, J., Flynn, C., Fralick, M., Kumar, R., Clemons, M. (2009). Survival outcomes for patients with metastatic triple-negative breast cancer: implications for clinical practice and trial design. *Clin. Breast Cancer* 9: 29-33.
- Katagiri, K., Hattori, S., Nakamura, S., Yamamoto, T., Yoshida, T., Katagiri, T. (1994). Activation of Ras and formation of GAP complex during TPA-induced monocytic differentiation of HL-60 cells. *Blood* 84: 1780-1789.
- Kathiria, A.S., Butcher, L.D., Feagins, L.A., Souza, R.F., Boland, C.R., Theiss A.L. (2012). Prohibitin 1 modulates mitochondrial stress-related autophagy in human colonic epithelial cells. *PLoS One* 7 (2): e31231.

- Kelland, L.R., Smith, V., Valenti, M., Patterson, L., Clarke, P.A., Detre, S., End, D., Howes, A.J., Dowsett, M., Workman, P., Johnston, S.R. (2001). Preclinical antitumor activity and pharmacodynamic studies with the farnesyl protein transferase inhibitor R115777 in human breast cancer. *Clin. Cancer Res.* (11): 3544-50.
- Kerbel, R.S. (2008). Tumor angiogenesis. *N. Engl. J. Med.* 358: 2039-49.
- Kijima, M., Yoshida, M., Sugita, K., Horinouchi, S., Beppu, T. (1993). Trapoxin, an antitumor cyclic tetrapeptide, is an irreversible inhibitor of mammalian histone deacetylase. *J. Biol. Chem.* 268: 22429-22435.
- Kim, S.H., Ahn, S., Han, J.W., Lee, H.W., Lee, H.Y., Lee, Y.W., Kim M.R., Kim, K.W., Kim, W.B., Hong, S. (2004). Apicidin is a histone deacetylase inhibitor with antiinvasive and anti-angiogenic potentials. *Biochem. Biophys. Res. Commun.* 315: 964-970.
- Kim, H.J., Bae, S.C. (2011). Histone deacetylase inhibitors: molecular mechanisms of action and clinical trials as anti-cancer drugs. *Am. J. Transl. Res.* 3: 166-179.
- Kim, M.S., Kwon, H.J., Lee, Y.M., Baek, J.H., Jang, J.E., Lee, S.W., Moon, E.J., Kim, H.S., Lee, S.K., Chung, H.Y., Kim, C.W., Kim, K.W. (2001). Histone deacetylase induce angiogenesis by negative regulation of tumor suppressor genes. *Nat. Med.* 7: 437-43.
- Kim, S.H., Jeong, J.W., Park, J.A., Lee, J.W., Seo, J.H., Jung, B.K., Bae, M.K., Kim, K.W. (2007). Regulation of the HIF-1 alpha stability by histone deacetylases. *Oncol. Rep.* 17: 647-5.
- Kim, J.W., Akiyama, M., Park, J.H., Lin, M.L., Shimo, A., Ueki, T., Daigo, Y., Tsunoda, T., Nishidate, T., Nakamura, Y., Katagiri, T. (2009). Activation of an estrogen/estrogen receptor signaling by BIG3 through its inhibitory effect on nuclear transport of PHB2/REA in breast cancer. *Cancer Sci.* 100 (8): 1468-78.
- Klionsky, D.J., Cregg, J.M., Dunn, W.A., Emr, S.D., Sakai, Y., Sandoval, I.V., Sibirny, A., Subramani, S., Thumm, M., Veenhuis, M., Ohsumi, Y. (2003). A unified nomenclature for yeast autophagy-related genes. *Dev. Cell* 5: 539-45.
- Knüsel, B., Rabin, S.J., Hefti, F., Kaplan, D.R. (1994). Regulated neurotrophin receptor responsiveness during neuronal migration and early differentiation. *J. Neurosci.* 14 (3 Pt 2): 1542-54.
- Knutson, A.K., Welsh, J., Taylor, T., Roy, S., Wang, W.L., Tenniswood, M. (2012). Comparative effects of histone deacetylase inhibitors on p53 target gene expression, cell cycle and apoptosis in MCF-7 breast cancer cells. *Oncol. Rep.* 27: 849-853.
- Körner, C., Keklikoglou, I., Bender, C., Wörner, A., Münstermann, E., Wiemann, S. (2013). MicroRNA-31 sensitizes human breast cells to apoptosis by direct targeting of protein kinase C epsilon (PKCepsilon). *J. Biol. Chem.* 288 (12): 8750-61.
- Kramer, O.H., Muller, S., Buchwald, M., Reichardt, S., Heinzl, T. (2008). Mechanism for ubiquitylation of the leukemia fusion proteins AML1-ETO and PML-RARalpha. *FASEB J.* 22 (5): 1369-79.
- Kotewicz, M.L., D'Alessio, J.M., Driftmier, K.M., Blodgett, K.P., Gerard, G.F. (1985). Cloning and overexpression of Moloney murine leukemia virus reverse transcriptase in *Escherichia coli*. *Gene.* 35 (3): 249-58.



- Kwiatkowski, D.J. (1988). Predominant induction of gelsolin and actin-binding protein during myeloid differentiation. *J. Biol. Chem.* 263: 13857-13862.
- Kwok, S.C., Liu, X., Daskal, I. (2001). Molecular cloning, expression, localization, and gene organization of PTX1, a human nuclear protein that is downregulated in prostate cancer. *DNA Cell Biol.* 20 (6): 349-57.
- Laurentiis, M.D., Cianniello, D., Caputo, R., Stanzone, B., Arpino, G., Cinieri, S., Lorusso, V. (2010). Treatment of triple-negative breast cancer (TNBC): Current options and future perspectives. *Cancer Treatment Reviews* 36S3: 580-586.
- Lee, H.B., Noh, H., Seo, J.Y., Yu, M.R., Ha, H. (2007). Histone deacetylase inhibitors a novel class of therapeutic agents in diabetic nephropathy. *Kidney Int. Suppl.* 106: S61-6.
- Levine, B., Klionsky, D.J. (2004). Development by self-digestion: molecular mechanisms and biological functions of autophagy. *Dev. Cell* 6: 463-77.
- Li, J., Liu, R., Lei, Y., Wang, K., Lau, Q.C., Xie, N., Zhou, S., Nie, C., Chen, L., Wei, Y., Huang, C. (2010). Proteomic analysis revealed association of aberrant ROS signaling with suberoylanilide hydroxamic acid-induced autophagy in Jurkat T-leukemia cells. *Autophagy* 6: 711-724.
- Li, Q., Yu, S., Wu, J., Zou, Y., Zhao, Y. (2013). Sulfiredoxin-1 protegge le cellule PC12 contro lo stress ossidativo indotto da perossido di idrogeno. *J. Neurosci. Res.* 91 (6): 861-70.
- Liang, X.H., Jackson, S., Seaman, M. Brown K., Kempkes, B., Hibshoosh, H., Levine, B. (1999). Induction of autophagy and inhibition of tumorigenesis by beclin 1. *Nature* 402: 672-6.
- Librizzi, M., Longo, A., Chiarelli, R., Amin, J., Spencer, J., Luparello, C. (2012). Cytotoxic effects of Jay Amin hydroxamic acid (JAHA), a ferrocene-based class I histone deacetylase inhibitor, on triple-negative MDA-MB231 breast cancer cells. *Chem. Res. Toxicol.* 19; 25 (11): 2608-16.
- Lin, R.K., Hsu, H.S., Chang, J.W., Chen, C.Y., Chen, J.T, Wang, Y.C. (2007). Alteration of DNA methyltransferases contributes to 5<sup>2</sup>CpG methylation and poor prognosis in lung cancer. *Lung Cancer* 55 (2): 205-213.
- Lindemann, R.K., Gabrielli, B., Johnstone, R.W. (2004). Histone-deacetylase inhibitors for the treatment of cancer. *Cell Cycle* 3: 779-88.
- Liu, Y.L., Yang, P.M., Shun, C.T., Wu, M.S., Weng, J.R., Chen, C.C. (2010). Autophagy potentiates the anti-cancer effects of the histone deacetylase inhibitors in hepatocellular carcinoma. *Autophagy* 6: 1057-1065.
- Liu, L.T., Chang, H.C., Chiang, L.C. Hung, W.C. (2003). Histone deacetylase inhibitor up-regulates RECK to inhibit MMP-2 activation and cancer cell invasion. *Cancer Res.* 63: 3069-72.
- López-Knowles, E., O'Toole, S.A., McNeil, C.M., Millar, E.K., Qiu, M.R., Crea, P., Daly, R.J., Musgrove, E.A., Sutherland, R.L. (2010). PI3K pathway activation in breast cancer is associated with the basal-like phenotype and cancer-specific mortality. *Int. J. Cancer* 126: 1121-1131.

- Lu, R., Wang, X., Chen, Z.F., Sun, D.F., Tian, X.Q., Fang, J.Y. (2007). Inhibition of the extracellular signal-regulated kinase/mitogen-activated protein kinase pathway decreases DNA methylation in colon cancer cells. *J. Biol. Chem.* 282: 12249-12259.
- Lucio-Eterovic, A.K., Cortez, M.A., Valera, E.T., Motta, F.J., Queiroz, R.G., Machado, H.R., Carlotti, C.G., Jr., Neder, L., Scrideli, C.A., Tone, L.G. (2008). Differential expression of 12 histone deacetylase (HDAC) genes in astrocytomas and normal brain tissue: class II and IV are hypoexpressed in glioblastomas. *BMC Cancer* 19 (8): 243.
- Lund, A.H., van Lohuizen, M. (2004). Epigenetics and cancer. *Genes Dev. Review* 18: 2315-2335.
- Luo, J., Su, F., Chen, D., Shiloh, A., Gu, W. (2000). Deacetylation of p53 modulates its effect on cell growth and apoptosis. *Nature* 408: 377-81.
- Mahlknecht, U., Hoelzer, D. (2000). Histone acetylation modifiers in the pathogenesis of malignant disease. *Mol. Med.* 6: 623-644.
- Mahon, P.C., Hirota, K., Semenza, G.L. (2001). FIH-1: a novel protein that interacts with HIF-1 alpha and VHL to mediate repression of HIF-1 transcription activity. *Genes Dev.* 15: 2675-86.
- Mai, A., Altucci, L. (2009). Epi-drugs to fight cancer: from chemistry to cancer treatment, the road ahead. *Int. J. Biochem. Cell Biol.* 41 (1): 199-213.
- Mann, B.S., Johnson, J.R., Cohen, M.H., Justice, R., Pazdur, R. (2007). FDA approval summary: vorinostat for treatment of advanced primary cutaneous T-cell lymphoma. *Oncologist* 12: 1247-1252.
- Manoharan, M., Ramachandran, K., Soloway, M.S., Singal, R. (2007). Epigenetic targets in the diagnosis and treatment of prostate cancer. *Int. Braz. J. Urol.* 33 (1): 11-18.
- Marks, P.A., Richon, V.M., Breslow, R. (2001). Histone deacetylase inhibitors as new cancer drugs. *Curr. Opin. Oncol.* 13: 477-83.
- Marks, P.A., Rifkind, R.A., Richon, V.M., Breslow, R., Miller, T., Kelly, W.K. (2001). Histone deacetylases and cancer: causes and therapies. *Nat. Rev. Cancer* 1: 194-202.
- Marks, P.A., Breslow, R. (2007). Dimethyl sulfoxide to vorinostat: development of this histone deacetylase inhibitor as an anticancer drug. *Nat Biotechnol* 25: 84-90.
- Martin, J., Magnino, F., Schmidt, K., Piguet, A.C., Lee, J.S., Semela, D., St-Pierre, M.V., Ziemiecki, A., Cassio, D., Brenner, C., Thorgeirsson, S.S., Dufour, J.F. (2006). Hint2, a mitochondrial apoptotic sensitizer down-regulated in hepatocellular carcinoma. *Gastroenterology.* 130 (7): 2179-88.
- Marty, B., Maire, V., Gravier, E., Rigaiil, G., Vincent-Salomon, A., Kappler, M., Lebigot, I., Djelti, F., Tourdès, A., Gestraud, P., Hupé, P., Barillot, E., Cruzalegui, F., Tucker, G. C., Stern, M.H., Thiery, J.P., Hickman, J.A., Dubois, T. (2008). Frequent PTEN genomic alterations and activated phosphatidylinositol 3-kinase pathway in basal-like breast cancer cells. *Breast Cancer Res.* 10: R101.
- Mathew, R., Karantza-Wadsworth, V., White, E. (2007). Role of autophagy in cancer. *Nat. Rev. Cancer* 7: 691-7.

- McCubrey, J.A., Steelman, L.S., Chappell, W.H., Abrams, S.L., Wong, E.W., Chang, F., Lehmann, B., Terrian, D.M., Milella, M., Tafuri, A., Stivala, F., Libra, M., Basecke, J., Evangelisti, C., Martelli, A.M., Franklin, R.A. (2007). Roles of the Raf/MEK/ERK pathway in cell growth, malignant transformation and drug resistance. *Biochim. Biophys. Acta* 1773 (8): 1263-84.
- Meech, S.J., Edelson, R., Walsh, P., Norris, D.A., Duke, R.C. (2001). Reversible resistance to apoptosis in cutaneous T cell lymphoma. *Ann. N. Y. Acad. Sci.* 941: 46-58.
- Meggers, E. (2009). Targeting proteins with metal complexes. *Chem. Commun.* 1001-10.
- Mielnicki, L.M., Ying, A.M., Head, K.L., Asch, H.L., Asch, B.B. (1999). Epigenetic regulation of gelsolin expression in human breast cancer cells. *Exp. Cell Res.* 249: 161-176.
- Miller, T.A., Witter, D.J., Belvedere, S. (2003). Histone deacetylase inhibitors. *J. Med. Chem.* 46: 5097-5116.
- Minucci, S., Pelicci, P.G. (2006). Histone deacetylase inhibitors and the promise of epigenetic (and more) treatments for cancer. *Nat. Rev. Cancer* 6: 38-51.
- Mizushima, N., Yoshimori, T. (2007). How to interpret LC3 immunoblotting. *Autophagy* 3: 542-545.
- Moreau, K., Ravikumar, B., Puri, C., Rubinsztein, D.C. (2012). Arf6 promotes autophagosome formation via effects on phosphatidylinositol 4,5-bisphosphate and phospholipase D. *J. Cell Biol.* 196: 483-496.
- Müller-Schiffmann, Al., Sticht, H., Korth, C. (2012). Hybrid compounds: from simple combinations to nanomachines. *BioDrugs* 26 (1): 21-31.
- Munshi, A., Kurland, J.F., Nishikawa, T., Tanaka, T., Hobbs, M.L., Tucker, S.L., Ismail, S., Stevens, C., Meyn, R.E. (2005). Histone deacetylase inhibitors radiosensitize human melanoma cells by suppressing DNA repair activity. *Clin. Cancer Res.* 11 (13): 4912-22.
- Muppirala, M., Gupta, V., Swarup, G. (2011). Syntaxin 17 cycles between the er and ergic and is required to maintain the architecture of ergic and golgi. *Biol. Cell.* 103: 333-350.
- Naselli, F., Catanzaro, I., Bellavia, D., Perez, A., Sposito, L., Caradonna F. (2014). Role and importance of polymorphisms with respect to DNA methylation for the expression of CYP2E1 enzyme. *Gene* 536 (1): 29-39.
- Niforou, K., Cheimonidou, C., Trougakos, I.P. (2014). Molecular chaperones and proteostasis regulation during redox imbalance. *Redox Biol.* 2: 323-332.
- Ng, H., Bird, A. (2000). Histone deacetylases: silencers for hire. *Trends Biochem. Sci.* 25: 21-6.
- Nishiyama, A., Matsui, M., Iwata, S., Hirota, K., Masutani, H., Nakamura, H., Takagi, Y., Sono, H., Gon, Y., Yodoi, J. (1999). Identification of thioredoxin-binding protein-2/vitamin D(3) up-regulated protein 1 as a negative regulator of thioredoxin function and expression. *J. Biol. Chem.* 274: 21645-21650.

- Noda, T., Oshumi, Y. (1998). Tor, a phosphatidylinositol kinase homologue, controls autophagy in yeast. *J. Biol. Chem.* 273: 3963-66.
- Noh, E.J., Lim, D.S., Jeong, G., Lee, J.S. (2009). An HDAC inhibitor, trichostatin A, induces a delay at G2/M transition, slippage of spindle checkpoint, and cell death in a transcription-dependent manner. *Biochem. Biophys. Res. Commun.* 378: 326-331.
- Okamoto, K. (2011). Mitochondria breathe for autophagy. *EMBO J.* 30: 2095-2096.
- Olsen, E., Rasmussen, H.H., Celis, J.E. (1995). Identification of proteins that are abnormally regulated in differentiated cultured human keratinocytes. *Electrophoresis* 16: 2241-2248.
- Olson, M.F., Marais, R. (2000). Ras protein signalling. *Semin. Immunol.* 12: 63-73.
- Osella, D., Homa Mahboobi, H., Colangelo, D., Cavigliolo, G., Vessieres, A., Jaouen, G. (2005). FACS analysis of oxidative stress induced on tumour cells by SERMs. *Inorg. Chim. Acta* 358: 1993-1998.
- Paget, J.A., Restall, I.J., Daneshmand, M., Mersereau, J.A., Simard, M.A., Parolin, D.A., Lavictoire, S.J., Amin, M.S., Islam, S., Lorimer, I.A. (2012) Repression of cancer cell senescence by PKC $\zeta$ . *Oncogene* 31 (31): 3584-96.
- Paglin, S., Hollister, T., Delohery, T., Hackett, N., McMahill, M., Sphicas, E., Domingo, D., Yahalom, J. (2001). A novel response of cancer cells to radiation involves autophagy and formation of acidic vesicles. *Cancer Res.* 61: 439-44.
- Pal, D., Outram, S.P., Basu, A. (2013). Upregulation of PKC $\eta$  by PKC $\epsilon$  and PDK1 involves two distinct mechanisms and promotes breast cancer cell survival. *Biochim. Biophys. Acta.* 1830 (8): 4040-5.
- Palani, C.D., Beck, J.F., Sonnemann, J. (2010). Histone deacetylase inhibitors enhance the anticancer activity of nutlin-3 and induce p53 hyperacetylation and downregulation of MDM2 e MDM4 gene expression. *Investig New Drugs* 3.
- Payne, D.M., Rossomando, A.J., Martino, P., Erickson, A.K., Her, J.H., Shabanowitz, J., Hunt, D.F., Weber, M.J., Sturgill, T.W. (1991). Identification of the regulatory phosphorylation sites in pp42/mitogen-activated protein kinase (MAP kinase). *EMBO J.* 10: 885-892.
- Peart, M.J., Tainton, K.M., Ruefli, A.A., Dear, A.E., Sedelies, K.A., O'Reilly, L.A., Waterhouse, N.J., Trapani, J.A., Johnstone, R.W. (2003). Novel mechanisms of apoptosis induced by histone deacetylase inhibitors. *Cancer Res.* 63: 4460-7.
- Polyak, K. (2011). Heterogeneity in breast cancer. *J Clin Invest* 121(10): 3786-3788.
- Portanova, P., Russo, T., Pellerito, O., Calvaruso, G., Giuliano, M., Vento, R., Tesoriere, G. (2008). The role of oxidative stress in apoptosis induced by the histone deacetylase inhibitor suberoylanilide hydroxamic acid in human colon adenocarcinoma HT-29 cells. *Int. J. Oncol.* 33: 325-331.
- Qadir, M.A., Kwok, B., Dragowska, W.H., To, K.H., Le, D., Bally, M.B., Gorski, S.M. (2008). Macroautophagy inhibition sensitizes tamoxifen-resistant breast cancer cells and enhances mitochondrial depolarization. *Breast Cancer Res. Treat.* 112: 389-403.

- Qian, D.Z., Kachhap, S.K., Collis, S.J., Verheul, H.M., Carducci, M.A., Atadja, P., Pili, R. (2006). Class II histone deacetylases are associated with VHL-independent regulation of hypoxia-inducible factor 1 alpha. *Cancer Res.* 66 (17): 8814-21.
- Qian, D.Z., Kato, Y., Shabbeer, S., Wei, Y., Verheul, H.M., Salumbides, B., Sanni, T., Atadja, P., Pili, R. (2006). Targeting tumor angiogenesis with histone deacetylase inhibitors: the hydroxamic acid derivative LBH589. *Clin. Cancer Res.* 12: 634-42.
- Qu, X., Yu, J., Bhagat, G., Furuya, N., Hibshoosh, H., Troxel, A., Rosen, J., Eskelinen, E. L., Mizushima, N., Ohsumi, Y. (2003). Promotion of tumorigenesis by heterozygous disruption of the beclin 1 autophagy gene. *J. Clin. Invest.* 112: 1809-20.
- Rao, R., Balusu, R., Fiskus, W., Mudunuru, U., Venkannagari, S., Chauhan, L., Smith, J. E., Hembruff, S.L., Ha, K., Atadja, P., Bhalla, K.N. (2012). Combination of pan-histone deacetylase inhibitor and autophagy inhibitor exerts superior efficacy against triple-negative human breast cancer cells. *Mol. Cancer Ther.* 11: 973-983.
- Reggiori, F., Klionsky, D.J. (2002). Autophagy in the eukaryotic cell. *Eukaryot Cell* 1: 11-21.
- Richon, V.M., Sandhoff, T.W., Rifkind, R.A., Marks, P.A. (2000). Histone deacetylase inhibitor selectively induces p21WAF1 expression and gene-associated histone acetylation. *Proc. Natl. Acad. Sci. USA* 97: 10014-19.
- Robertson, K.D. (2001). DNA methylation, methyltransferases, and cancer. *Oncogene* 20 (24): 3139-3155.
- Rogalska, A., Koceva-Chyla, A., Józwiak, Z. (2008). Aclarubicin-induced ROS generation and collapse of mitochondrial membrane potential in human cancer cell lines. *Chem. Biol. Interact.* 176: 58-70.
- Ropero, S., Fraga, M.F., Ballestar, E., Hamelin, R., Yamamoto, H., Boix-Chornet, M., Caballero, R., Alaminos, M., Setien, F., Paz, M.F., Herranz, M., Palacios, J., Arango, D., Orntoft, T.F., Aaltonen, L.A., Schwartz, S.Jr., Esteller, M.A (2006). Truncating mutation of HDAC2 in human cancers confers resistance to histone deacetylase inhibition. *Nat. Genet.* 38: 566-9.
- Rossi, D., Gaidano, G. (2003). Messengers of cell death: apoptotic signaling in health and disease. *Haematologica* 88: 212-18.
- Rossig, L., Li, H., Fisslthaler, B., Urbich, C., Fleming, I., Forstermann, U., Zeiher, A.M. Dimmeler, S. (2002). Inhibitors of histone deacetylation downregulate the expression of endothelial nitric oxide synthase and compromise endothelial cell function in vasorelaxation and angiogenesis. *Circ. Res.* 91: 837-44.
- Saito, A., Yamashita, T., Mariko, Y., Nosaka, Y., Tsuchiya, K., Ando, T., Suzuki, T., Tsuruo, T., Nakanishi, O. (1999). A synthetic inhibitor of histone deacetylase, MS-27-275, with marked in vivo antitumor activity against human tumors. *Proc. Natl. Acad. Sci. USA* 96: 4592-97.
- Samaddar, J.S., Gaddy, V.T., Duplantier, J., Thandava, S.P., Shah, M., Smith, M.J., Browning, D., Rawson, J., Smith, S.B., Barrett, J.T., Schoenlien, P.V. (2008). A role for macroautophagy in protection against 4-hydroxytamoxifen-induced cell death and the development of antiestrogen resistance. *Mol. Cancer Ther.* 7: 2977-87.

- Sauter, P.K., Saurin, A.T., Durgan, J., Cameron, A.J., Faisal, A., Marber, M.S., Parker, P.J. (2008). The regulated assembly of a PKCepsilon complex controls the completion of cytokinesis. *Nat. Cell Biol.* 10 (8): 891-901.
- Schneider-Stock, R., Ocker, M. (2007). Epigenetic therapy in cancer: molecular background and clinical development of histone deacetylase and DNA methyltransferase inhibitors. *Drugs* 10 (8): 557-561.
- Schwartz, S.B., Higgins, P.J., Rajasekaran, A.K., Staiano, C.L. (1994). Gelsolin expression in normal human keratinocytes is a function of induced differentiation. *Adv. Exp. Med. Biol.* 358: 169-181.
- Seger, R., Ahn, N.G., Posada, J., Munar, E.S., Jensen, A.M., Cooper, J.A., Cobb, M.H., Krebs, E.G. (1992). Purification and characterization of mitogen-activated protein kinase activator(s) from epidermal growth factor-stimulated A431 cells. *J. Biol. Chem.* 267: 14373-14381.
- Sibaji, S., Abujamre, L., Loew, E. (2011). Histone Deacetylase Inhibitors Reverse CpG Methylation by Regulating DNMT1 through ERK Signaling. *Anticancer Research.* 31: 2723-2732.
- Sokolov, B.P., Prockop, D.J. (1994). A rapid and simple PCR-based method for isolation of cDNAs from differentially expressed genes. *Nucleic Acids Res.* 22 (19): 4009-15.
- Sowa, Y., Orita, T., Minamikawa-Hiranabe, S., Mizuno, T., Nomure, H., Sakai, T. (1999). Sp3, but not Sp1, mediates the transcriptional activation of the p21/WAF1/Cip1 gene promoter by histone deacetylase inhibitor. *Cancer Res.* 59: 4266-70.
- Spange, S., Wagner, T., Heinzl, T., Krämer, O.H. (2009). Acetylation of non-histone proteins modulates cellular signaling at multiple levels. *Int. J. Biochem Cell Biol.* 41: 185-98.
- Spencer, J., Amin, J., Boddiboyena, R., Packham, G., Cavell, B.E., Syed Alwi, S.S., Paranal, R.M., Heightman, T.D., Wang, M., Marsden, B., Coxhead, P., Guille, M., Tizzard, G.J., Coles, S.J., Bradner, J.E. (2012). Click JAHAs: conformationally restricted ferrocene-based histone deacetylase inhibitors. *Med. Chem. Commun.* 3: 61-64.
- Spencer, J., Amin, J., Wang, M., Packham, G., Tizzard, G.J., Coles, S.J., Paranal, R., Bradner, J.E., Heightman, T. (2011). Synthesis and biological evaluation of JAHAs: ferrocene-based class I histone deacetylase inhibitors. *ACS Med. Chem. Lett.* 2: 358-62.
- Steelman, L.S., Pohnert, S.C., Shelton, J.G., Franklin, R.A., Bertrand, F.E., McCubrey, J.A. (2004). JAK/STAT, Raf/MEK/ERK, PI3K/Akt and BCR-ABL in cell cycle progression and leukemogenesis. *Leukemia* 18: 189-218.
- Strahl, B.D., Allis, C.D. (2000). The language of covalent histone modifications. *Nature* 403: 41-45.
- Tagaya, Y., Maeda, Y., Mitsui, A., Kondo, N., Matsui, H., Hamuro, J., Brown, N., Arai, K., Yokota, T., Wakasugi, H., (1989). ATL-derived factor (ADF), an IL-2 receptor/Tac inducer homologous to thioredoxin; possible involvement of dithiol-reduction in the IL-2 receptor induction. *EMBO J.* 8: 757-764.

- Tan, B., Young, D.A., Lu, Z.H., Wang, T., Meier, T.I., Shepard, R.L., Roth, K., Zhai, Y., Huss, K., Kuo, M.S., Gillig, J., Parthasarathy, S., Burkholder, T.P., Smith, M.C., Geeganage, S., Zhao, G. (2013). Pharmacological inhibition of nicotinamide phosphoribosyltransferase (NAMPT), an enzyme essential for NAD<sup>+</sup> biosynthesis, in human cancer cells: metabolic basis and potential clinical implications. *J. Biol. Chem.* 288 (5): 3500-11.
- Tanaka, M., Mullauer, L., Ogiso, Y., Fujita, H., Moriya, S., Furuuchi, K., Harabayashi, T., Shinohara, N., Koyanagi, T., Kuzumaki, N. (1995). Gelsolin: a candidate for suppressor of human bladder cancer. *Cancer Res.* 55: 3228-3232.
- Tanaka, M., Sazawa, A., Shinohara, N., Kobayashi, Y., Fujioka, Y., Koyanagi, T., Kuzumaki, N. (1999). Gelsolin gene therapy by retrovirus producer cells for human bladder cancer in nude mice. *Cancer Gene Ther.* 6: 482-487.
- Tang, Y., Zhao, W., Chen, Y., Zhao, Y., Gu, W. (2008). Acetylation is indispensable for p53 activation. *Cell* 133: 612-26.
- Tanida, I., Sou, Y. S., Ezaki, J., Minematsu-Ikeguchi, N., Ueno, T., Kominami, E. (2004 a). HsAtg4B/HsApg4B/ Autophagin-1 cleaves the carboxyl termini of three human Atg8 homologues and dilapidates microtubule-associated protein-phospholipid conjugates. *J. Biol. Chem.* 279: 36268-76.
- Tanida, I., Ueno, T., Kominami, E. (2004 b). Human light chain 3/MAP1LC3B is cleaved at its carboxyl-terminal Met121 to expose Gly120 for lipidation and targeting to autophagosomal membranes. *J. Biol. Chem.* 279: 47704-10.
- Taunton, J., Hassig, C.A., Schreiber, S.L. (1996). A mammalian histone deacetylase related to the yeast transcriptional regulator Rpd3p. *Science* 272 (5260): 408-11.
- Thornberry, N.A., Lazebnik, Y. (1998). Caspase: enemies within. *Science* 281: 1312-16.
- Tong, A., Zhang, H., Li, Z., Gou, L., Wang, Z., Wei, H., Tang, M., Liang, S., Chen, L., Huang, C., Wei, Y. (2008). Proteomic analysis of liver cancer cells treated with suberoylanilide hydroxamic acid. *Cancer Chemother Pharmacol.* 61 (5): 791-802.
- Tsai, H.Y., Yang, Y.F., Wu, A.T., Yang, C.J., Liu, Y.P., Jan, Y.H., Lee, C.H., Hsiao, Y.W., Yeh, C.T., Shen, C.N., Lu, P.J., Huang, M.S., Hsiao, M. (2013). Endoplasmic reticulum ribosome-binding protein 1 (RRBP1) overexpression is frequently found in lung cancer patients and alleviates intracellular stress-induced apoptosis through the enhancement of GRP78. *Oncogene.* 32 (41): 4921-31.
- Ueda, T., Takai, N., Nishida, M., Nasu, K., Narahara, H. (2007). Apicidin, a novel histone deacetylase inhibitor, has profound anti-growth activity in human endometrial and ovarian cancer cells. *Int. J. Mol. Med.* 19: 301-308.
- Valerie, K., Yacoub, A., Hagan, M.P., Curiel, D.T., Fisher, P.B., Grant, S., Dent, P. (2007). Radiation-induced cell signaling: inside-out and outside-in. *Mol. Cancer Ther.* 6: 789-80.
- Van Lint, C., Emiliani, S., Verdin, E. (1996). The expression of a small fraction of cellular gene is changes in response to histone hyperacetylation. *Gene Expr.* 5: 245-254.

- Vannini, A., Volpari, C., Filocamo, G., Casavola E.C., Brunetti, M., Renzoni, D., Chakravarty, P., Paolini, C., De Francesco, R., Gallinari, P., Steinkühler, C., Di Marco, S. (2004). Crystal structure of a eukaryotic zinc-dependent histone deacetylase, human HDAC8, complexed with a hydroxamic acid inhibitor. *Proc Natl Acad Sci USA* 101 (42): 15064-9.
- Vaquero, A., Loyola, A., Reinberg, D. (2003). The constantly changing face of chromatin. *Sci Aging Knowledge Environ* (14): RE4.
- Vermeulen, K., Van Bockstaele, D.R., Berneman, Z.N. (2005). Apoptosis: mechanisms and relevance in cancer. *Ann. Hematol.* 84: 627-39.
- Viale, G. (2012). The current state of breast cancer classification. *Ann. Oncol.* 23: 207-210.
- Villa, R., Morey, L., Raker, V.A., Buschbeck, M., Gutierrez, A., De Santis, F., Corsaro, M., Varas, F., Bossi, D., Minucci, S., Pelicci, P.G., Di Croce, L. (2006). The methyl-CpG binding protein MBD1 is required for PML-RARalpha function. *Proc. Natl. Acad. Sci. USA* 103 (5): 1400-5.
- Wade, P.A. (2001). Transcriptional control at regulatory checkpoints by histone deacetylases: molecular connections between cancer and chromatin. *Hum. Mol.Genet.* 10: 693-698.
- Wakasugi, N., Tagaya, Y., Wakasugi, H., Mitsui, A., Maeda, M., Yodoi, J., Tursz, T. (1990). Adult T-cell leukemia-derived factor/thioredoxin, produced by both human T-lymphotropic virus type I- and Epstein-Barr virus-transformed lymphocytes, acts as an autocrine growth factor and synergizes with interleukin 1 and interleukin 2. *Proc. Natl. Acad. Sci. U.S.A.* 87: 8282-8286.
- Wang, C.W., Klionsky, D.J.(2003). The molecular mechanism of autophagy. *Mol. Med.* 9: 65-76.
- Wang, B., David, M.D., Schrader, J.W. (2005). Absence of caprin-1 results in defects in cellular proliferation. *J. Immunol.* 175 (7): 4274-82.
- Xu, W.S., Perez, G., Ngo, L., Gui, C.Y., Marks, P.A. (2005). Induction of polyploidy by histone deacetylase inhibitor: a pathway for antitumor effects. *Cancer Res.* 65: 7832-7839.
- Yamamoto, A., Tagawa, Y., Yoshimori, T., Moriyama, Y., Masaki, R., Tashiro, Y. (1998). Bafilomycin A1 prevents maturation of autophagic vacuoles by inhibiting fusion between autophagosomes and lysosomes in rat hepatoma cell line, H-4-II-E cells. *Cell Struct. Funct.* 23: 33-42.
- Yamamoto, S., Tanaka, K., Sakimura, R., Okada, T., Nakamura, T., Li, Y., Takasaki, M., Nakabeppu, Y., Iwamoto, Y. (2008). Suberoylanilide hydroxamic acid (SAHA) induces apoptosis or autophagy-associated cell death in chondrosarcoma cell lines. *Anticancer Res.* 28: 1585-1591.
- Yang, X., Martin, T.A., Jiang, W.G. (2012). Int Biological influence of brain-derived neurotrophic factor on breast cancer cells. *J. Oncol.* 41 (4): 1541-6.



- 
- Yang, X., Young, L.H., Voigt, J.M. (1998). Expression of a vitamin D-regulated gene (VDUP-1) in untreated- and MNU-treated rat mammary tissue. *Breast Cancer Res. Treat.* 48: 33-44.
  - Yoshida, M., Horinouchi, S., Beppu, T. (1995). Trichostatin A and trapoxin: novel chemical probes for the role of histone acetylation in chromatin structure and function. *Bioassays* 17: 423-430.
  - Yoshida, M., Matsuyama, A., Komatsu, Y., Nishino, N. (2003). From discovery to the coming generation of histone deacetylase inhibitors. *Curr. Med. Chem.* 10: 2351-2358.
  - Young, L.H., Yang, X., Voigt, J.M. (1996). Alteration of gene expression in rat mammary tumors induced by N-methyl-N-nitrosourea. *Mol. Carcinog.* 15: 251-260.
  - Žak, M., Bress, A., Brandt, N., Franz, C., Ruth, P., Pfister, M., Knipper, M. Blin, N. (2012). Ergic2, a brain specific interacting partner of Otoferlin. *Cell Physiol. Biochem.* 29 (5-6): 941-8.
  - Zhang, Y., Reinberg, D. (2001). Transcription regulation by histone methylation: interplay between different covalent modifications of the core histone tails. *Genes Dev. Review* 15: 2343-2360.
  - Zhao, Y., Lu, S., Wu, L., Chai, G., Wang, H., Chen, Y., Sun, J., Yu, Y., Zhou, W., Zheng, Q., Wu, M., Otterson, G.A., Zhu, W.G. (2006). Acetylation of p53 at lysine 373/382 by the histone deacetylase inhibitor depsipeptide induce expression of p21 (Waf1/Cip1). *Mol. Cell Biol.* 26: 2782-90.
  - Zordoky, B.N.M., Bark, D., Soltys, C.L., Sung, M.M., Dyck, J.R.B. (2014). The antiproliferative effect of metformin in triple-negative MDA-MB231 breast cancer cells is highly dependent on glucose concentration: Implications for cancer therapy and prevention. *Biochimica et Biophysica Acta* 1840: 1943-1957.

## **Sitography**

- <http://www.autophagy.lu>
- <http://www.bouzoki.files.wordpress.com>
- <http://www.discoverymedicine.com>
- [http://www.en.wikipedia.org/wiki/Trichostatin\\_A](http://www.en.wikipedia.org/wiki/Trichostatin_A)
- <http://www.genenames.org>
- <http://www.hindawi.com>
- <http://www.labmed.ascpjournals.org>
- <http://www.mun.ca>
- <http://www.nature.com>
- <http://www.planetorbitrap.com>
- <http://www.primer3.wi.mit.edu>
- <http://www.proteom.ibb.waw.pl>
- <http://www.wormbook.org>